ISM Dynamics and Star Formation

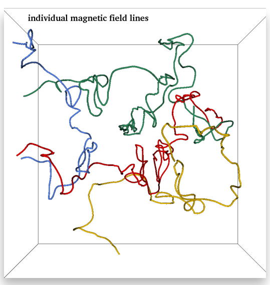

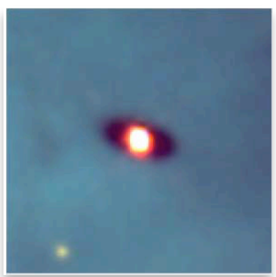
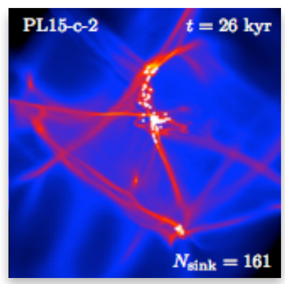

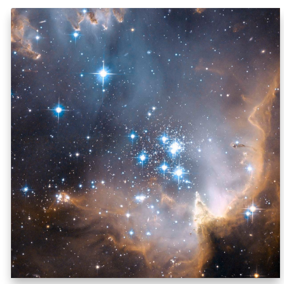
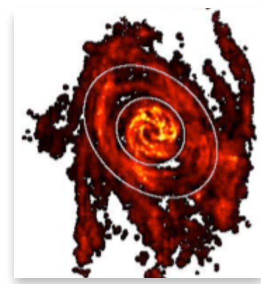
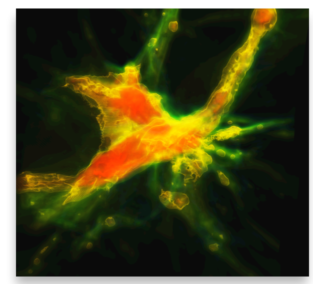

Ralf Klessen

Zentrum für Astronomie der Universität Heidelberg
Institut für Theoretische Astrophysik

thanks to ...

... people in the star formation group at Heidelberg University:

Christian Baczynski, Erik Bertram, Frank Bigiel, Andre Bubel, Diane Cormier, Volker Gaibler, Simon Glover, Dimitrious Gouliermis, Tilman Hartwig, Juan Ibanez, Christoph Klein, Lukas Konstandin, Mei Sasaki, Jennifer Schober, Rahul Shetty, Rowan Smith, László Szűcs

... former group members:

Robi Banerjee, Ingo Berentzen, Paul Clark, Christoph Federrath, Philipp Girichidis, Thomas Greif, Milica Micic, Thomas Peters, Dominik Schleicher, Stefan Schmeja, Sharanya Sur, . . .

... many collaborators abroad!

Deutsche
Forschungsgemeinschaft
DFG

DFG Priority Program 1573
ISM-SPP
Interstellar Medium

BADEN-
WÜRTTEMBERG
STIFTUNG
Wir stiften Zukunft

HGSFP

IMPRS

erc
European
Research
Council

agenda

- introductory remarks
  - relation between measurement and underlying physics
- applications / controversies / puzzles
  - global star formation relations
    are we sure we see universal dependencies?
  - molecular gas
    are we sure we see all H_2 gas?
  - filaments
    are they real (ly everywhere)?

NGC 3324 (Hubble, NASA/ESA)

prolegomena

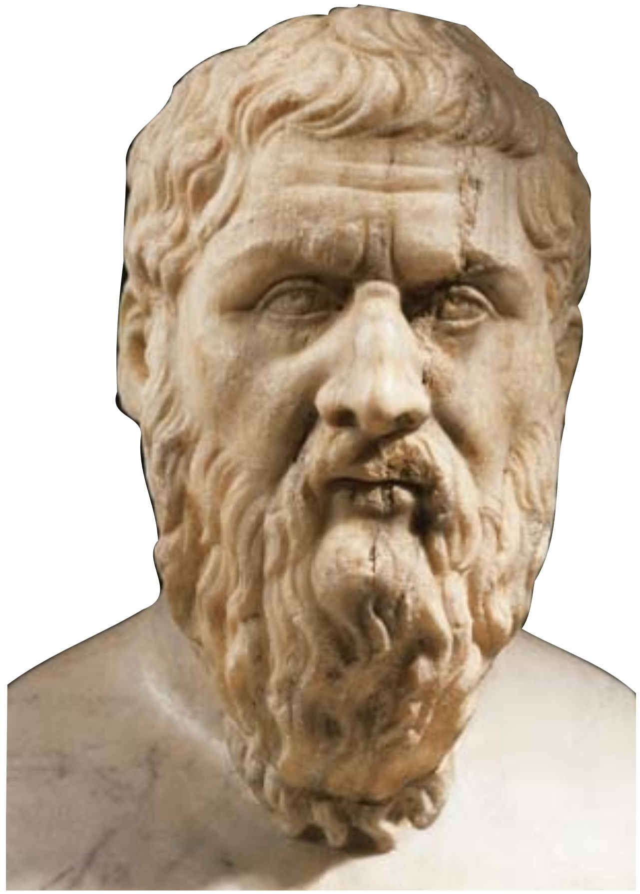

Platon
428/427–348/347 BC

Capitoline Museum, Rome.

Plato's allegory of the cave*

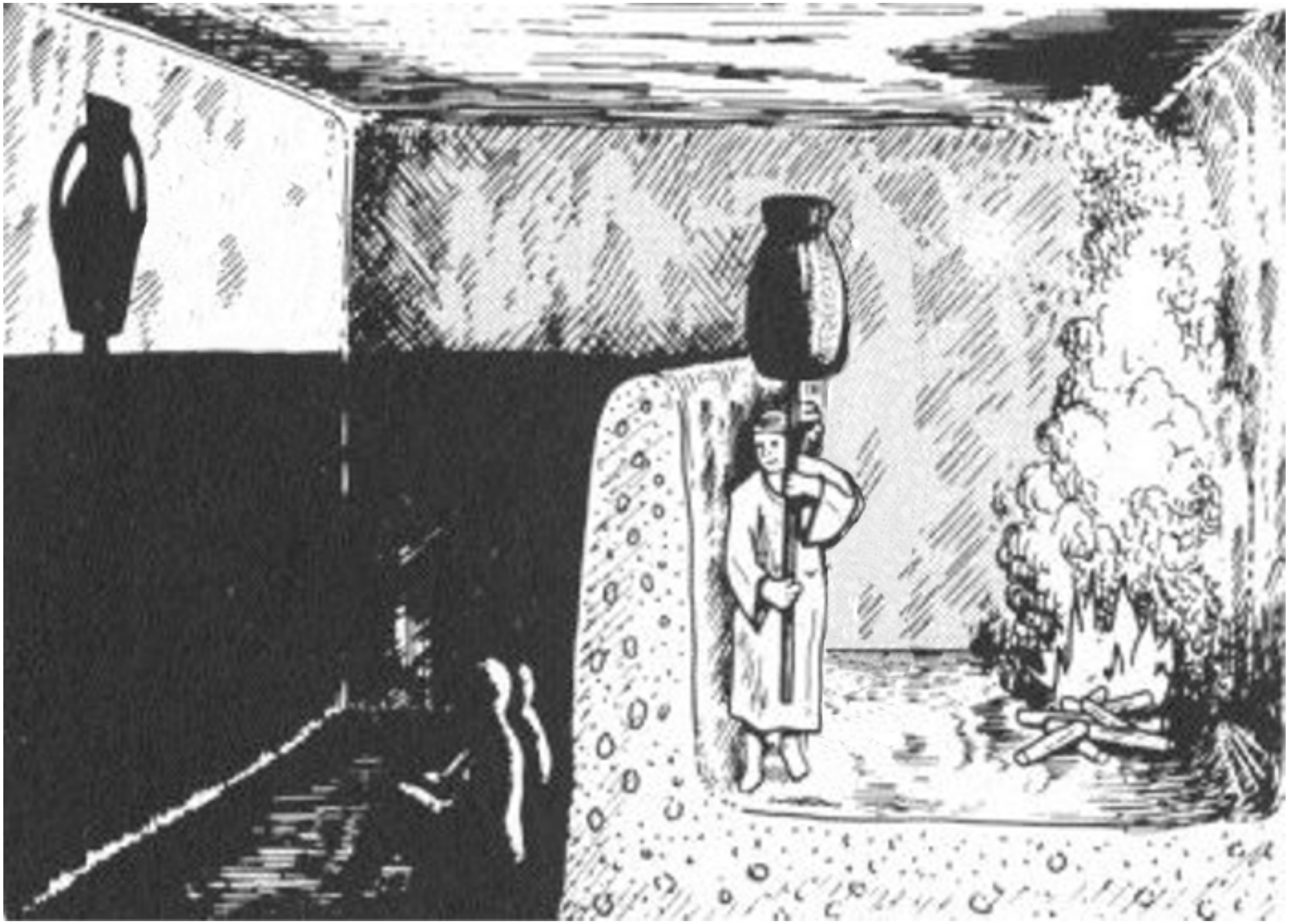

Laszlo Szücs, image from criticalthinking-mc205.wikispaces.com

* The Republic (514a-520a)

Plato's allegory of the cave*

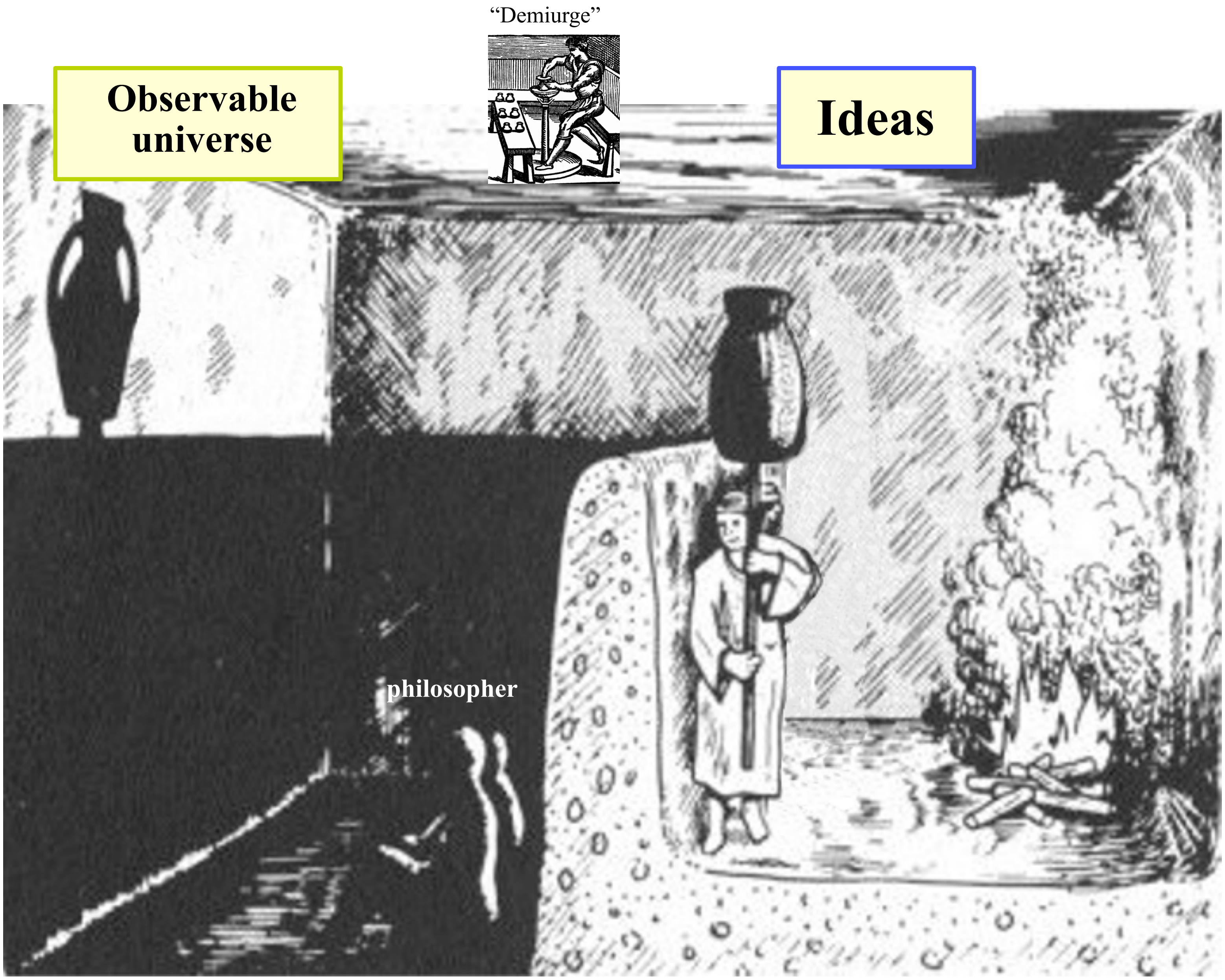

Laszlo Szücs, image from criticalthinking-mc205.wikispaces.com

* The Republic (514a-520a)

Plato's allegory of the cave* ↔ Astronomical observations

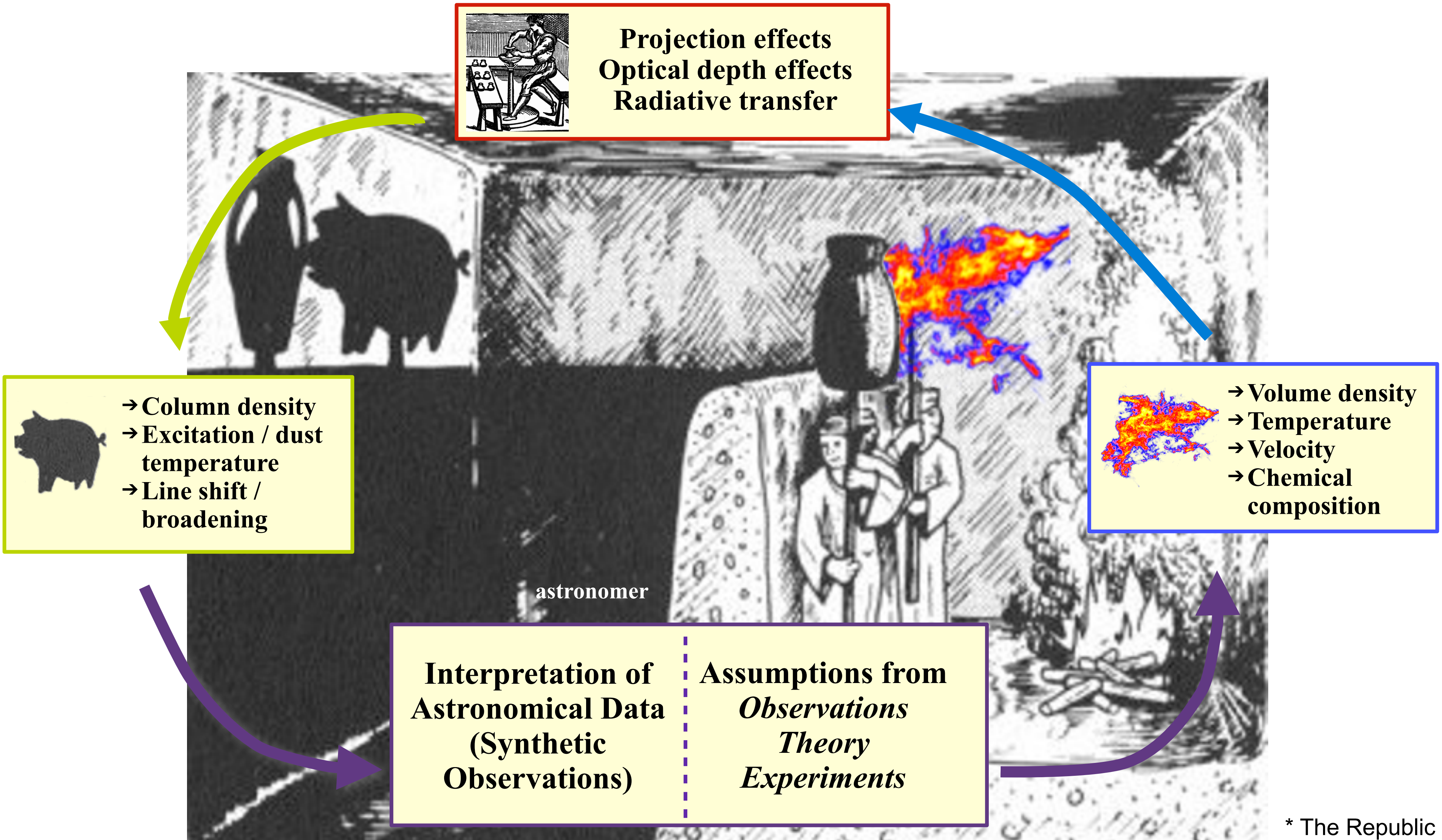

Laszlo Szücs, image from criticalthinking-mc205.wikispaces.com

* The Republic (514a-520a)

Example: from CO emission to total column density

J=1-0

I(^{12}CO)
115.271 GHz

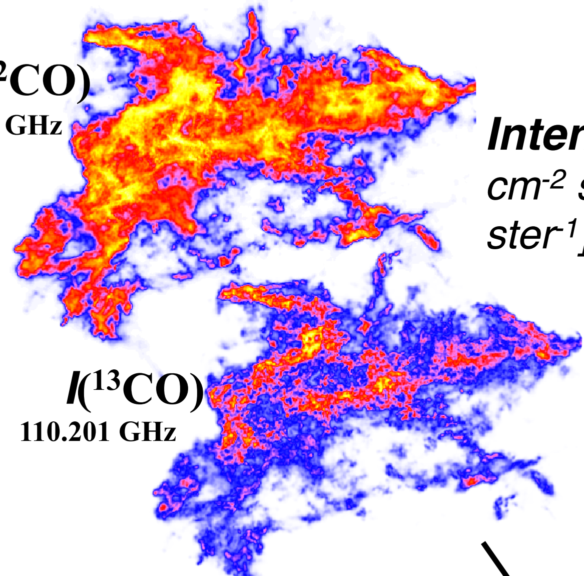

I(^{13}CO)
110.201 GHz

Intensity *[erg cm^{-2} s^{-1} Hz^{-1} ster^{-1}]*

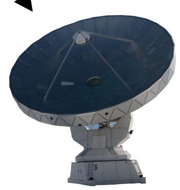

Brightness temperature *[K]*

T_B^{12}

T_B^{13}

Following Wilson et al. 2009

Assumptions I.

I(^{12}CO) is optically thick

I(^{13}CO) is optically thin

Along a line of sight uniform T_{ex} and same for ^{12}CO and ^{13}CO

$$T_{\rm ex} = 5.5/\ln\left(1 + \frac{5.5}{T_B^{12} + 0.82}\right)$$

$$\tau_{13}(v) = -\ln\left[1 - \frac{T_{\rm B}^{13}}{5.3}\left\{\exp\left(\frac{5.3}{T_{\rm ex}} - 1\right)^{-1} - 0.16\right\}^{-1}\right],$$

LTE

$$N(^{13}{\rm CO}) = 3.0 \times 10^{14}\frac{T_{\rm ex}\int \tau_{13}(v)dv}{1 - \exp(-5.3/T_{\rm ex})}$$

Assumptions II.

Uniform N(^{12}CO)/N(^{13}CO) ~ 60 *

N(H_2)/N(^{12}CO) ratio ~ 6.6×10^3 **

Column density *[cm^{-2}]*

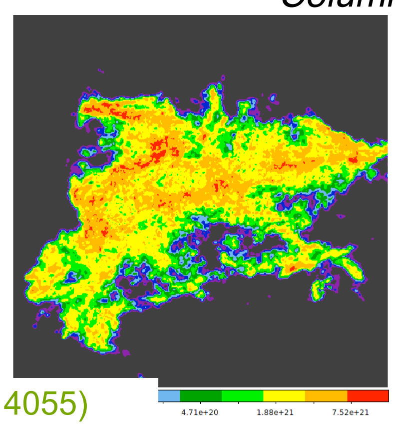

Astrophysical interpretation

Laszlo Szücs et al. (2014, MNRAS, 445, 4055)

* Langer & Penzias (1990)
** Pineda et al. (2009)

global SF relations

1. radial distribution in spirals

- HI versus H_2:
  - H_2 is restricted to the optical disk
  - while the HI extends 2 - 4 x optical radius
- HI hole or depression in the centers, sometimes compensated by H_2
- often H_2 is exponential like stars, HI does *not* follow in most cases

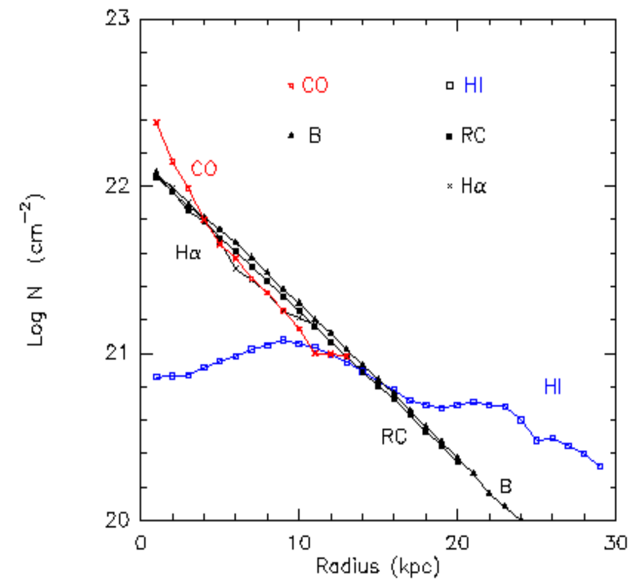

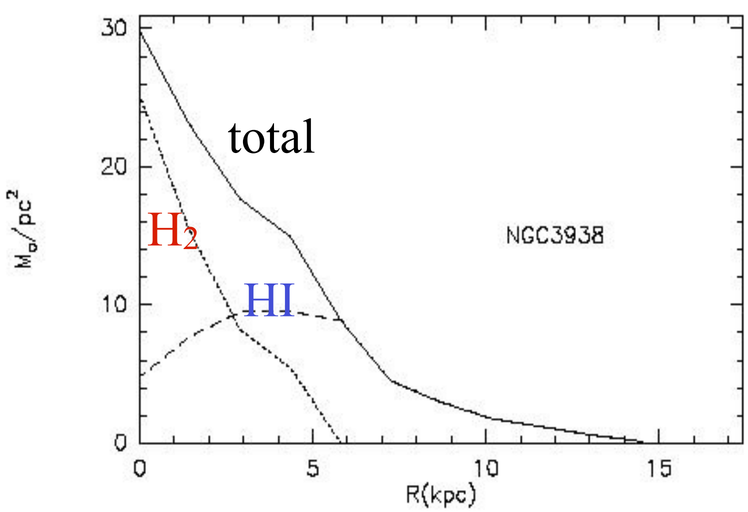

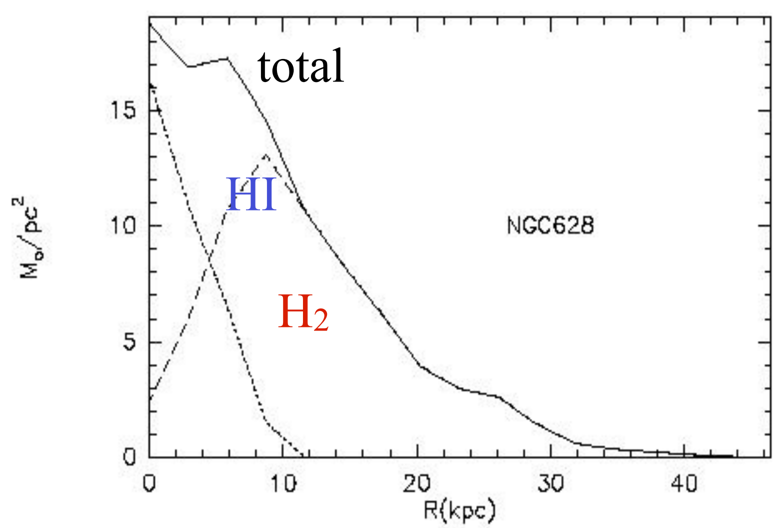

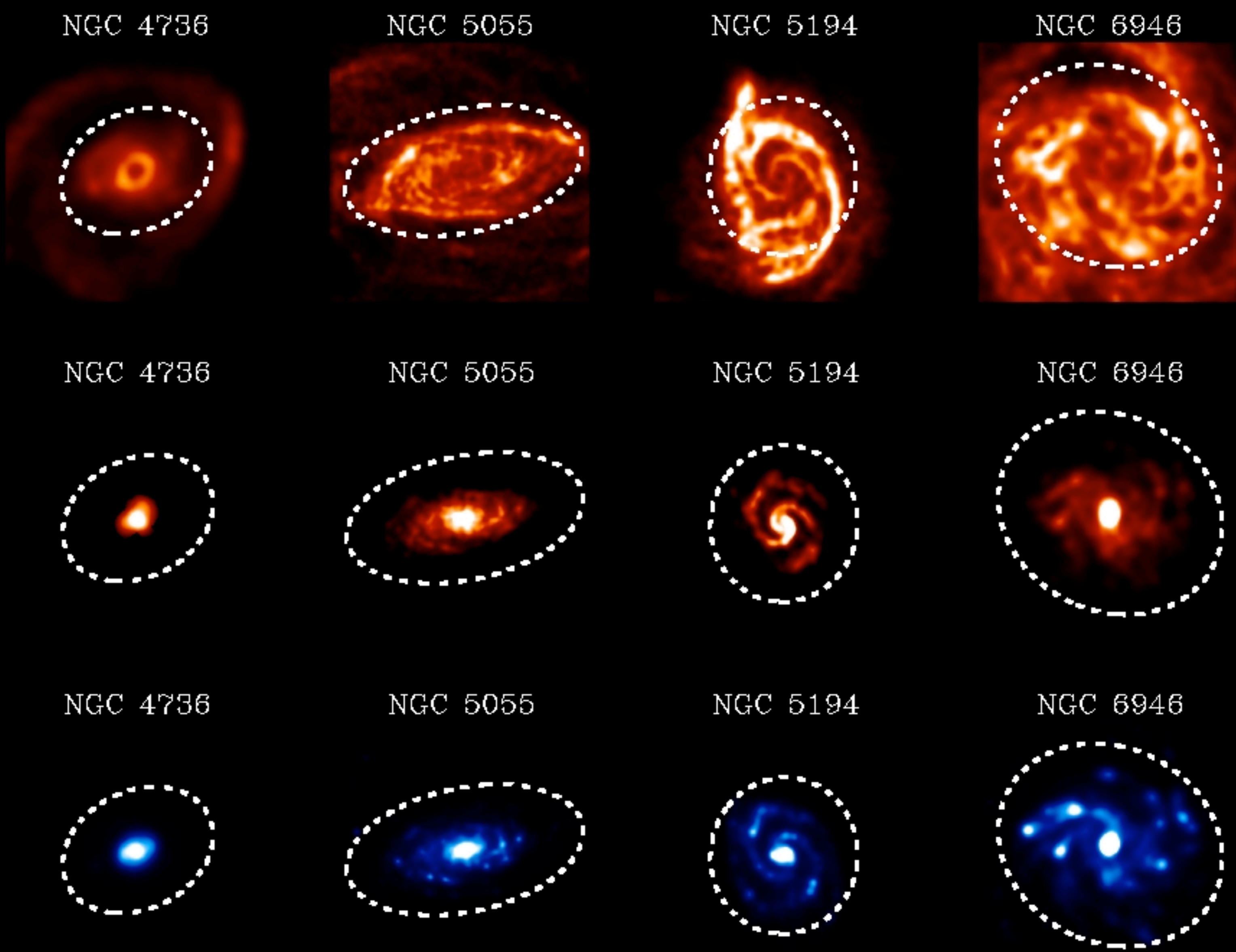

atomic hydrogen

molecular hydrogen

star formation

- HI gas more extended
- H2 and SF well correlated

galaxies from THINGS and HERACLES survey
(images from Frank Bigiel, ZAH/ITA)

2. correlation with star formation

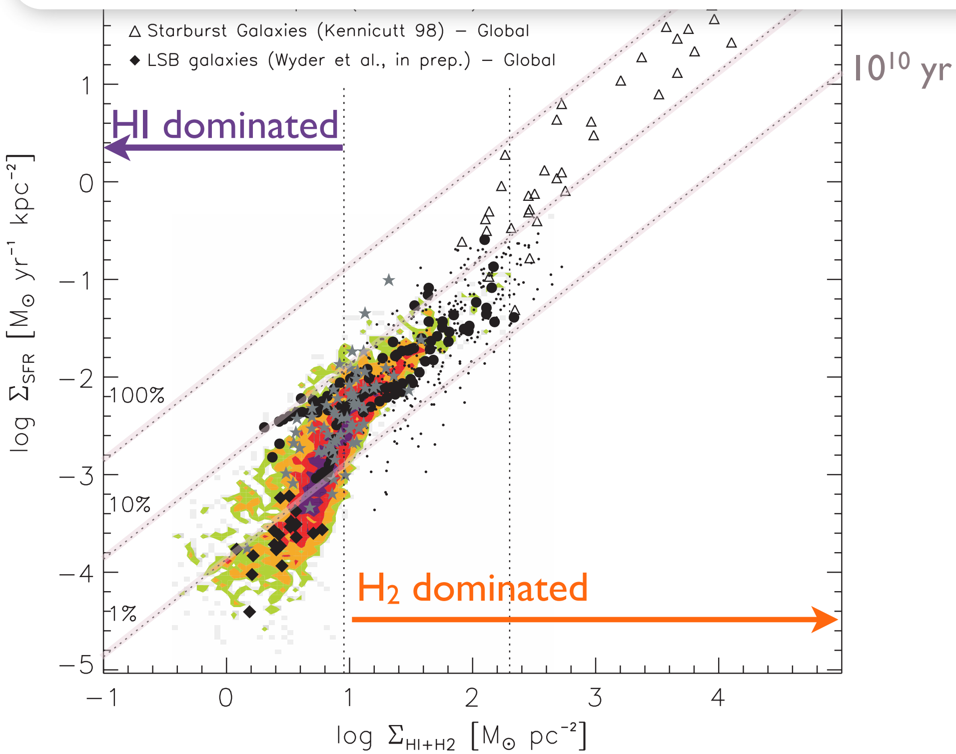

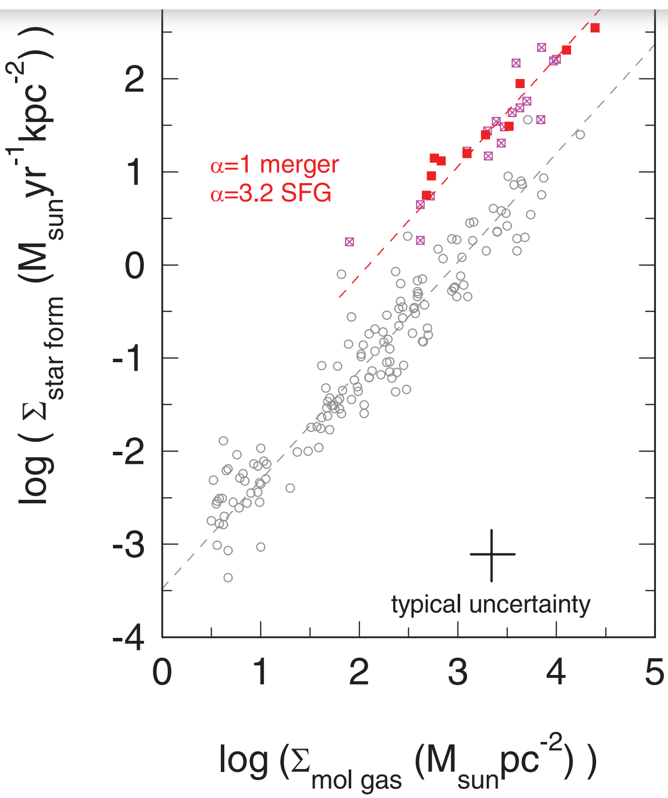

Bigiel et al. (2008, AJ, 136, 2846)

Genzel et al. (2010, MNRAS, AJ, 407, 2091)

- standard model: roughly linear relation between H
- standard model: roughly constant depletion time: few x 10
- super linear relation between total gas and SFR

data from STING survey (Rahman et al. 2011, 2012)

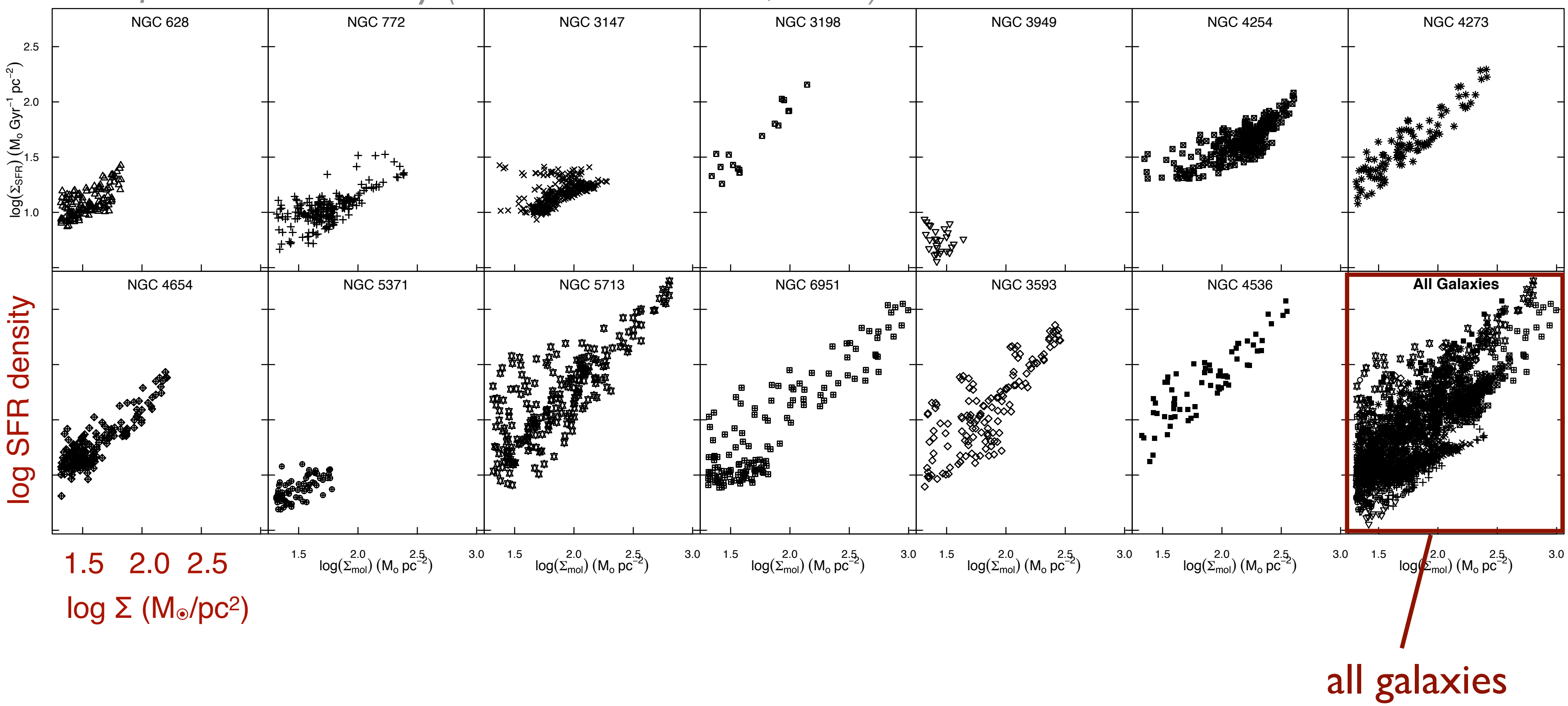

- QUIZ: do you see a universal

Shetty et al. (2014, MNRAS, 437, L61, see also Shetty, Kelly, Bigiel, 2013, MNRAS, 430, 288)

data from STING survey (Rahman et al. 2011, 2012)

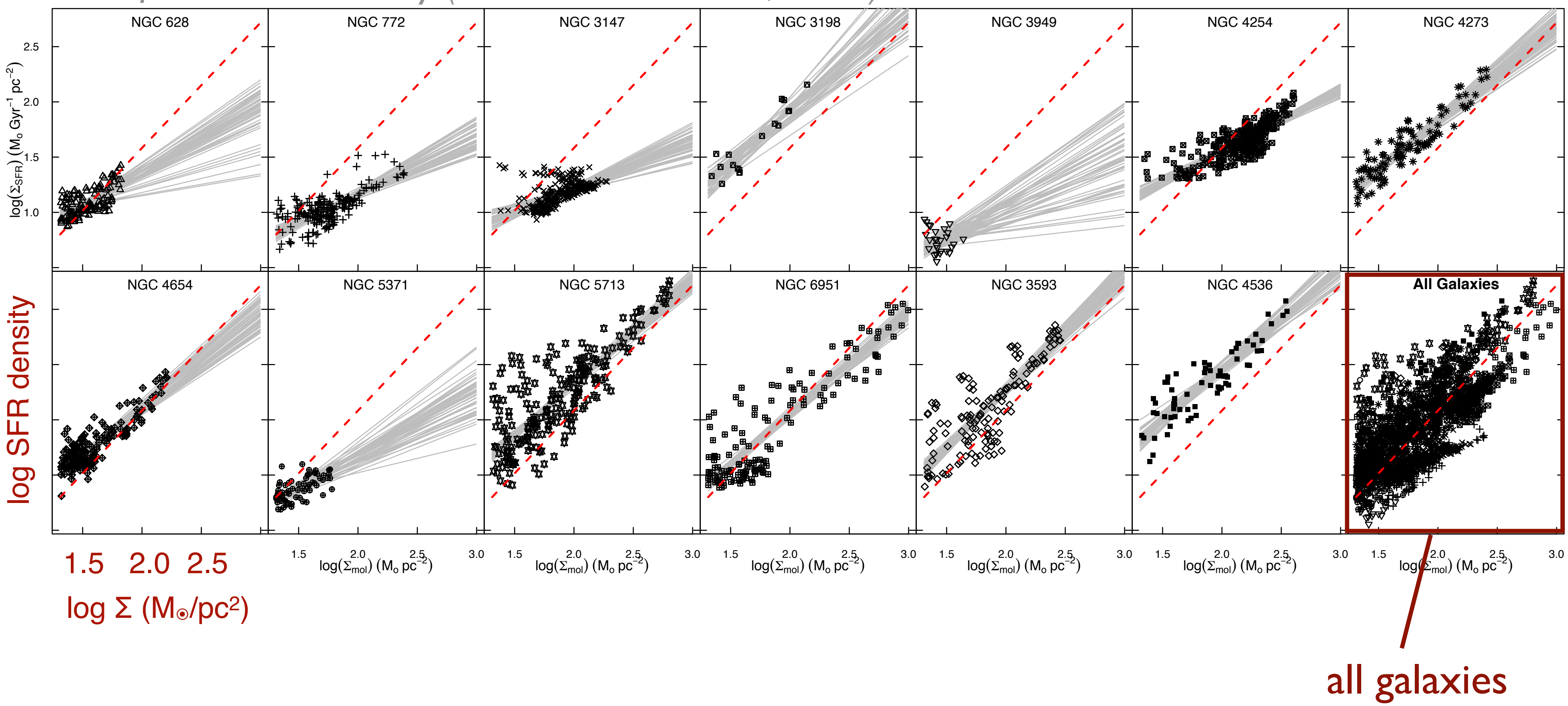

- QUIZ: do you see a universal
- ANSWER: - probably not
  - in addition, the relation often is sublinear

Shetty et al. (2014, MNRAS, 437, L61, see also Shetty, Kelly, Bigiel, 2013, MNRAS, 430, 288)

Hierarchical Bayesian models give more reliable estimates of the *slope* and the *intercept* of a power-law fit compared to least-square fits (or bisector fits).

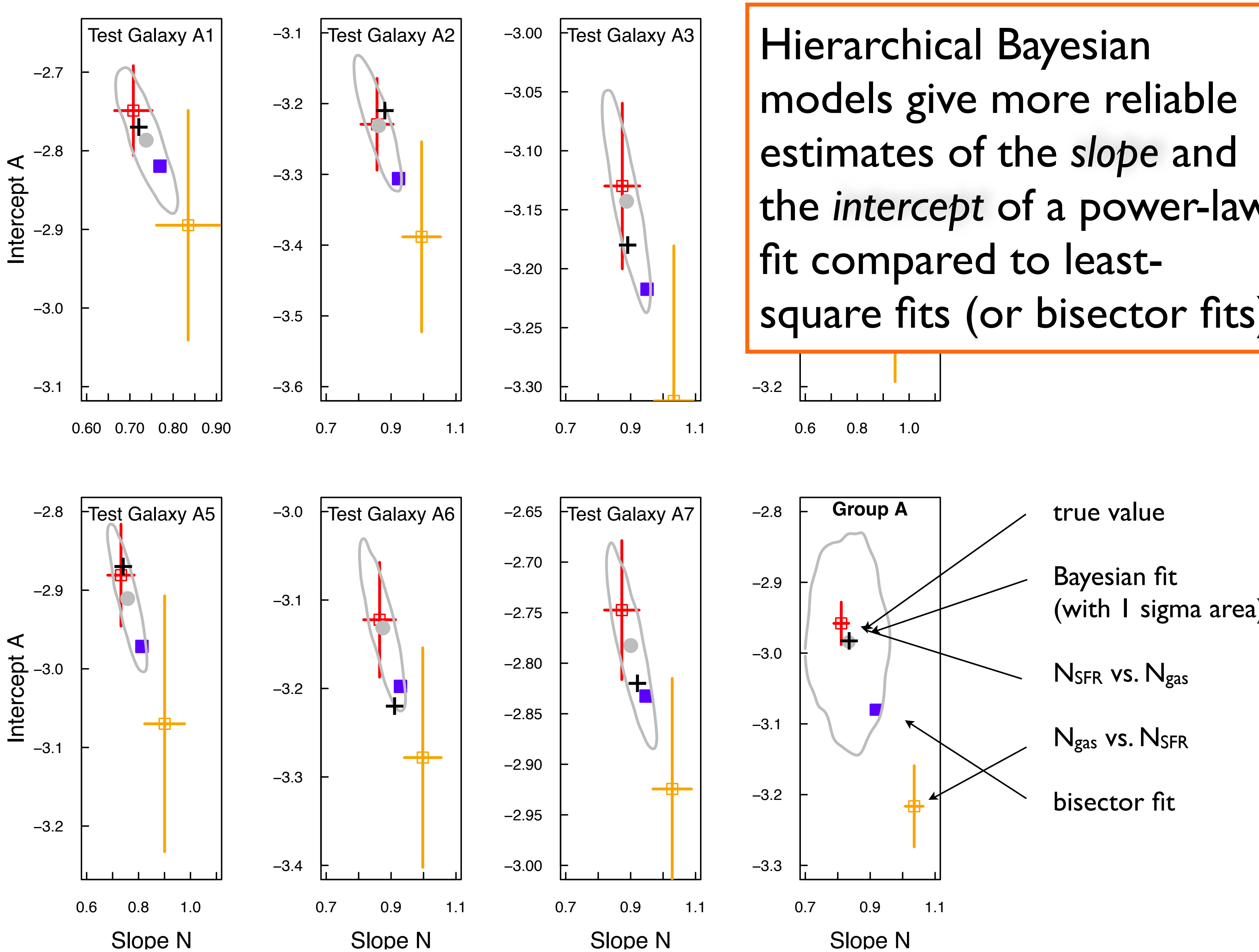

Figure 1. Slope and intercept of test galaxies in Group A. Black cross shows the true values. Red and orange squares show the OLS($\Sigma_{\rm SFR}|\Sigma_{\rm mol}$) and OLS($\Sigma_{\rm mol}|\Sigma_{\rm SFR}$) results, with their 1σ uncertainties, respectively. The gray circles indicate the estimate provided by the median of hierarchical Bayesian posterior result, and the contours mark the 1σ deviation. The filled blue squares mark the bisector estimates. The last panel on the bottom row shows the group parameters and fit estimates.

Shetty et al. (2013, MNRAS, 430, 288)

data from STING survey (Rahman et al. 2011, 2012)

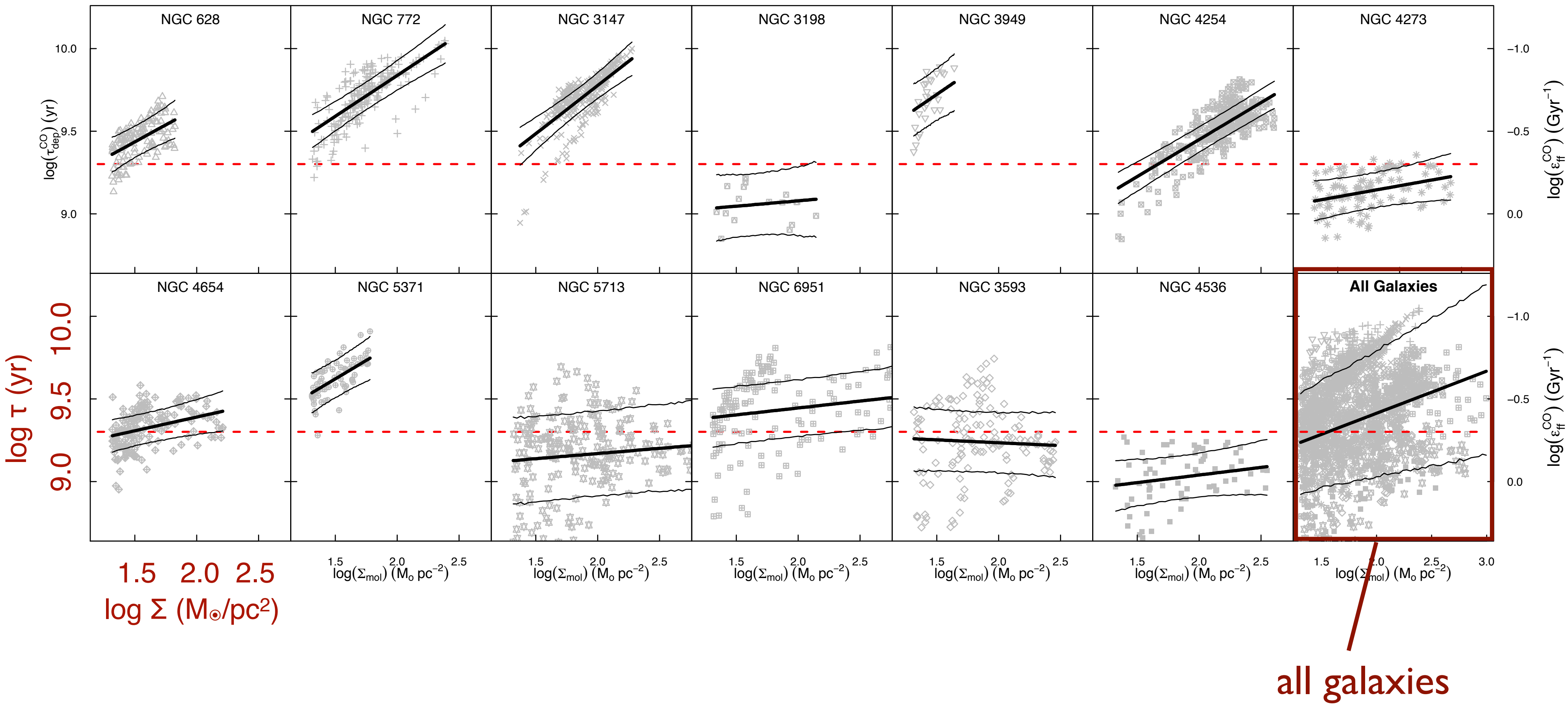

Hierarchical Bayesian model for STING galaxies indicate *varying depleting times.*

Shetty et al. (2014, MNRAS, 437, L61)

data from STING survey (Rahman et al. 2011, 2012)

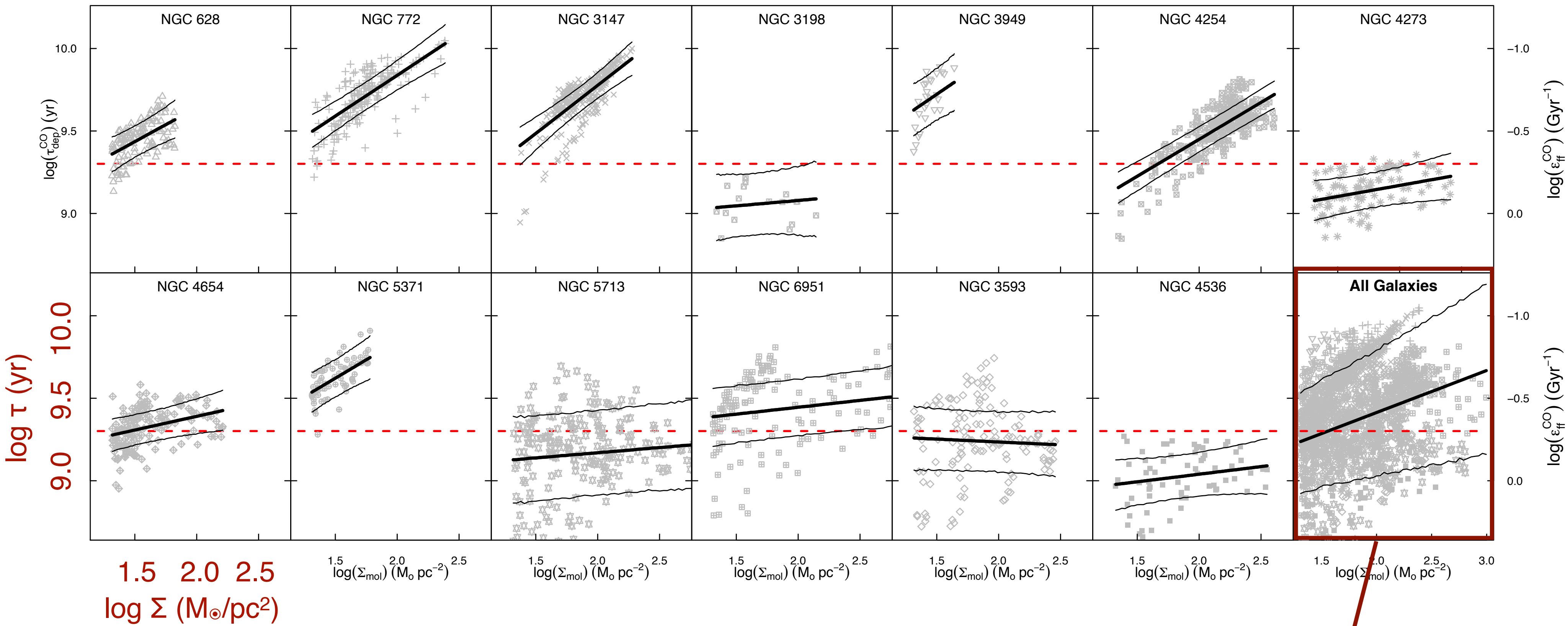

all galaxies

physical origin of this behavior?

- maybe strong shear in dense arms (example M51, Meidt et al. 2013)...
- maybe non-star forming H densities (recall H

Shetty et al. (2013, MNRAS, 437, L61, see also Shetty, Kelly, Bigiel, 2013, MNRAS, 430, 288)

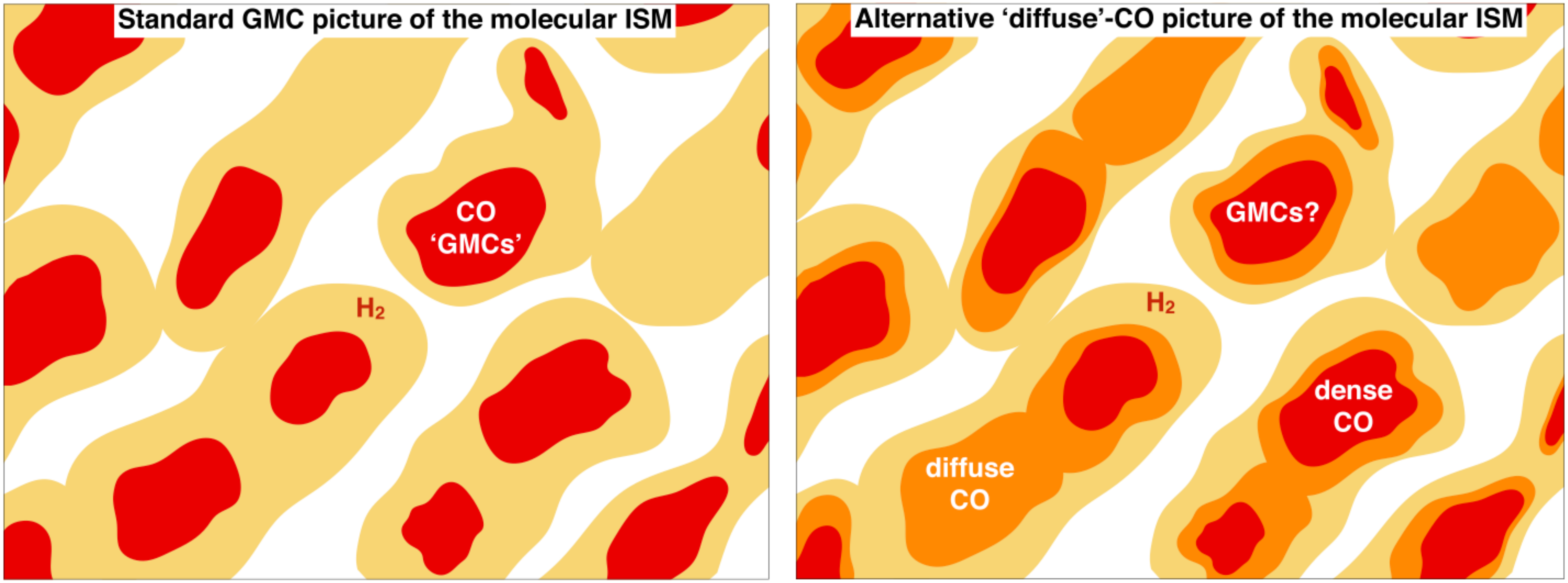

in addition:

- maybe a large fraction of H
  dense clouds, but in a diffuse state!

Shetty et al. (2014, MNRAS, 422, 2208)

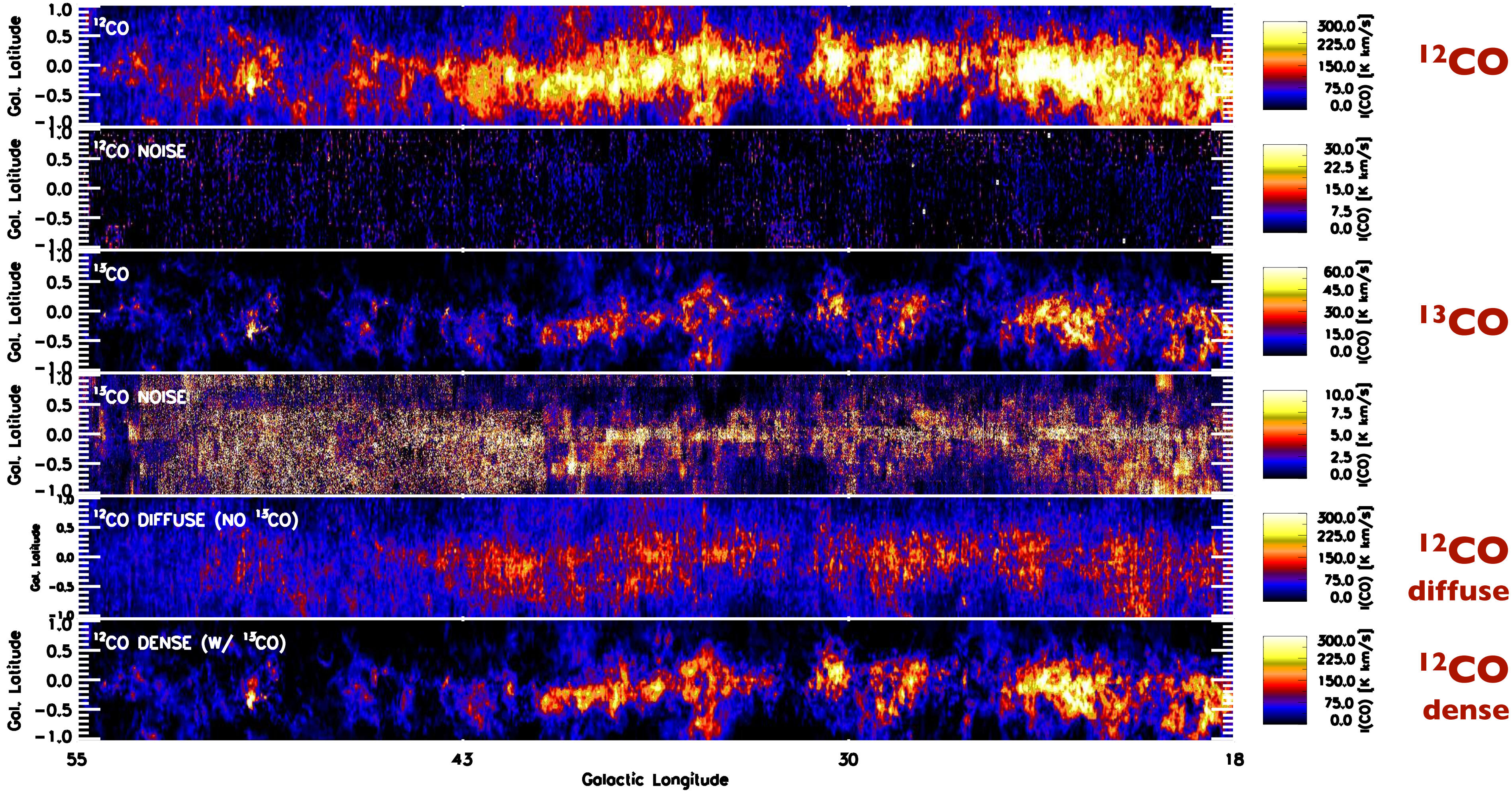

Galactic Ring Survey (GRS)

- comparison of
  tracing all the gas (including the more diffuse component)

Roman-Duval et al. (2015, in prep.)

data from STING survey (Rahman et al. 2011, 2012)

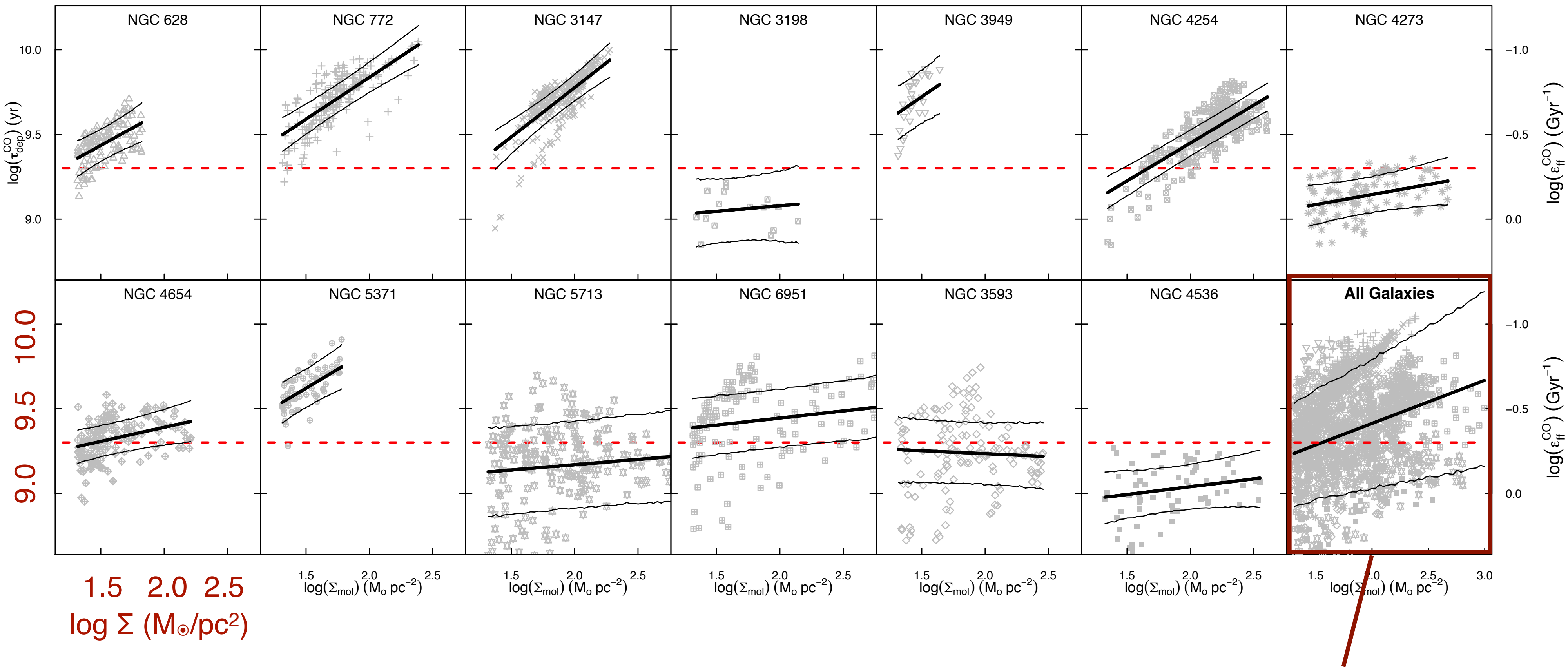

physical origin of this behavior?

- maybe strong shear in dense arms (example M51, Meidt et al. 2013)...
- ***maybe non-star forming H densities (recall H***

Shetty et al. (2013, MNRAS, 437, L61, see also Shetty, Kelly, Bigiel, 2013, MNRAS, 430, 288)

molecular cloud formation

molecular cloud formation

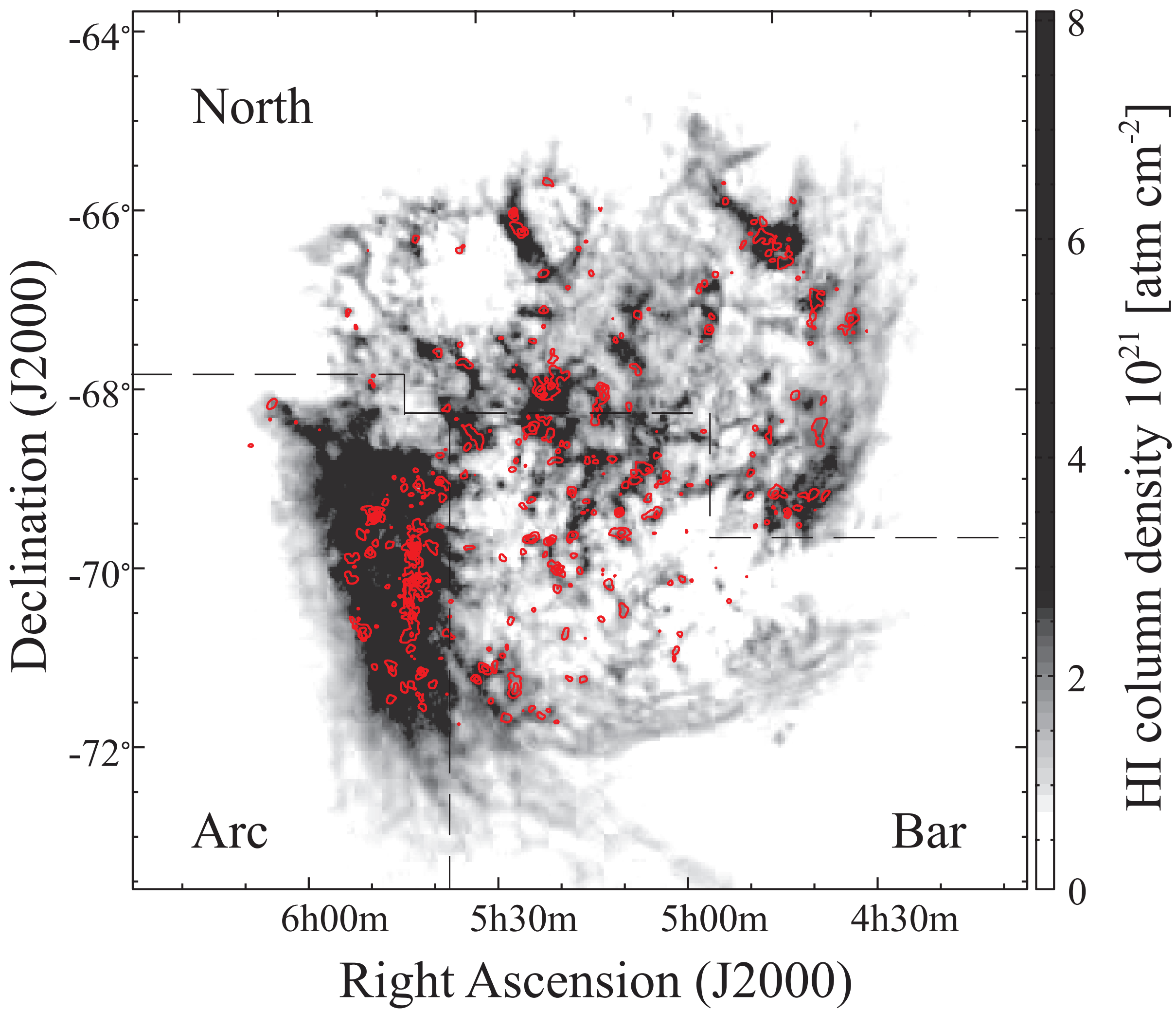

Idea:

Molecular clouds form at *stagnation points* of large-scale convergent flows, mostly triggered by global (or external) perturbations. Their internal turbulence is driven by accretion, i.e. by the process of cloud formation

- molecular clouds grow in mass
- this is inferred by looking at molecular clouds in different evolutionary phases in the LMC (Fukui et al. 2008, 2009)

Fukui et al. (2009)

zooming in ...

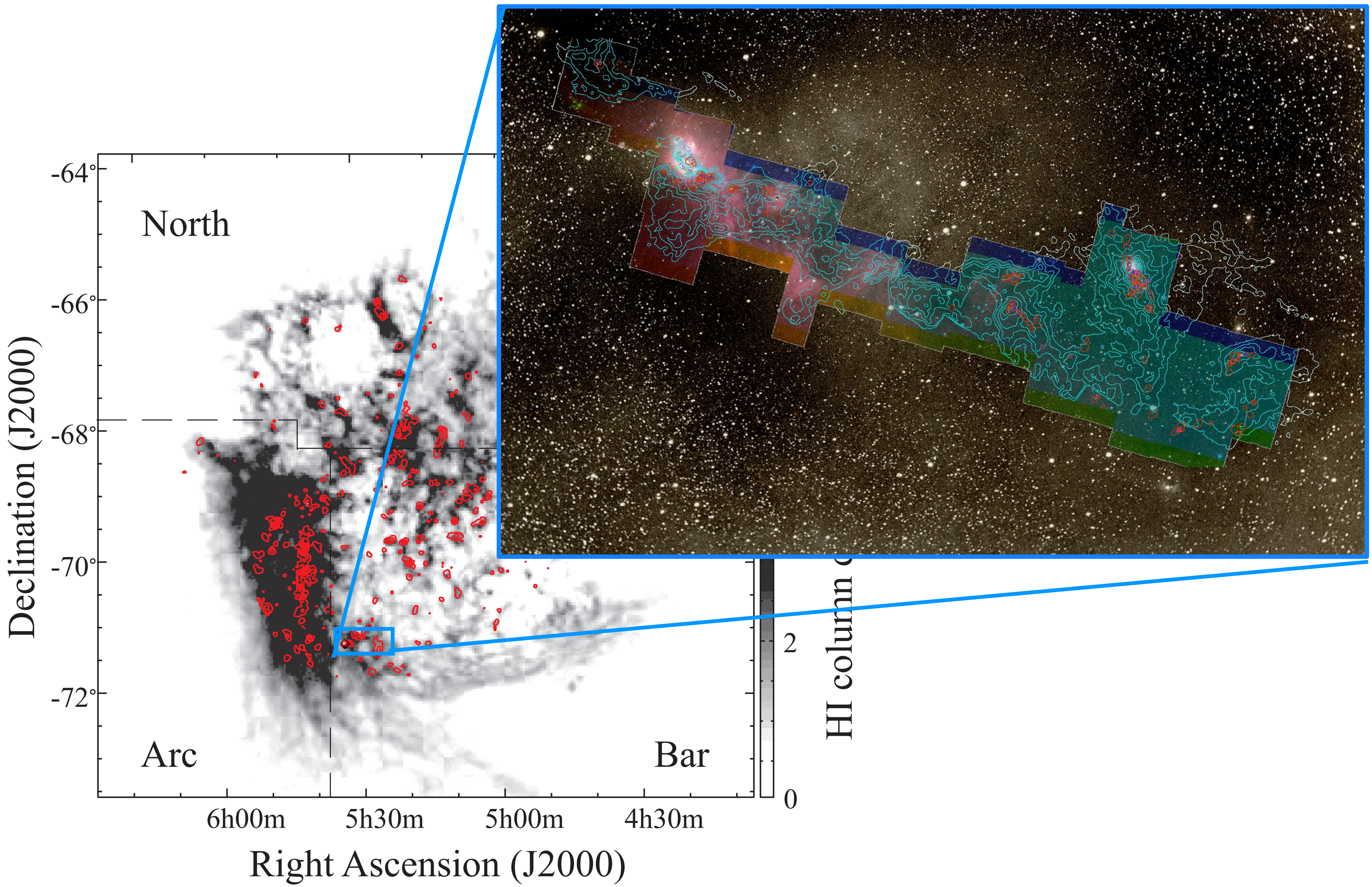

North
Arc
Bar
-64°
-66°
-68°
-70°
-72°
6h00m
5h30m
5h00m
4h30m
Declination (J2000)
Right Ascension (J2000)
HI column
2
0

position-position-velocity structure of the Perseus cloud

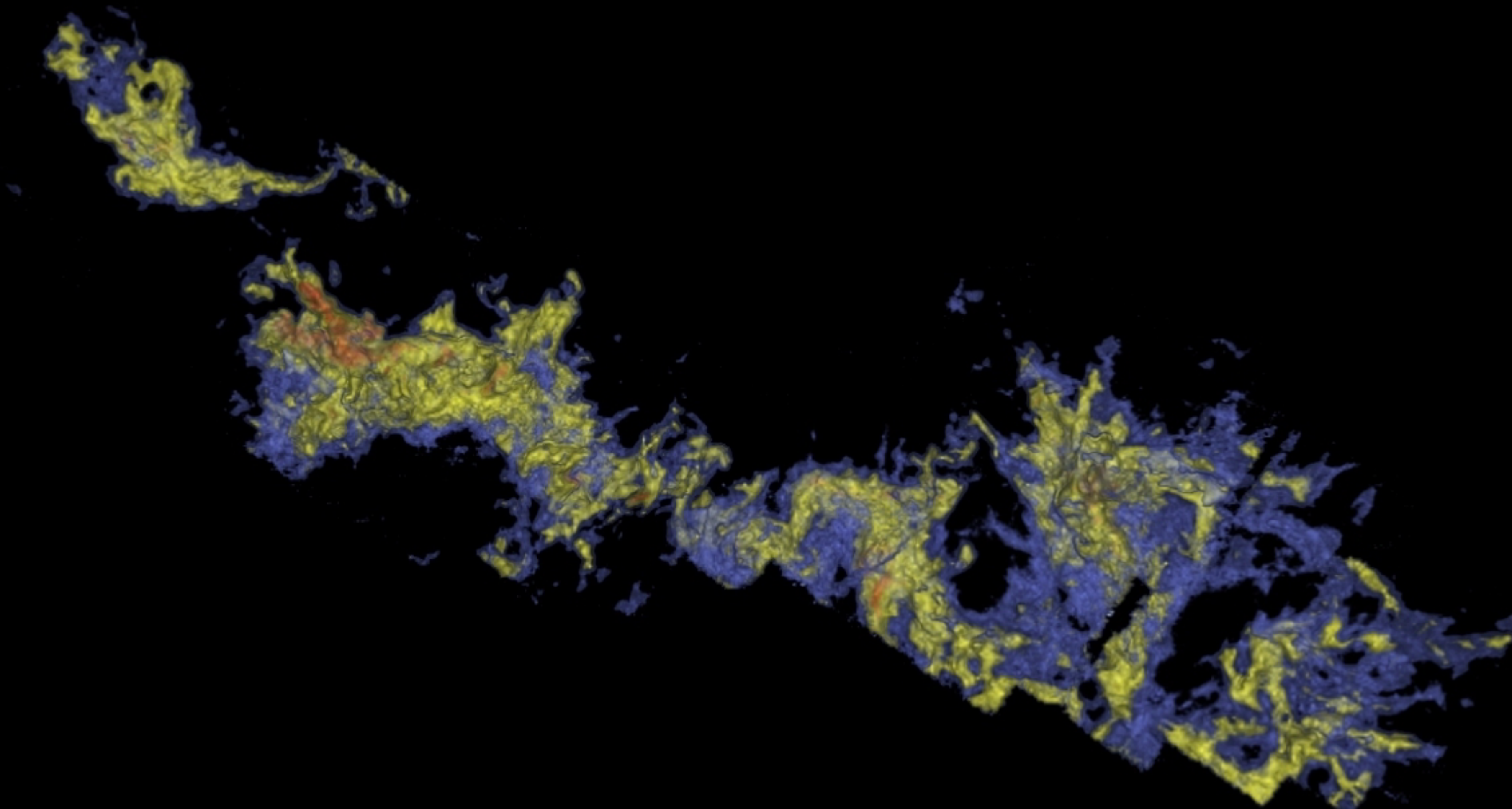

image from Alyssa Goodman: COMPLETE survey

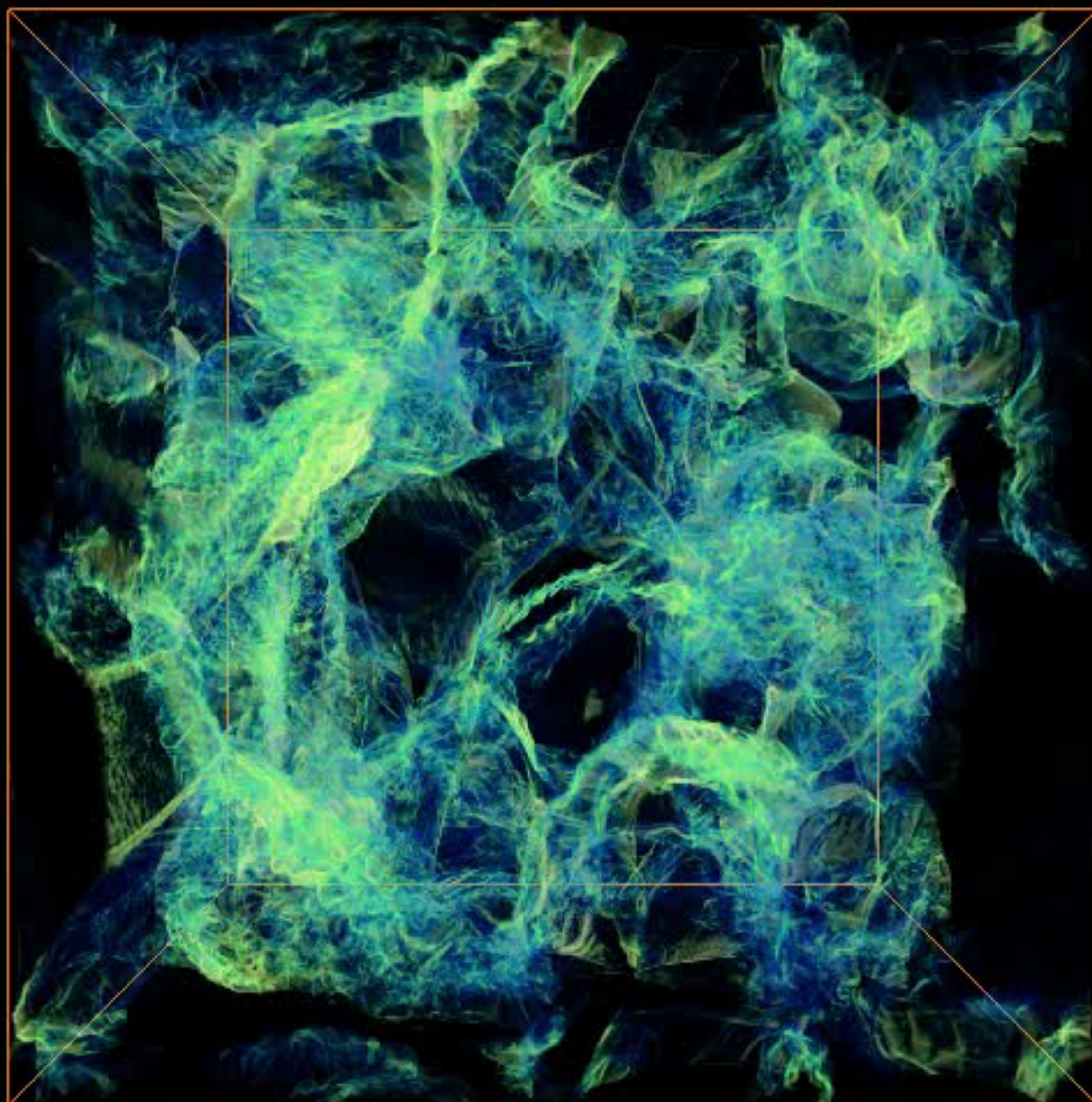

Schmidt et al. (2009, A&A, 494, 127)

caveat of numerical simulations

- most astrophysical turbulence simulations use an ***LES*** approach to model the flow
- principal problem: only large scale flow properties
  - Reynolds number: Re = LV/ν ***($Re_{nature} >> Re_{model}$)***
  - dynamic range much smaller than true physical one
  - need *subgrid model* (often only dissipation)
  - but what to do for more complex when processes on subgrid scale determine large-scale dynamics (chemical reactions, nuclear burning, etc)
  - Turbulence is "space filling" --> difficulty for AMR (don't know what criterion to use for refinement)
- how *large* a Reynolds number do we need to catch basic dynamics right?

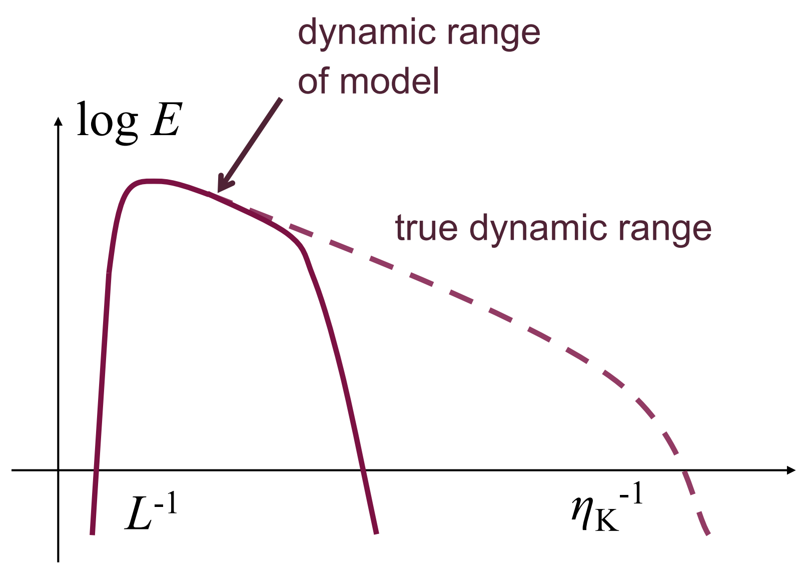

including detailed chemistry

experimental set-up

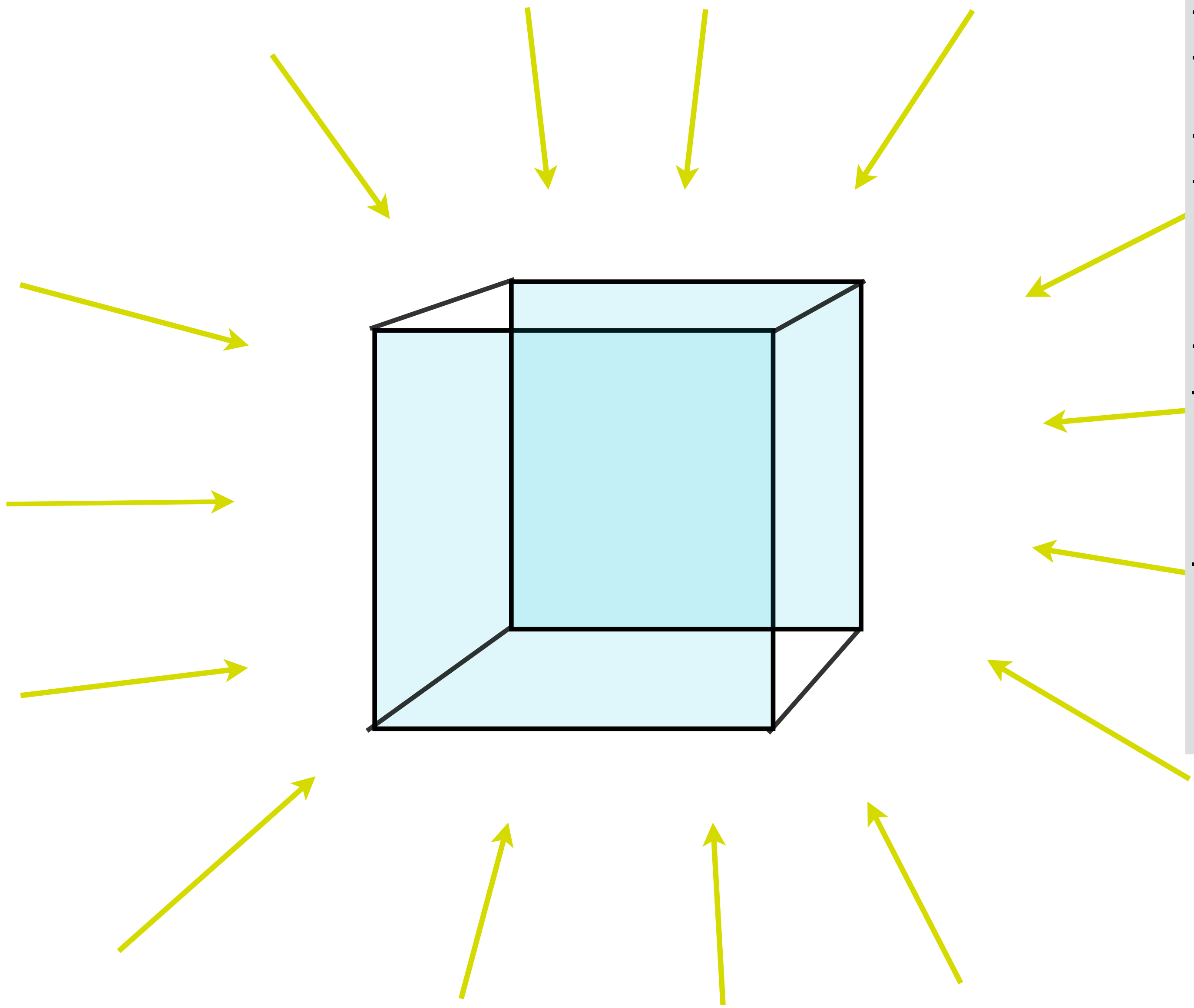

- Arepo and FLASH
- stochastic forcing
  (Ornstein-Uhlenbeck)
- self-gravity
- time-dependent chemistry
  (DVODE, standard variable-coefficient ordinary differential equation solver)
- cooling & heating processes
- gives you mathematically well defined boundary conditions
  --> good for statistical studies
- gives external radiation with TreeCol (a new approximative scheme to calculate column densities from the gravity solver)

chemical model 0

- 32 chemical species
  - 17 in instantaneous equilibrium:

H^-, H_2^+, H_3^+, CH^+, CH_2^+, OH^+, H_2O^+, H_3O^+, CO^+, HOC^+, O^-, C^- and O_2^+

  - 19 full non-equilibrium evolution

e^-, H^+, H, H_2, He, He^+, C, C^+, O, O^+, OH, H_2O, CO,

C_2, O_2, HCO^+, CH, CH_2 and CH_3^+

- 218 reactions
- various heating and cooling processes

long series of publications by Simon Glover and collaborators, e.g. Glover & Mac Low (2007ab), Glover, Federrath, Mac Low, Klessen (2010), Glover & Clark (2012, 2013), Clark & Clover (2012, 2013)

chemical model 1

Process	Reference(s)
Cooling:	
C fine structure lines	Atomic data – Silva & Viegas (2002)
	Collisional rates (H) – Abrahamsson, Krems & Dalgarno (2007)
	Collisional rates (H_2) – Schroder et al. (1991)
	Collisional rates (e^-) – Johnson et al. (1987)
	Collisional rates (H^+) – Roueff & Le Bourlot (1990)
C^+ fine structure lines	Atomic data – Silva & Viegas (2002)
	Collisional rates (H_2) – Flower & Launay (1977)
	Collisional rates (H, $T < 2000$ K) – Hollenbach & McKee (1989)
	Collisional rates (H, $T > 2000$ K) – Keenan et al. (1986)
	Collisional rates (e^-) – Wilson & Bell (2002)
O fine structure lines	Atomic data – Silva & Viegas (2002)
	Collisional rates (H) – Abrahamsson, Krems & Dalgarno (2007)
	Collisional rates (H_2) – see Glover & Jappsen (2007)
	Collisional rates (e^-) – Bell, Berrington & Thomas (1998)
	Collisional rates (H^+) – Pequignot (1990, 1996)
H_2 rovibrational lines	Le Bourlot, Pineau des Forêts & Flower (1999)
CO and H_2O rovibrational lines	Neufeld & Kaufman (1993); Neufeld, Lepp & Melnick (1995)
OH rotational lines	Pavlovski et al. (2002)
Gas-grain energy transfer	Hollenbach & McKee (1989)
Recombination on grains	Wolfire et al. (2003)
Atomic resonance lines	Sutherland & Dopita (1993)
H collisional ionization	Abel et al. (1997)
H_2 collisional dissociation	See Table B1
Compton cooling	Cen (1992)
Heating:	
Photoelectric effect	Bakes & Tielens (1994); Wolfire et al. (2003)
H_2 photodissociation	Black & Dalgarno (1977)
UV pumping of H_2	Burton, Hollenbach & Tielens (1990)
H_2 formation on dust grains	Hollenbach & McKee (1989)
Cosmic ray ionization	Goldsmith & Langer (1978)

(Glover, Federrath, Mac Low, Klessen, 2010, MNRS, 404, 2)

chemical model 2

No.	Reaction	Rate coefficient	Ref.
88	$H_2 + He^+ \rightarrow He + H_2^+$	$k_{88} = 7.2 \times 10^{-15}$	63
89	$H_2 + He^+ \rightarrow He + H + H^+$	$k_{89} = 3.7 \times 10^{-14} \exp\left(\frac{35}{T}\right)$	63
90	$CH + H^+ \rightarrow CH^+ + H$	$k_{90} = 1.9 \times 10^{-9}$	28
91	$CH_2 + H^+ \rightarrow CH_2^+ + H$	$k_{91} = 1.4 \times 10^{-9}$	28
92	[illegible]	[illegible]	28
93	[illegible]	[illegible]	28
94	$OH + H^+ \rightarrow OH^+ + H$	$k_{94} = 2.1 \times 10^{-9}$	28
95	$OH + He^+ \rightarrow O^+ + He + H$	$k_{95} = 1.1 \times 10^{-9}$	28
96	$H_2O + H^+ \rightarrow H_2O^+ + H$	$k_{96} = 6.9 \times 10^{-9}$	64
97	$H_2O + He^+ \rightarrow OH + He + H^+$	$k_{97} = 2.04 \times 10^{-10}$	65

Table B2. List of photochemical reactions included in our chemical model

No.	Reaction	Optically thin rate (s^{-1})	γ	Ref.
166	$H^- + \gamma \rightarrow H + e^-$	$R_{166} = 7.1 \times 10^{-7}$	0.5	1
167	$H_2^+ + \gamma \rightarrow H + H^+$	$R_{167} = 1.1 \times 10^{-9}$	1.9	2
168	$H_2 + \gamma \rightarrow H + H$	$R_{168} = 5.6 \times 10^{-11}$	See §2.2	3
169	$H_3^+ + \gamma \rightarrow H_2 + H^+$	$R_{169} = 4.9 \times 10^{-13}$	1.8	4
170	$H_3^+ + \gamma \rightarrow H_2^+ + H$	$R_{170} = 4.9 \times 10^{-13}$	2.3	4
171	$C + \gamma \rightarrow C^+ + e^-$	[illegible]	[illegible]	[illegible]
172	$C^- + \gamma \rightarrow$ …			
173	$CH + \gamma \rightarrow$ …			
174	$CH + \gamma \rightarrow$ …			
175	$CH^+ + \gamma$ …			
176	$CH_2 + \gamma$ …			
177	$CH_2 + \gamma$ …			
178	$CH_2^+ + \gamma$ …			
179	$CH_3^+ + \gamma$ …			
180	$CH_3^+ + \gamma$ …			
181	$C_2 + \gamma \rightarrow$ …			
182	$O^- + \gamma \rightarrow$ …			
183	$OH + \gamma \rightarrow$ …			
184	$OH + \gamma \rightarrow$ …			
185	$OH^+ + \gamma$ …			
186	$H_2O + \gamma$ …			
187	$H_2O + \gamma$ …			
188	$H_2O^+ +$ …			
189	$H_2O^+ +$ …			
190	$H_2O^+ +$ …			
191	$H_2O^+ +$ …			
192	$H_3O^+ +$ …			
193	$H_3O^+ +$ …			
194	$H_3O^+ +$ …			
195	$H_3O^+ +$ …			
196	$O_2 + \gamma \rightarrow$ …			
197	$O_2 + \gamma \rightarrow O + O$	$R_{197} = 7.0 \times 10^{-10}$	1.8	7
198	$CO + \gamma \rightarrow C + O$	$R_{198} = 2.0 \times 10^{-10}$	See §2.2	13

Table B3. List of reactions included in our chemical model that involve cosmic rays or cosmic-ray induced UV emission

No.	Reaction	Rate ($s^{-1}\zeta_H^{-1}$)	Ref.
199	$H + c.r. \rightarrow H^+ + e^-$	$R_{199} = 1.0$	—
200	$He + c.r. \rightarrow He^+ + e^-$	$R_{200} = 1.1$	1
201	$H_2 + c.r. \rightarrow H^+ + H + e^-$	$R_{201} = 0.037$	1
202	$H_2 + c.r. \rightarrow H + H$	$R_{202} = 0.22$	1
203	$H_2 + c.r. \rightarrow H^+ + H^-$	$R_{203} = 6.5 \times 10^{-4}$	1
204	$H_2 + c.r. \rightarrow H_2^+ + e^-$	$R_{204} = 2.0$	1
205	$C + c.r. \rightarrow C^+ + e^-$	$R_{205} = 3.8$	1
206	$O + c.r. \rightarrow O^+ + e^-$	$R_{206} = 5.7$	1
207	$CO + c.r. \rightarrow CO^+ + e^-$	$R_{207} = 6.5$	1
208	$C + \gamma_{c.r.} \rightarrow C^+ + e^-$	$R_{208} = 2800$	2
209	$CH + \gamma_{c.r.} \rightarrow C + H$	$R_{209} = 4000$	3
210	$CH^+ + \gamma_{c.r.} \rightarrow C^+ + H$	$R_{210} = 960$	3
211	$CH_2 + \gamma_{c.r.} \rightarrow CH_2^+ + e^-$	$R_{211} = 2700$	1
212	$CH_2 + \gamma_{c.r.} \rightarrow CH + H$	$R_{212} = 2700$	1
213	$C_2 + \gamma_{c.r.} \rightarrow C + C$	$R_{213} = 1300$	3
214	$OH + \gamma_{c.r.} \rightarrow O + H$	$R_{214} = 2800$	3
215	$H_2O + \gamma_{c.r.} \rightarrow OH + H$	$R_{215} = 5300$	3
216	$O_2 + \gamma_{c.r.} \rightarrow O + O$	$R_{216} = 4100$	3
217	$O_2 + \gamma_{c.r.} \rightarrow O_2^+ + e^-$	$R_{217} = 640$	3
218	$CO + \gamma_{c.r.} \rightarrow C + O$	$R_{218} = 0.21 T^{1/2} x_{H_2} x_{CO}^{-1/2}$	4

(Glover, Federrath, Mac Low, Klessen, 2010, MNRS, 404, 2)

effects of chemistry

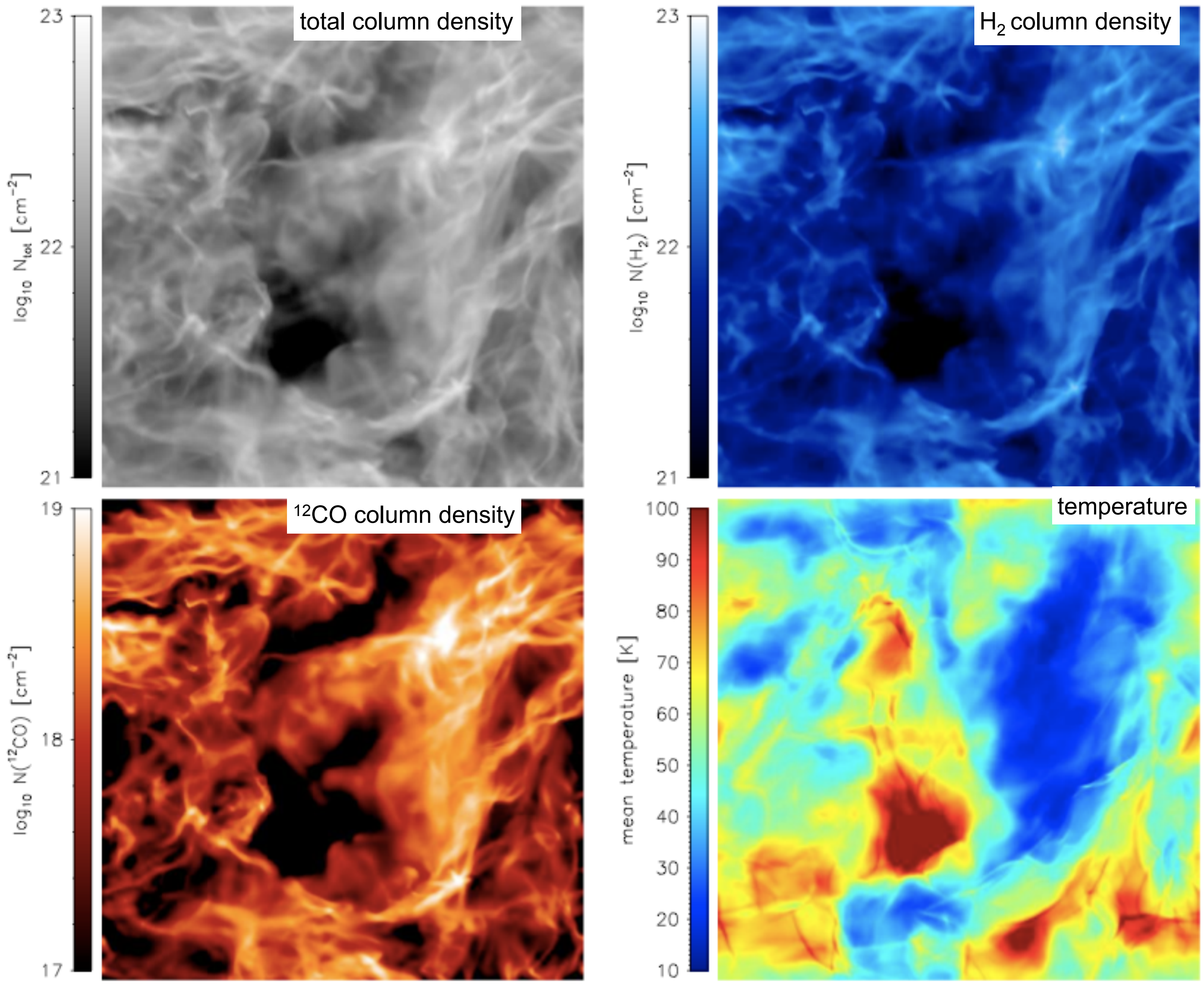

(Glover et al. 2010)

effects of chemistry

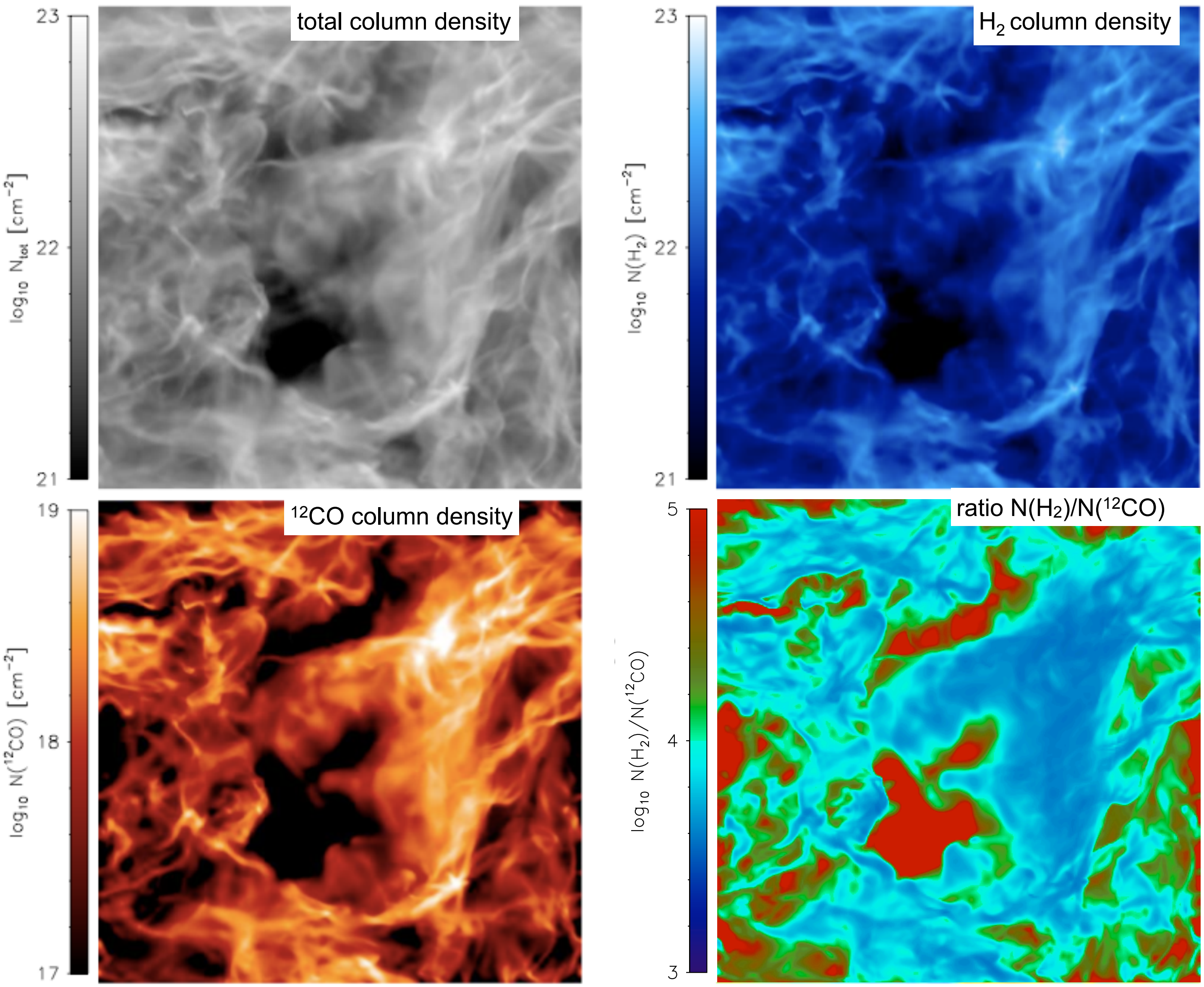

(Glover et al. 2010)

Xco factor

x-factor

- conversion rate between H_2 column density and CO emission (equivalent width W)

$$X = \frac{N_{\mathrm{H}_2}}{W} \ (\mathrm{cm}^{-2}\,\mathrm{K}^{-1}\,\mathrm{km}^{-1}\,\mathrm{s})$$

- most mass H_2 determinations depend on X*!*
- in Milky Way X ~ few x 10^{22} cm^{-2} K^{-1} km^{-1} s ~ const.
- why is it constant?
- how does it vary with environmental condition?
  - metallicity
  - density, radiation field, etc.
    ("normal" gal. vs star burst)

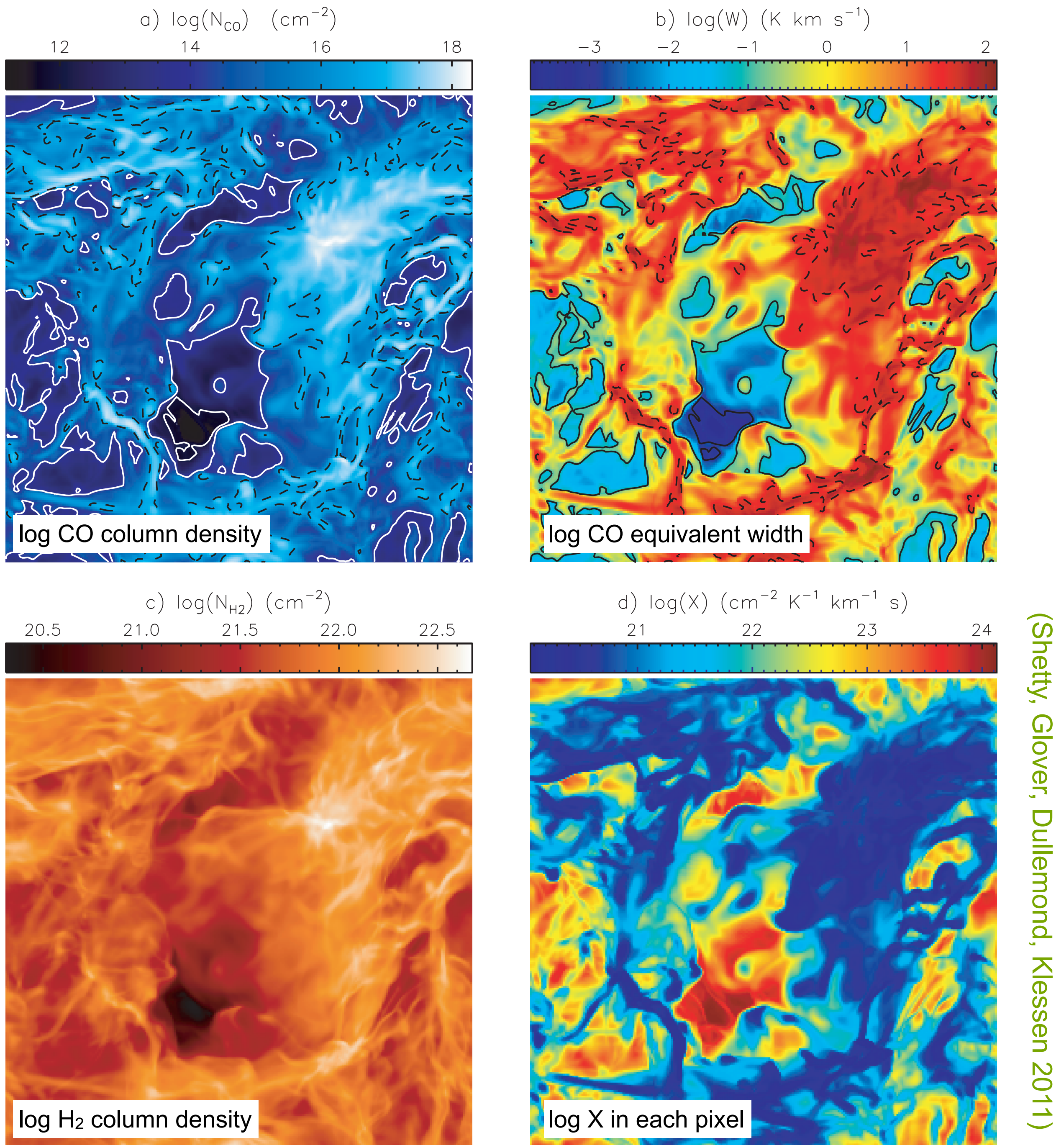

Figure 4. Images of (a) N_{CO}, (b) W, (c) N_{H_2} and (d) the X factor of model n300-Z03. Each side has a length of 20 pc. In (a) and (b), solid contours indicate $\log(N_{CO}) = 12, 14$ and $\log(W) = -3, -1$; dashed contours are $\log(N_{CO}) = 16.5$ and $\log(W) = 1.5$ (see the text and Fig. 2d).

detailed analysis of typical Galactic model cloud: solar metallicity and mean density 300 cm^{-3}

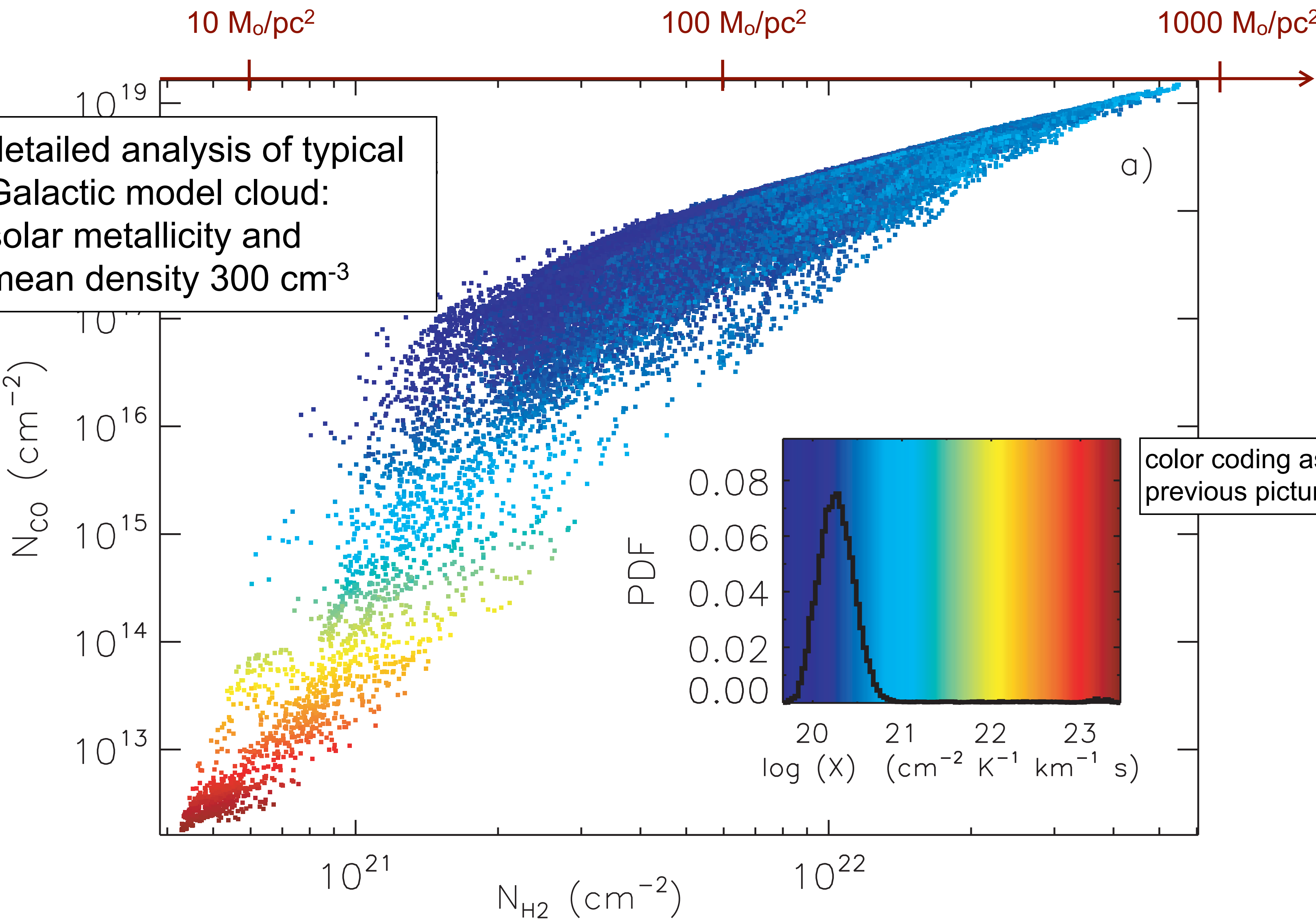

color coding as in previous picture

(Shetty, Glover, Dullemond, Klessen 2011)

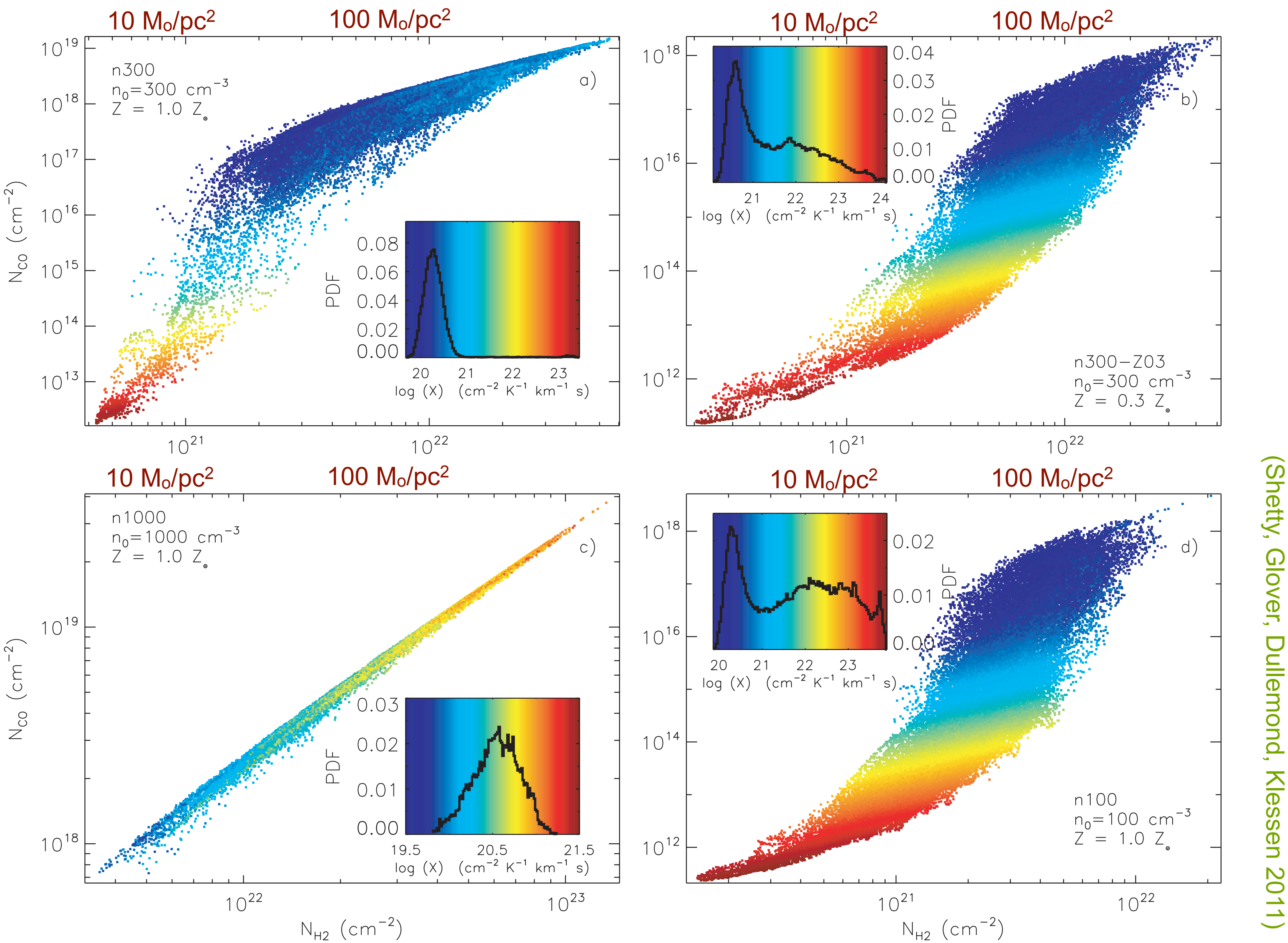

Figure 5. X factor for four models. $N_{\rm CO}$ is plotted as a function of $N_{\rm H_2}$. The colour of each point indicates the X factor. Inset figures show the colour scale and PDF of the X factor. The corresponding maps of $N_{\rm H_2}$, $N_{\rm CO}$ and the X factor from model n300-Z03 are shown in Fig. 4.

observed x-factor

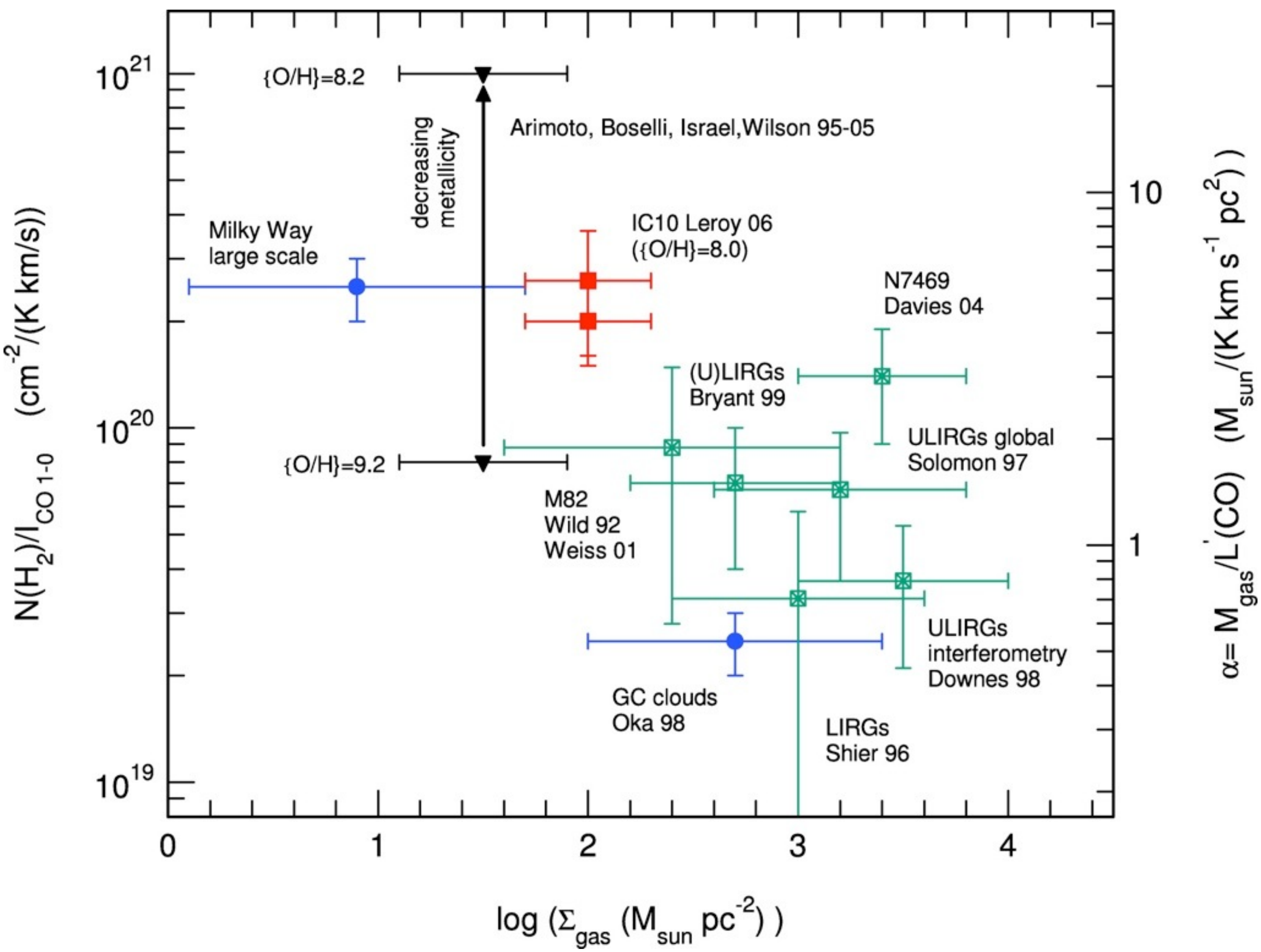

Tacconi et al. (2008)

derived x-factor

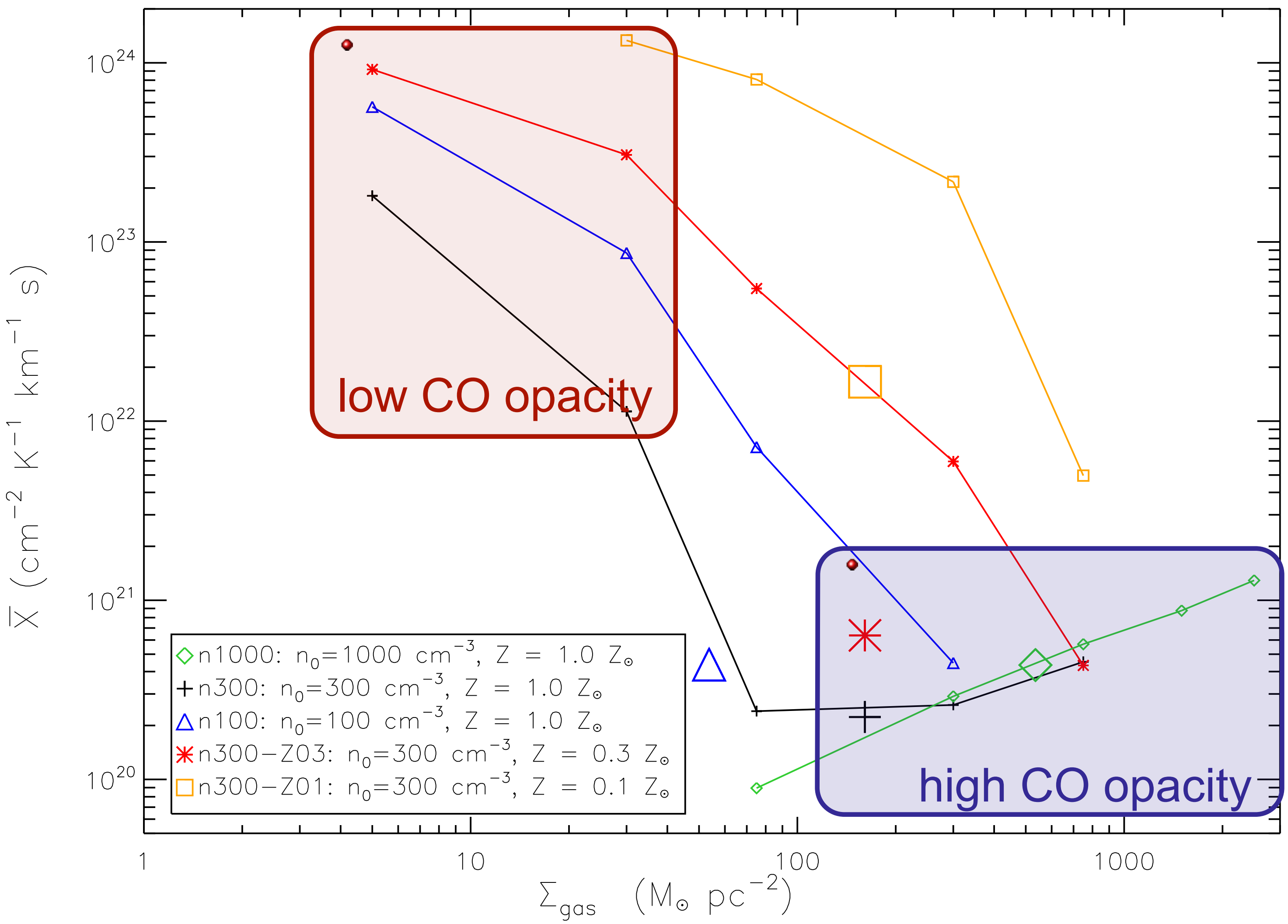

(Shetty, Glover, Dullemond, Klessen, MNRAS, 2011)

^{12}CO / ^{13}CO ratio

CO chemistry in GMCs

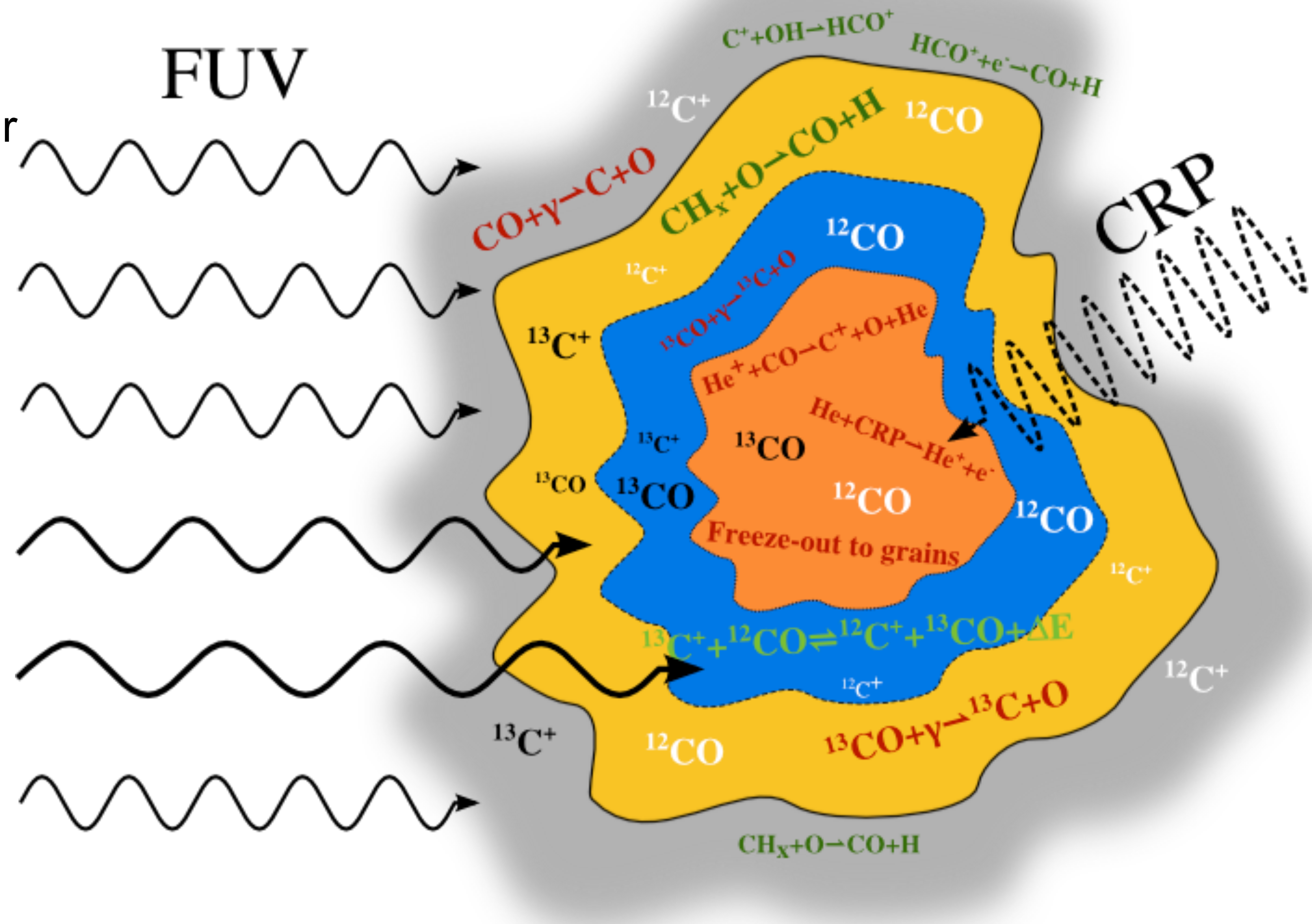

Based on van Dishoeck & Black (1988)

Non-isotope selective reactions

$C^+ + OH \rightarrow HCO^+$ $HCO^+ + e^- \rightarrow H + CO$ $CH_x + O \rightarrow CO + H_x$	**Production**
$He + CRP \rightarrow He^+ + e^-$ $He^+ + CO \rightarrow C^+ + O + He$	**Destruction**
Accretion to grains	**Depletion**

I. Diffuse region ($A_v < 0.5^m$)

$CO + \gamma \rightarrow C + O$

II. Translucent region ($1^m < A < 2^m$)

a) **preferential ^{13}CO photo-dissociation**

b) **Fractionation reaction**

$^{12}CO + ^{13}C \leftarrow\rightarrow ^{13}CO + ^{12}C + 36K$

III. Dense core ($A_v \approx 5^m$)

C^+ depletes

Freeze-out & CRP destruction

Hydrodynamic simulation setup

- GADGET 2 (Springel 2005) – SPH
- **Chemical network** including reactions with H, C and O
  Nelson & Langer (1999)
- Fractionation and photo-dissociation of ^{13}CO
- **TreeCol** for attenuation of ISRF: ^{12}CO, ^{13}CO self- and H_2 shielding
  Clark et al. (2012)
- Self gravity→**Sink particles**
- CO freeze-out not included
- Initial abundances: fully molecular (H_2 but no CO), $^{12}C/^{13}C = 60$

Model	n_0 [cm^{-3}]	Metallicity [$Z_\odot$]	ISRF [G_0]	Time [Myr]
a	300	0.3	1	2.046
b	300	0.6	1	1.930
c	300	1	0.1	2.124
d	300	1	1	2.150
e	300	1	10	2.022
f	1000	1	1	0.973

Results – $N(^{12}CO)/N(^{13}CO)$ column densities ratio

N_0 = 300 cm^{-3}
ISRF = 1 G_0
Z = 1 $Z_\odot$
Before first sink particle forms

White contour shows 5×10^{21} cm^{-2}

Around the $^{12}C/^{13}C$ ratio

$\langle\rho\rangle \approx 10^{-20}$ g cm^{-3}
$\langle Av\rangle > 1.5^m$
$\langle Tgas\rangle \approx 15$ K

Chemical fractionation

$\langle\rho\rangle \approx 10^{-21}$ g cm^{-3}
$\langle Av\rangle \approx 1^m$
$\langle Tgas\rangle \approx 20$ K

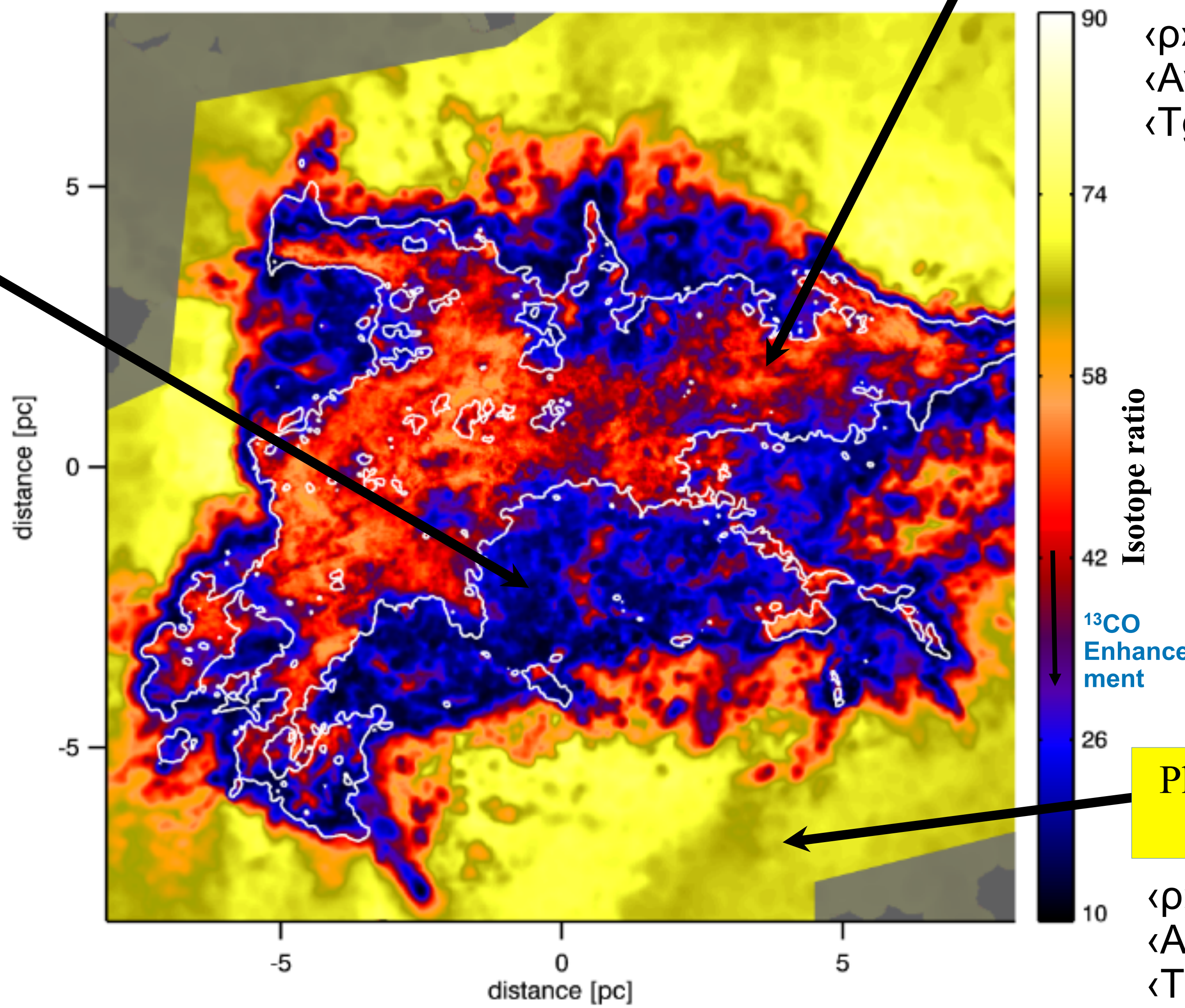

Photo-dissociation dominates

$\langle\rho\rangle \approx 10^{-22}$ g cm^{-3}
$\langle Av\rangle << 1^m$
$\langle Tgas\rangle \approx 40$ K

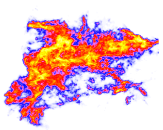

Results – N(^{12}CO)/N(^{13}CO) column densities ratio

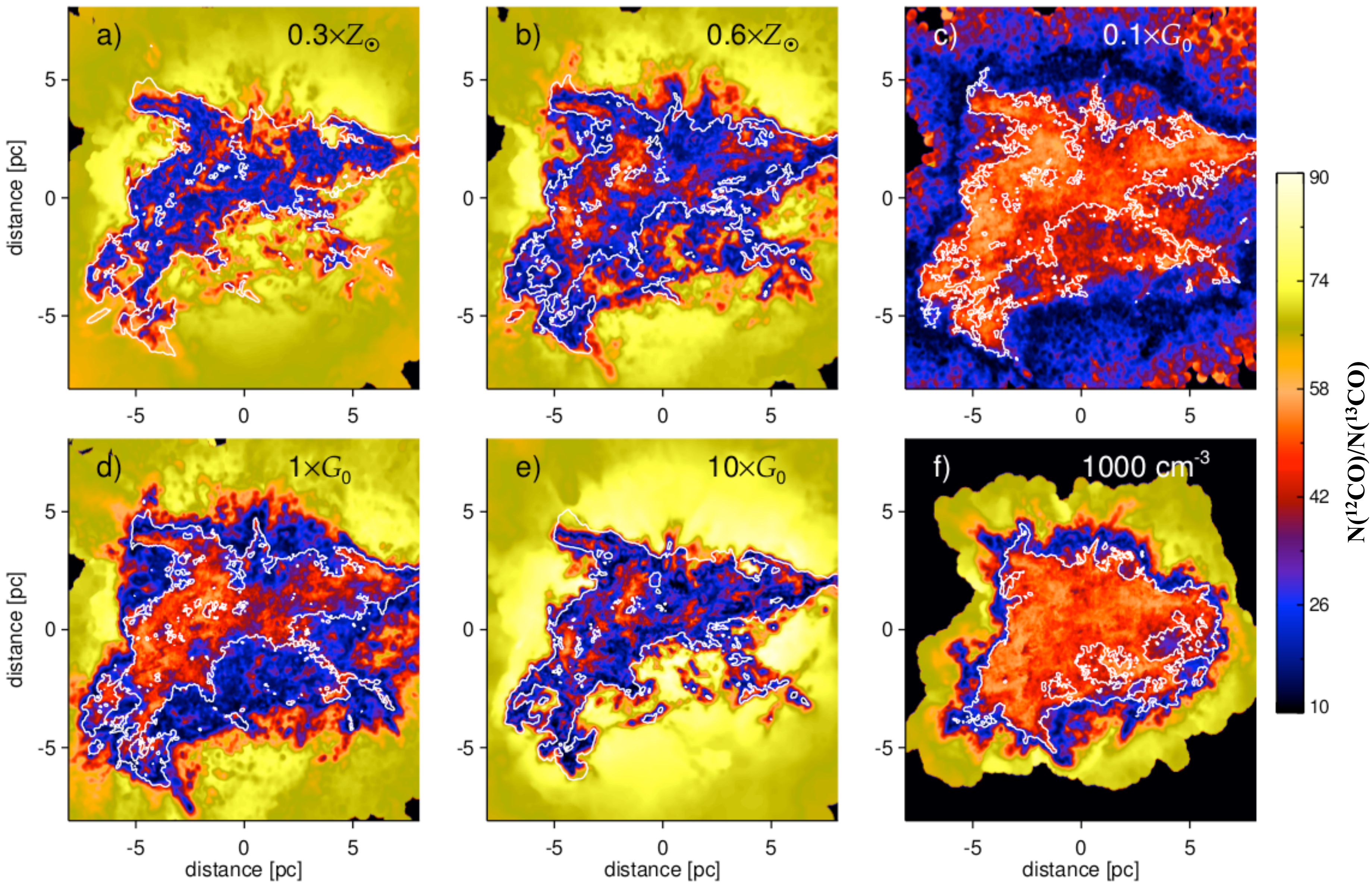

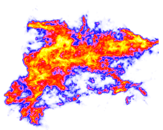

White contour shows 5×10^{21} cm^{-2} → overall density is not changing significantly

Results – N(^{12}CO)/N(^{13}CO) column densities ratio

r

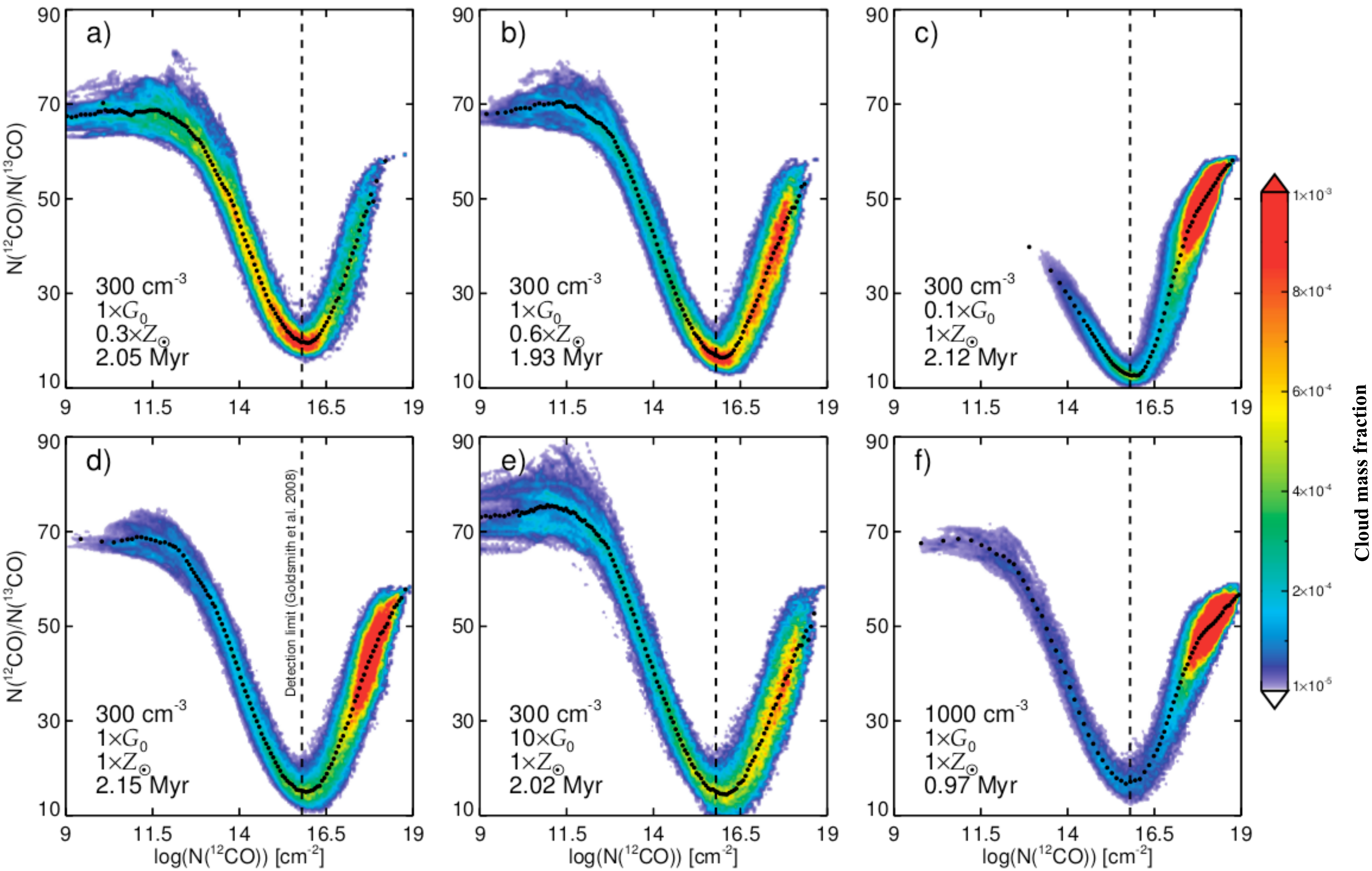

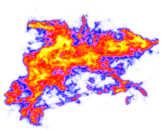

Fitting formula

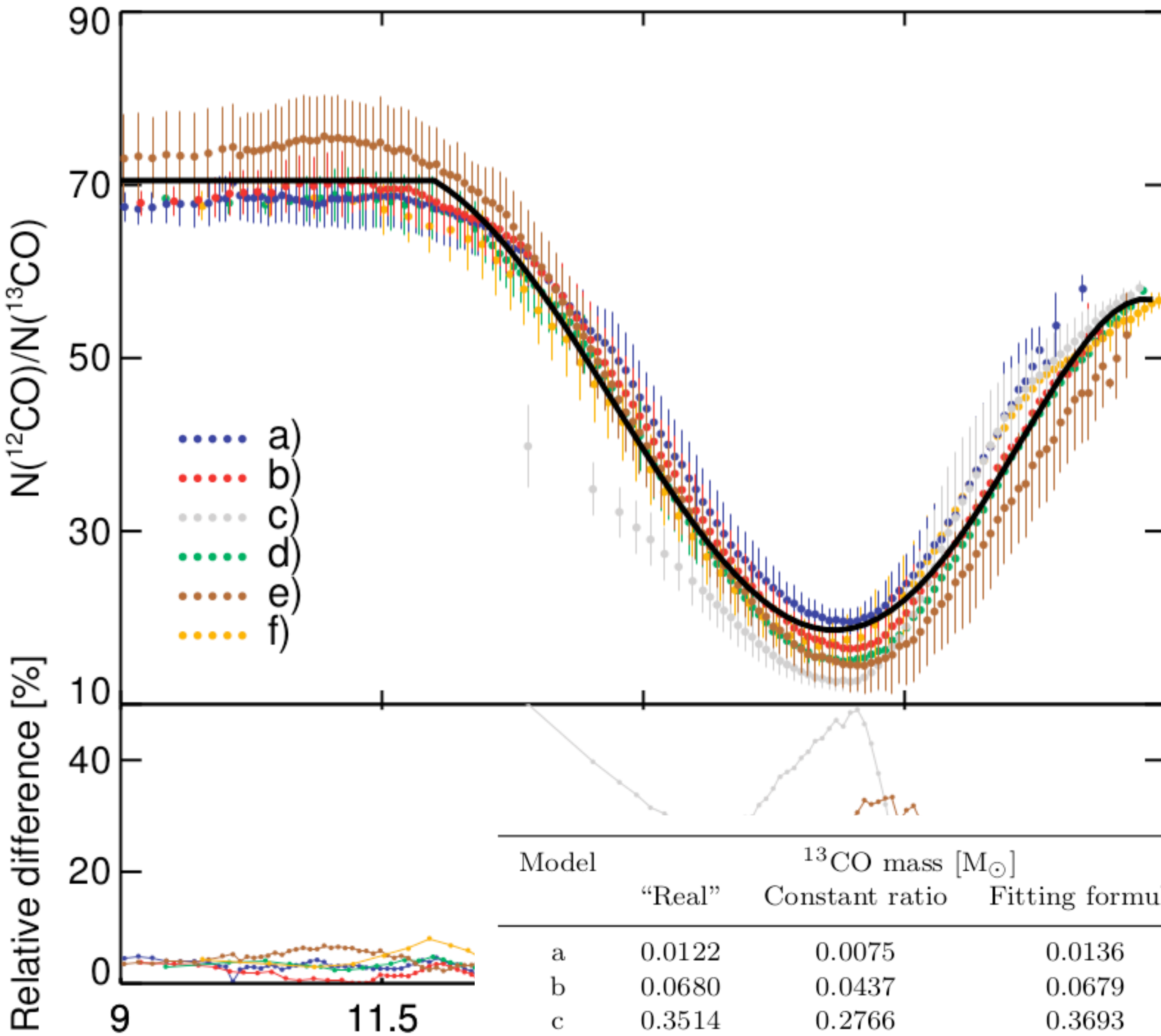

5th order polynomial

Model (c) excluded

Bellow 10^{12} cm^{-2} constant

Above 10^{19} cm^{-2} eq. 60

Model	^{13}CO mass [$M_\odot$]			Relative difference [%]	
	"Real"	Constant ratio	Fitting formula	Constant ratio	Fitting formula
a	0.0122	0.0075	0.0136	38.3	12.0
b	0.0680	0.0437	0.0679	35.7	0.2
c	0.3514	0.2766	0.3693	21.3	5.1
d	0.1969	0.1399	0.1896	28.9	3.7
e	0.0849	0.0522	0.0732	38.5	13.8
f	0.3477	0.2913	0.3453	16.2	0.7

CO-dark gas

modeling molecular cloud formation

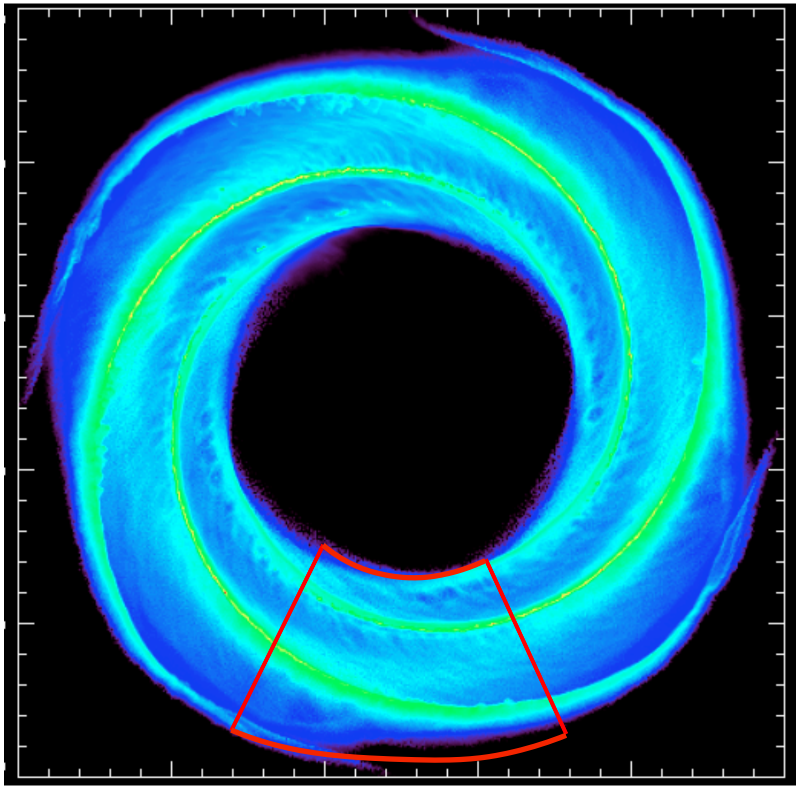

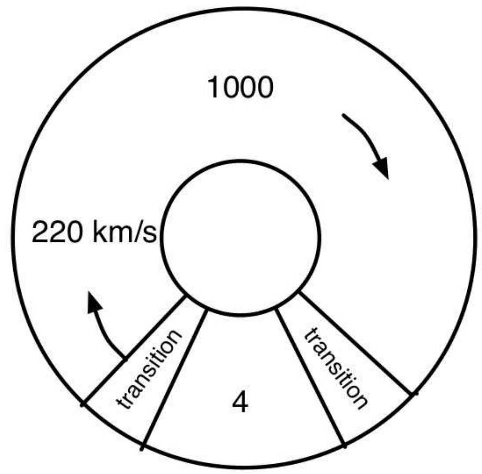

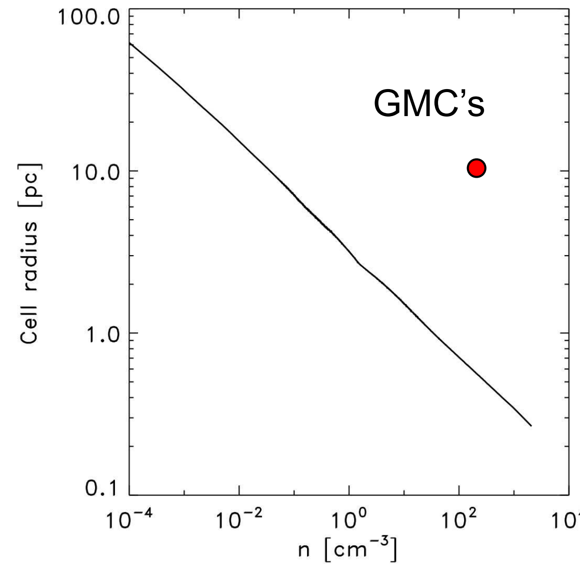

Simulation	Surface Density $M_\odot\ pc^{-2}$	Radiation Field G_0
Milky Way	10	1
Low Density	4	1
Strong Field	10	10
Low & Weak	4	0.1

- Arepo moving mesh code *(Springel 2010)*
- time dependent chemistry *(Glover et al. 2007)* gives heating & cooling in a 2 phase medium
- two layers of refinement with mass resolution down to 4 $M_\odot$ in full Galaxy simulation
- UV field and cosmic rays
- TreeCol *(Clark et al. 2012)*
- external spiral potential *(Dobbs & Bonnell 2006)*
- no gas self-gravity, SN, or magnetic fields yet

(Smith et al., 2014, MNRAS, 441, 1628)

numerical method

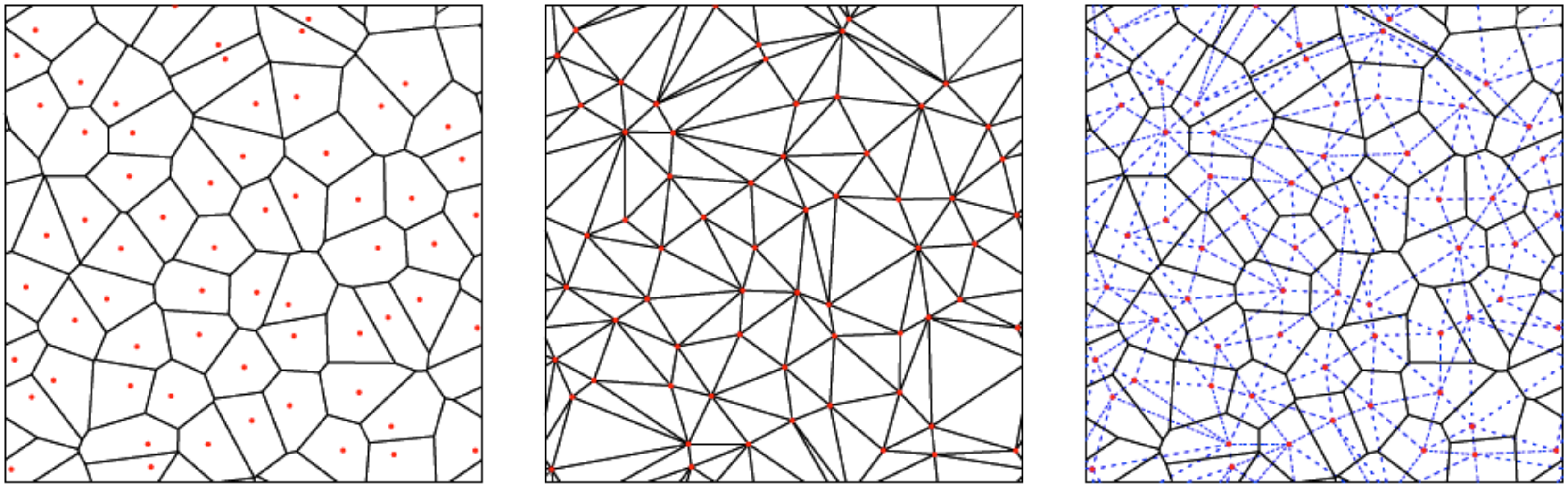

*moving mesh code **Arepo**:*

- semi-Lagrangian
- flexible refinement
- fluid instabilities and no artificial clumping
  (Agertz et al. 2007)
- can also handle sub-sonic turbulence
  (Bauer & Springel 2012)
- no preferred geometry

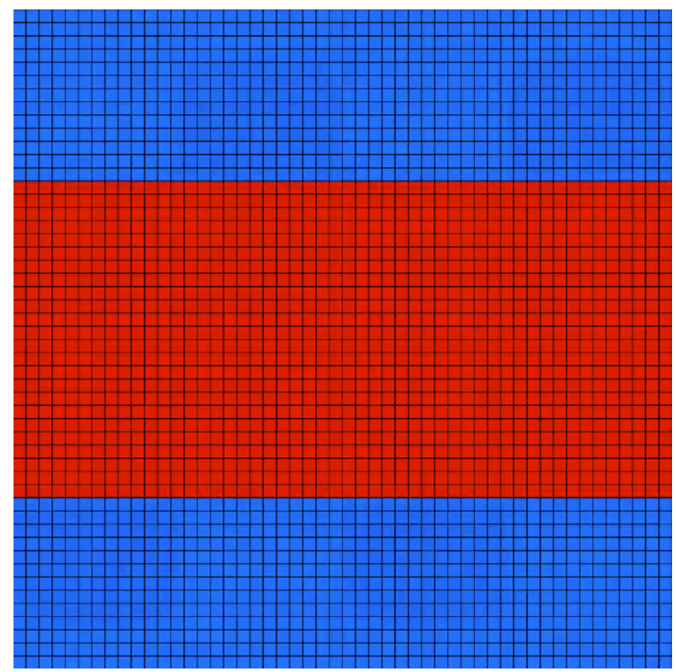

Springel (2010, MNRAS, 401, 791)

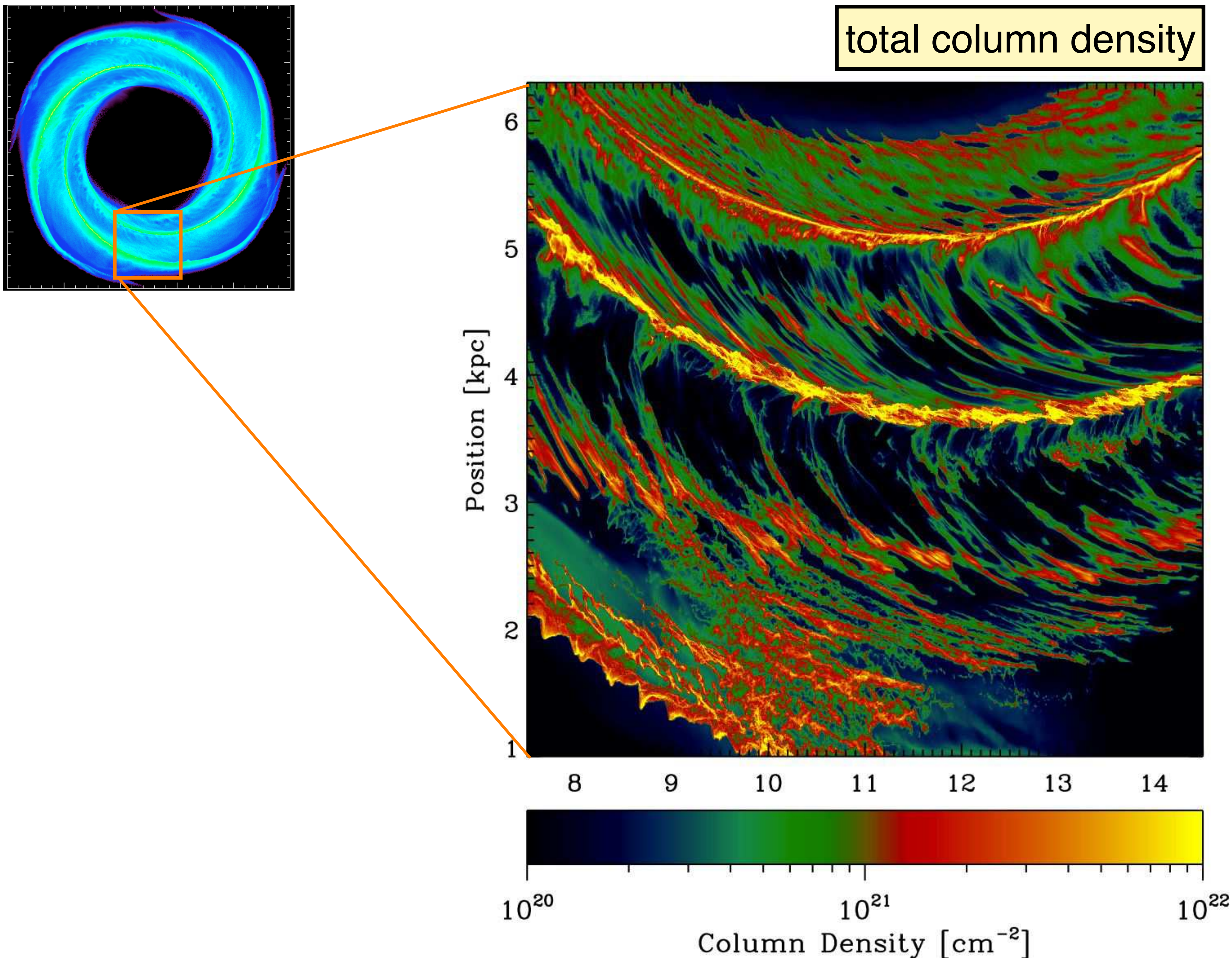

(Smith et al., 2014, MNRAS, 441, 1628)

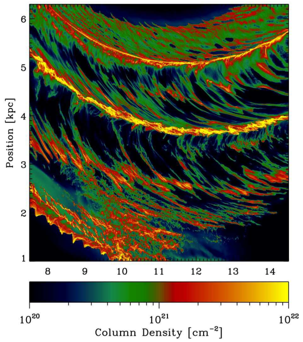

HI column density

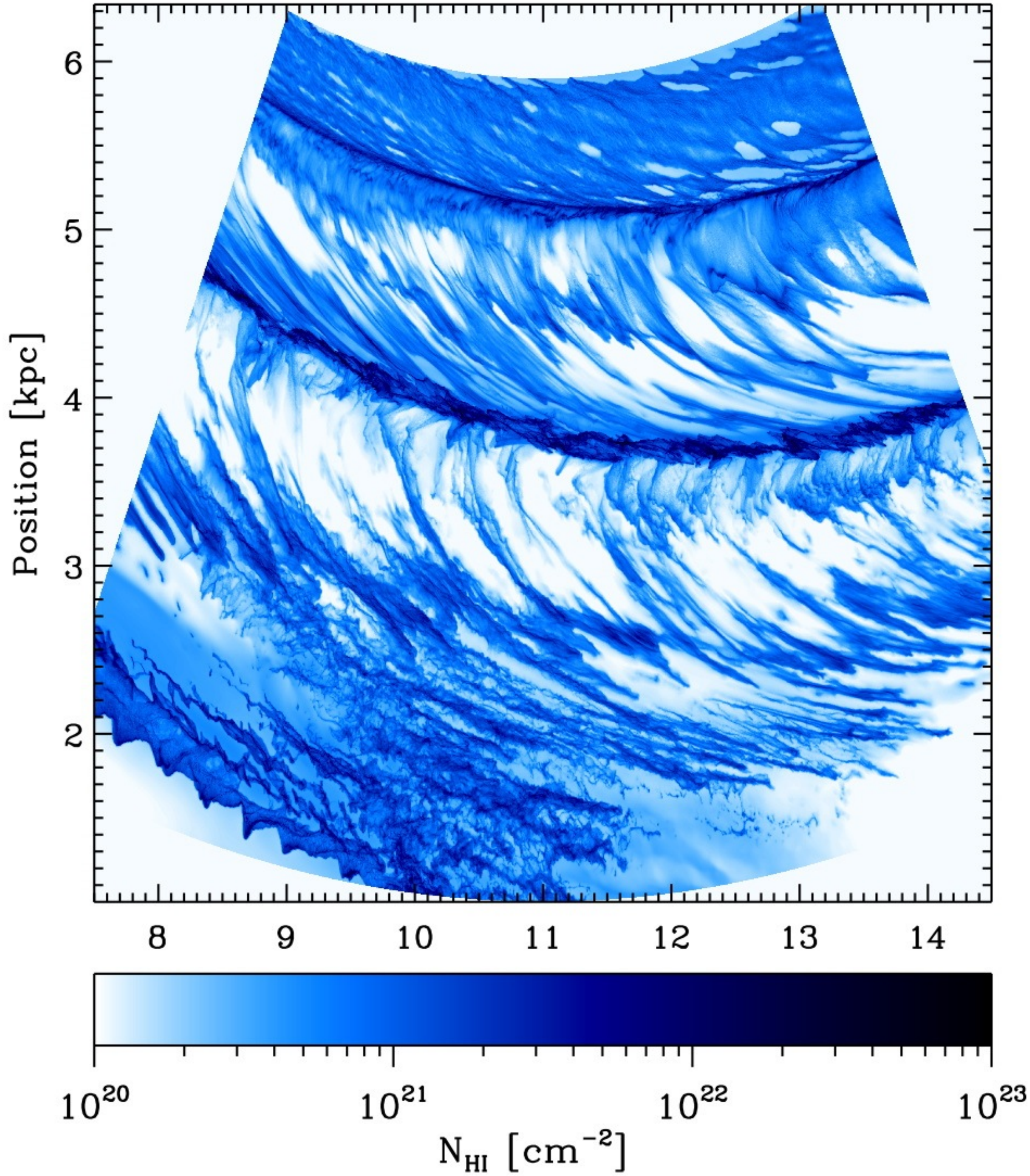

(Smith et al., 2014, MNRAS, 441, 1628)

preliminary image from THOR Galactic plane survey (PI H. Beuther): continuum emission around 21 cm

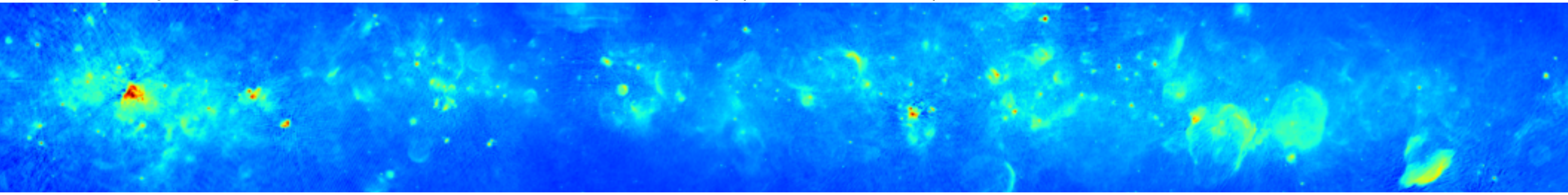

next step: produce all sky maps at various positions in the model galaxy (use RADMC-3D)

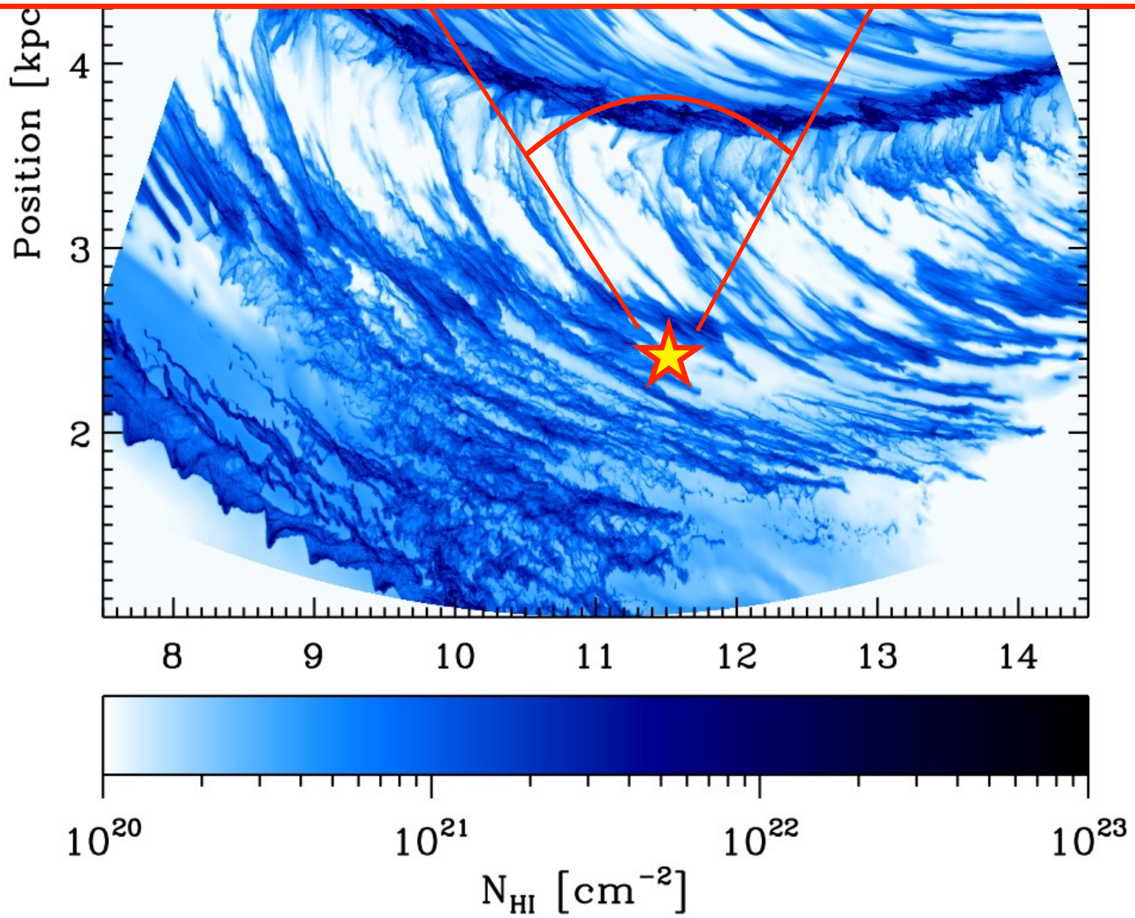

(Smith et al., 2014, MNRAS, 441, 1628)

preliminary image from THOR Galactic plane survey (PI H. Beuther): continuum emission around 21 cm

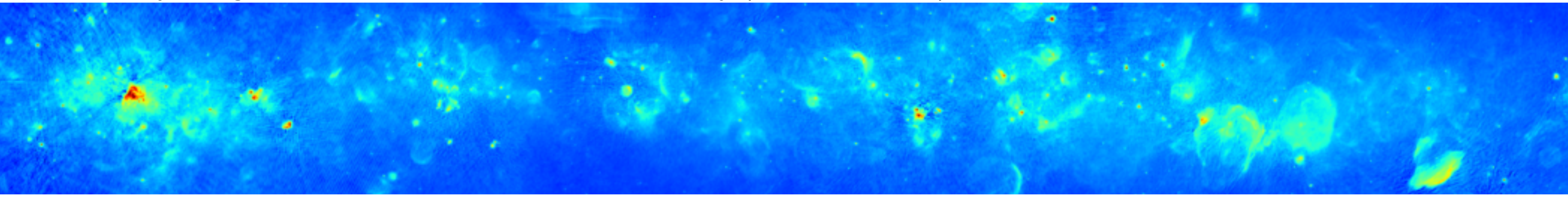

next step: produce all sky maps at various positions in the model galaxy (use RADMC-3D)

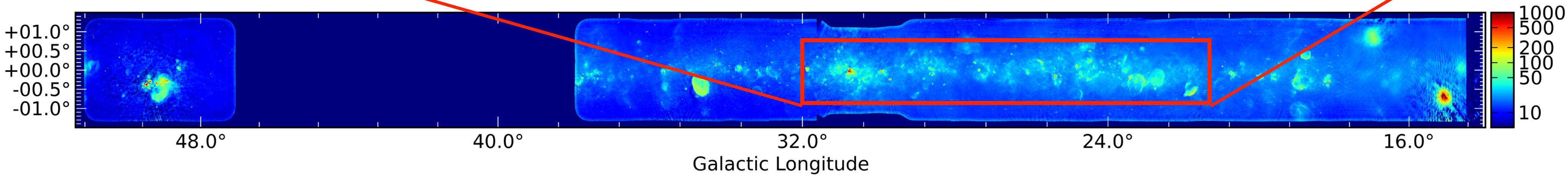

http://www.mpia.de/thor/Overview.html

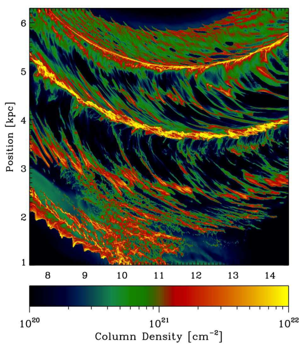

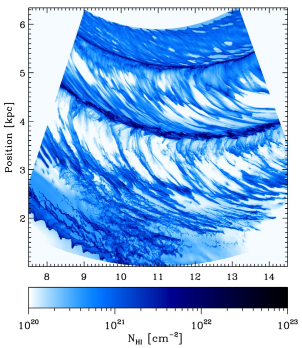

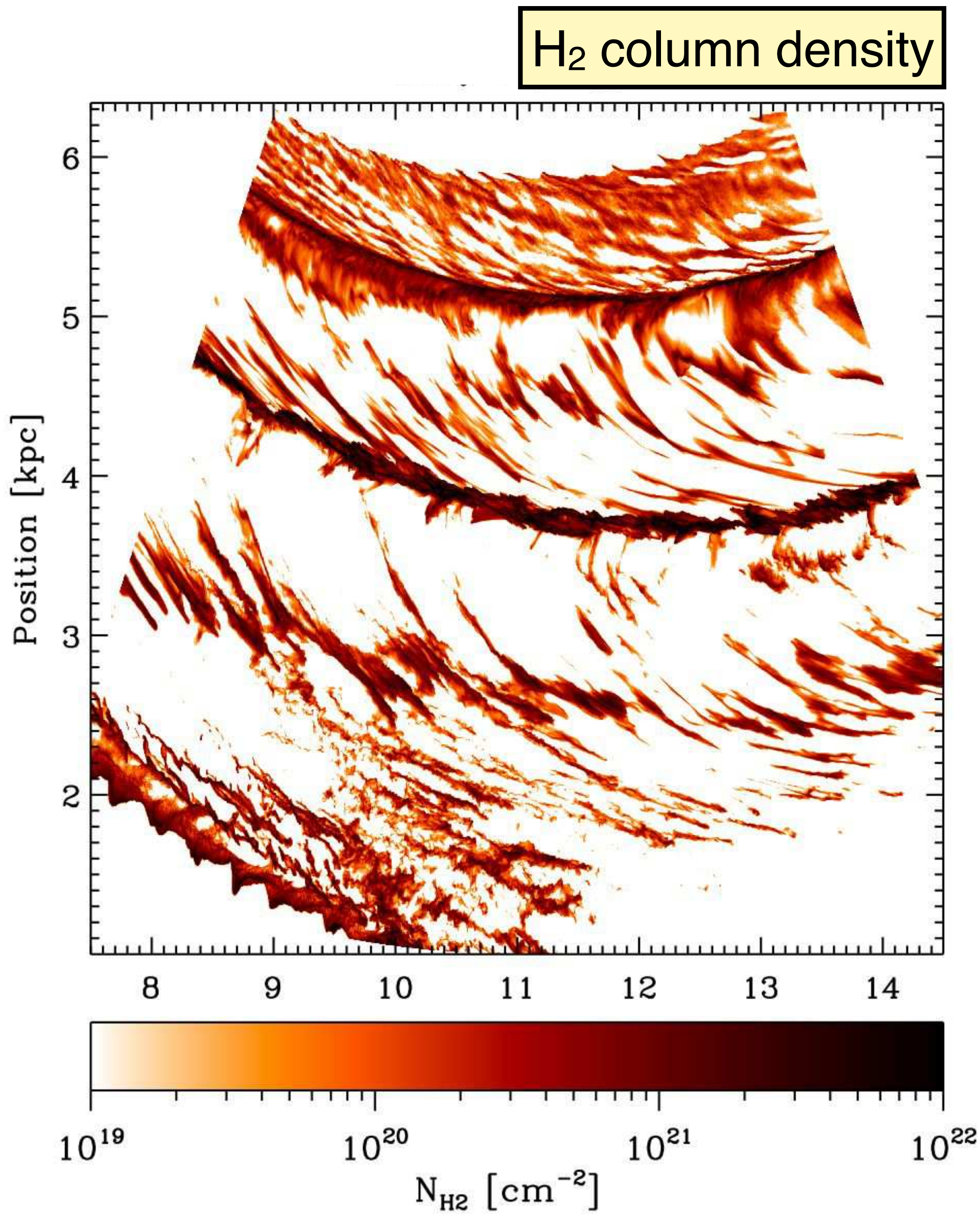

(Smith et al., 2014, MNRAS, 441, 1628)

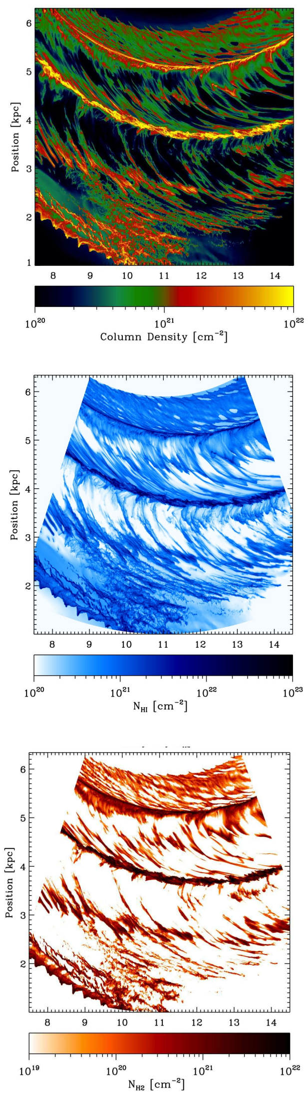

CO column density

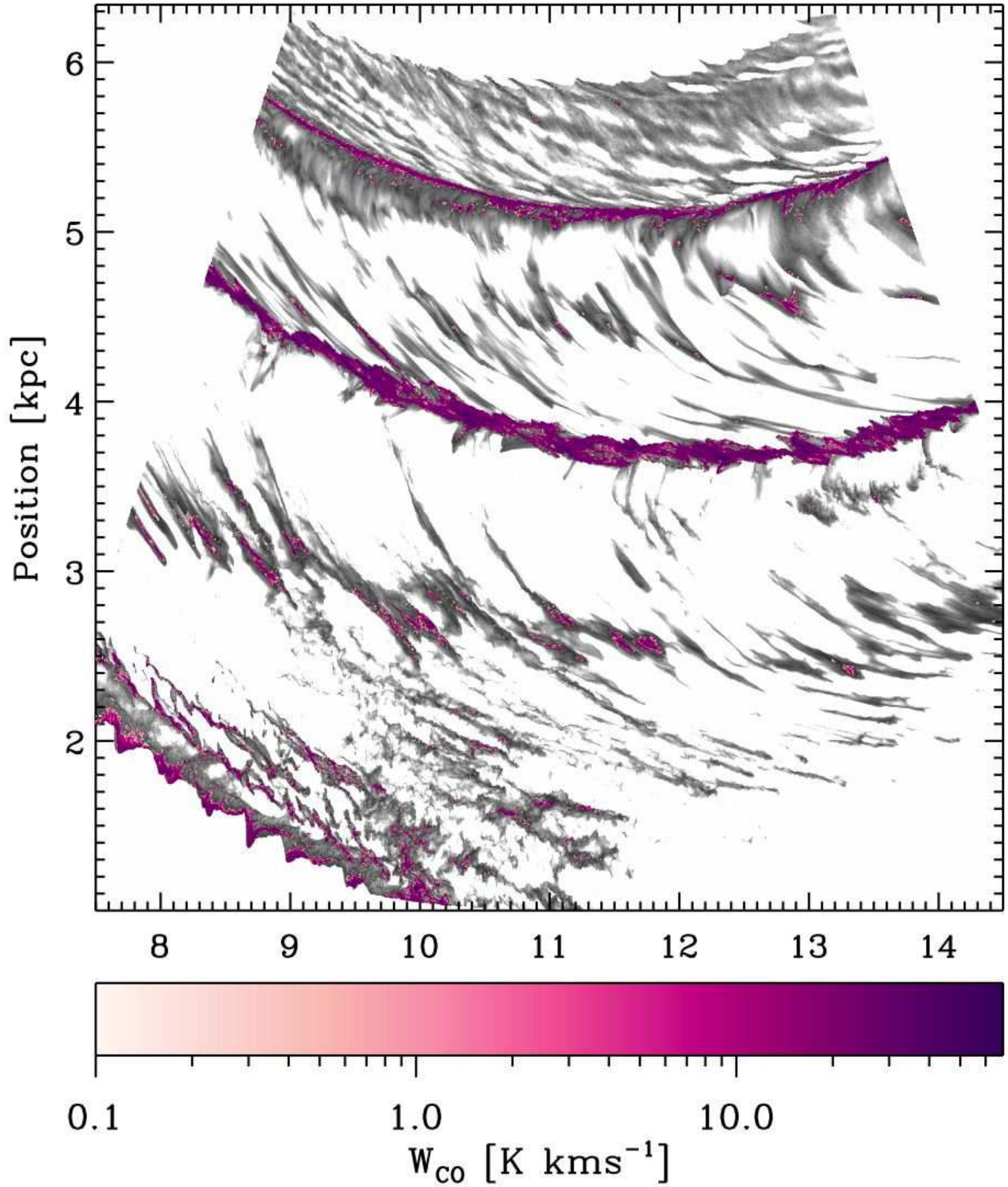

(Smith et al., 2014, MNRAS, 441, 1628)

H_2 fraction vs. column density N

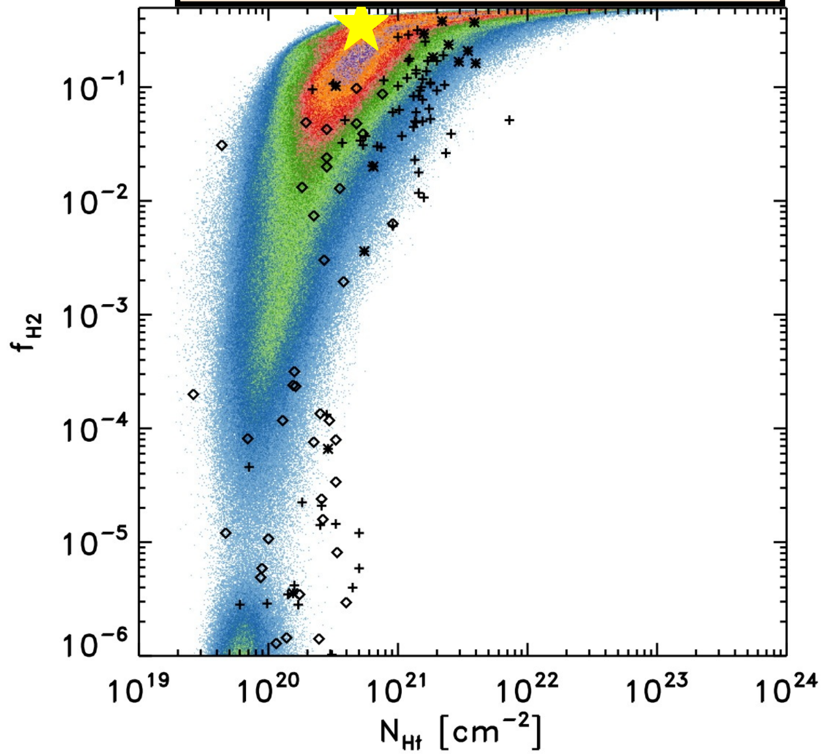

CO col. density vs. H_2 col. density

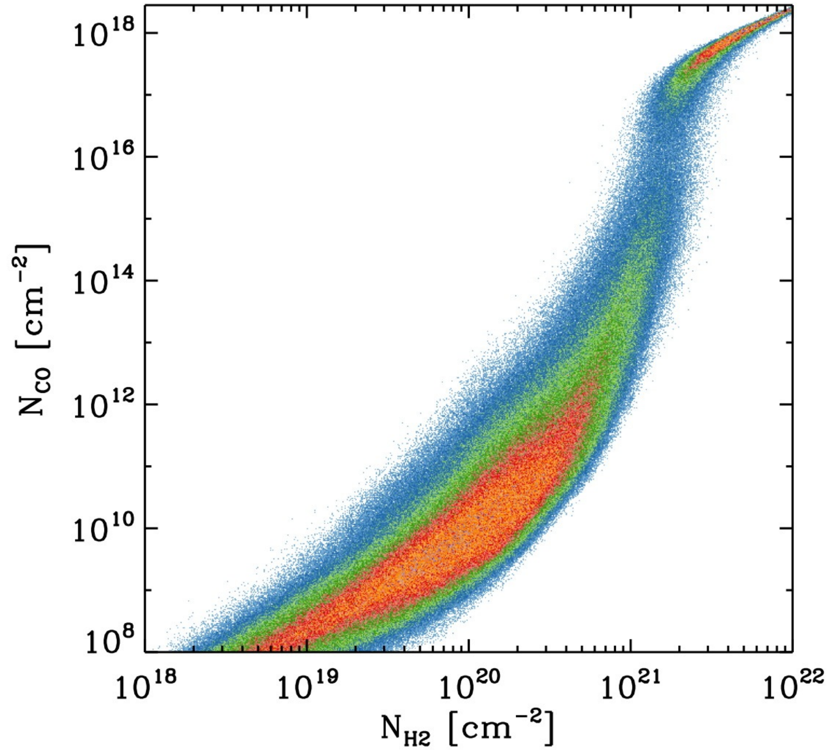

H_2 forms above column densities of 10^{20} cm^{-2}

CO columns jump after $N_{H2} \sim 10^{21}$ cm^{-2}

$$log(Z_{CO}[cm^{-2}]) = -18.1 log(N_{CO}[cm^{-2}]) + 0.8.$$

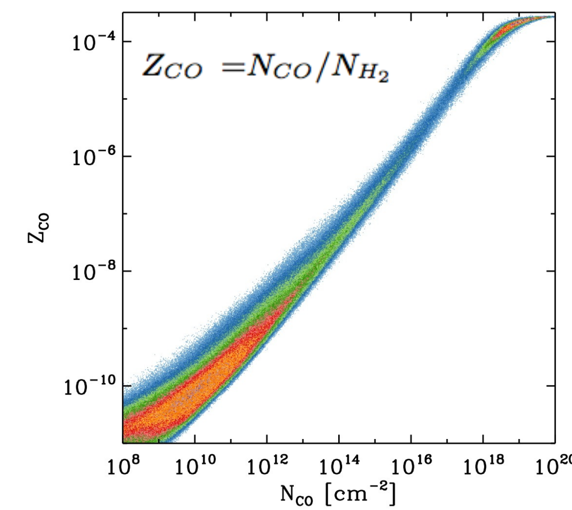

(Smith et al., 2014, MNRAS, 441, 1628)

details of CO emission

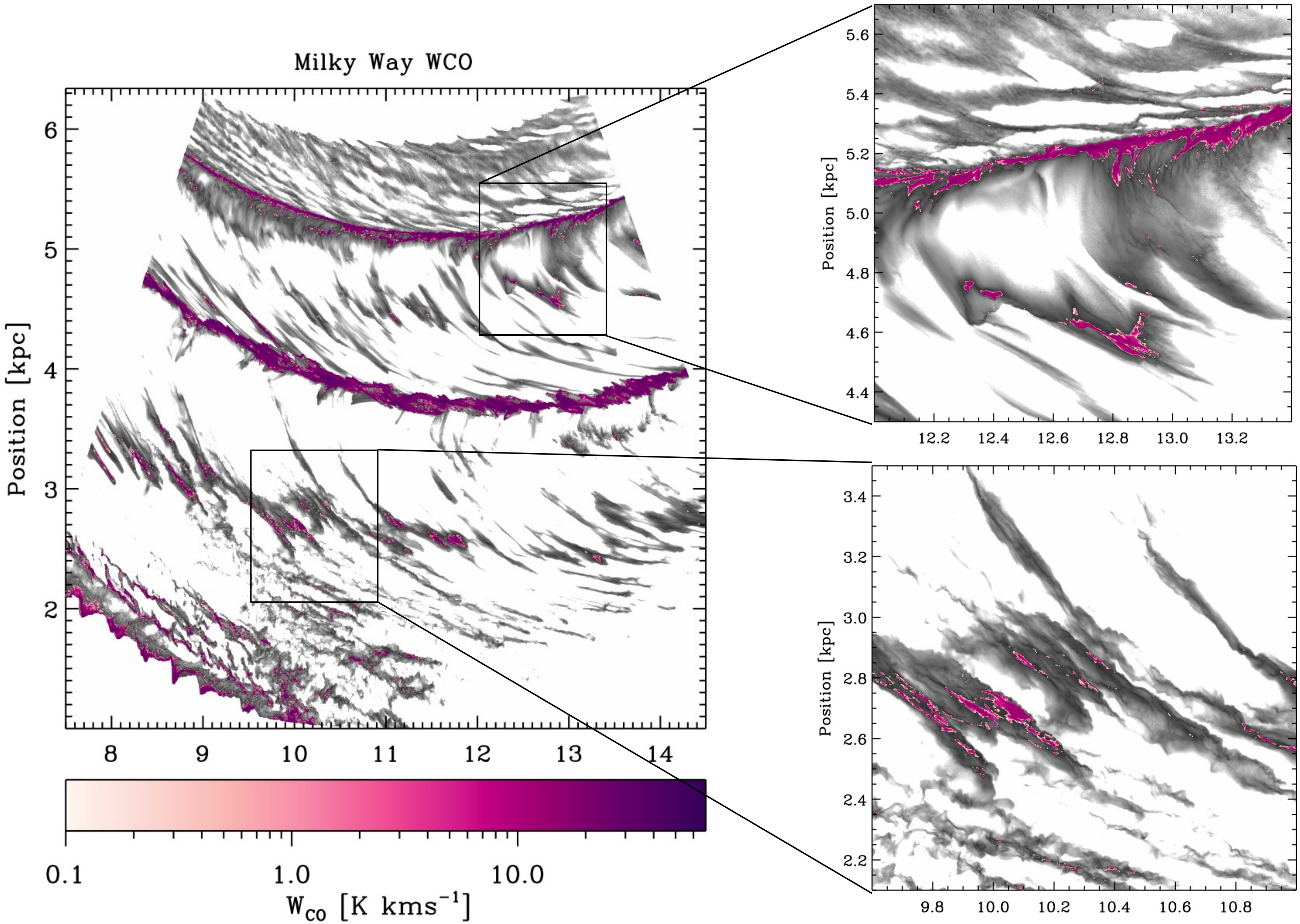

(Smith et al., 2014, MNRAS, 441, 1628)

relation between CO and H_2

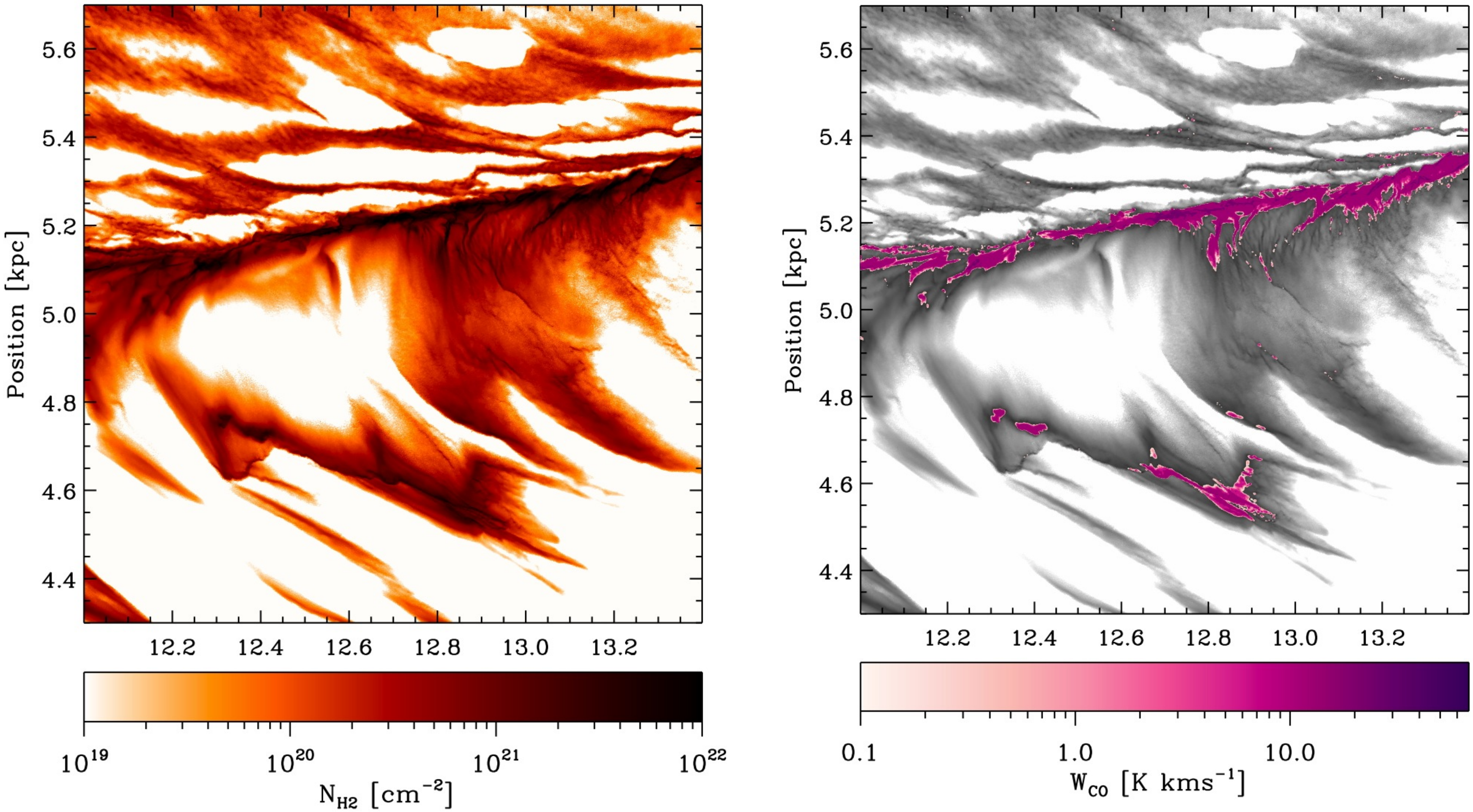

(Smith et al., 2014, MNRAS, 441, 1628)

relation between CO and H_2

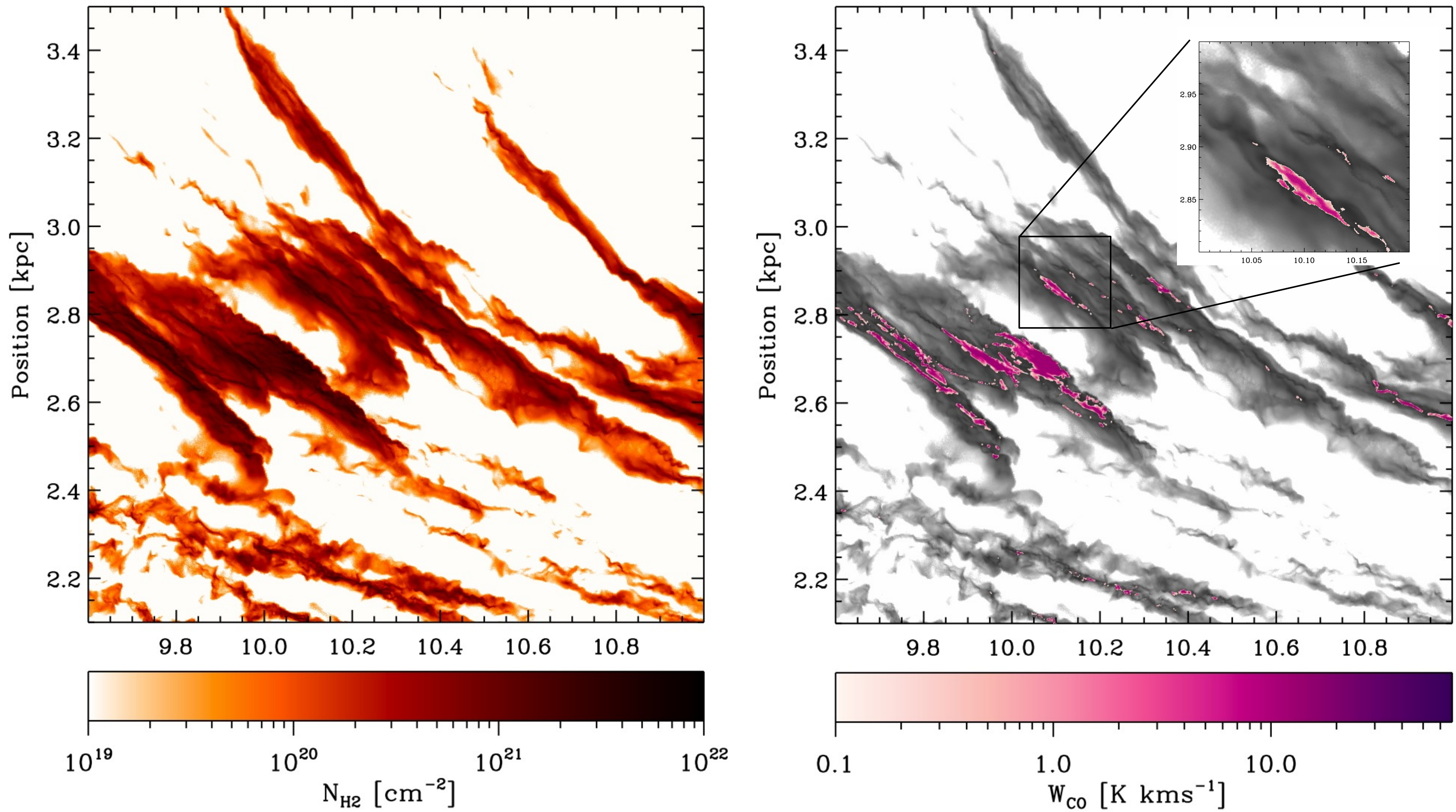

Filamentary molecular clouds in inter-arm regions are likely only the observable parts of much larger structures.

dark gas fraction

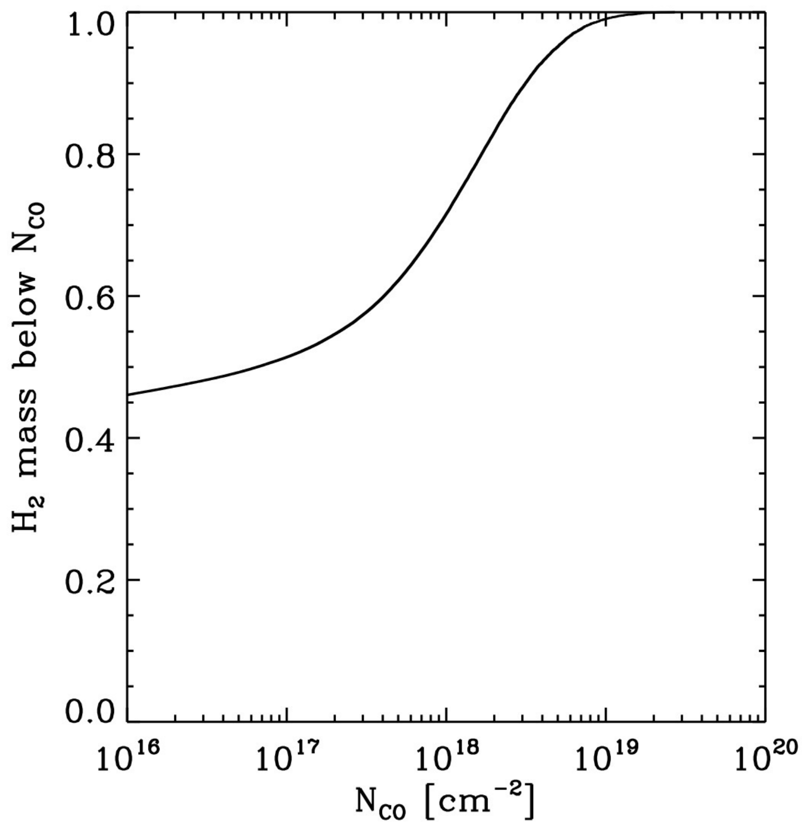

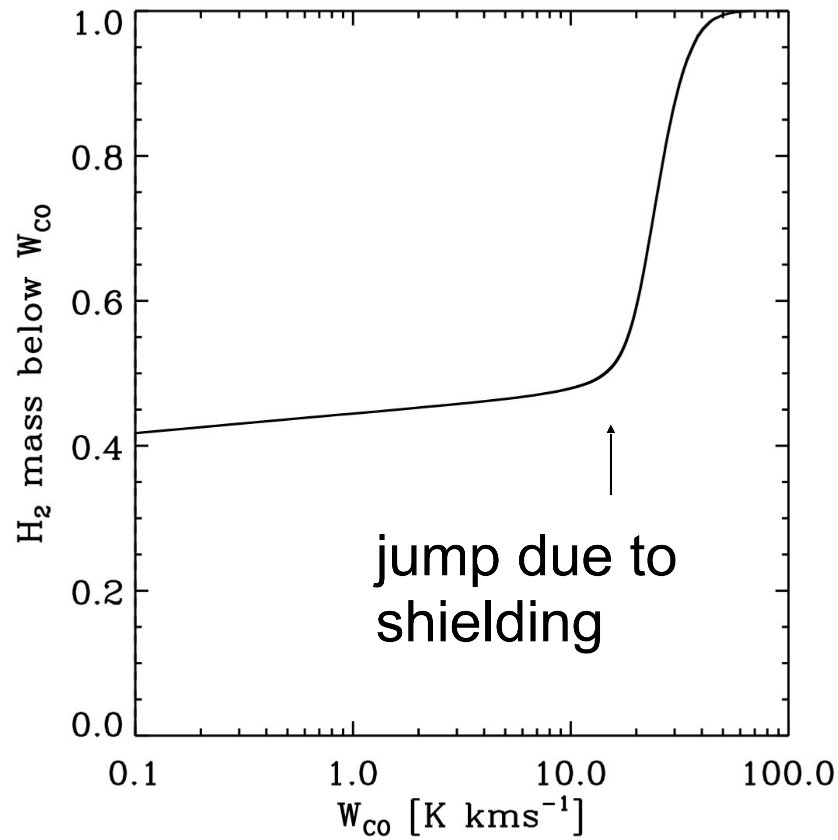

46% molecular gas below CO column densities of 10^{16} cm^{-2}

42% has an integrated CO emission of less than 0.1 K kms^{-1}

$f_{DG} = 0.42$ $\qquad$ $X_{co}=2.2 \times 10^{20}\ cm^{-2}K^{-1}km^{-1}s$

(Smith et al., 2014, MNRAS, 441, 1628)

dark gas fraction

Observational estimates:

Grenier et al. (2005) f_{DG} = 0.33-0.5

Planck coll. (2011)* f_{DG} = 0.54

Paradis et al. (2012)* f_{DG} = 0.62

(inner f_{DG} = 0.71, outer f_{DG} = 0.43)

Pineda et al. (2013) f_{DG}= 0.3

Roman-Duval et al. (in prep.) f_{DG} ~ 0.5

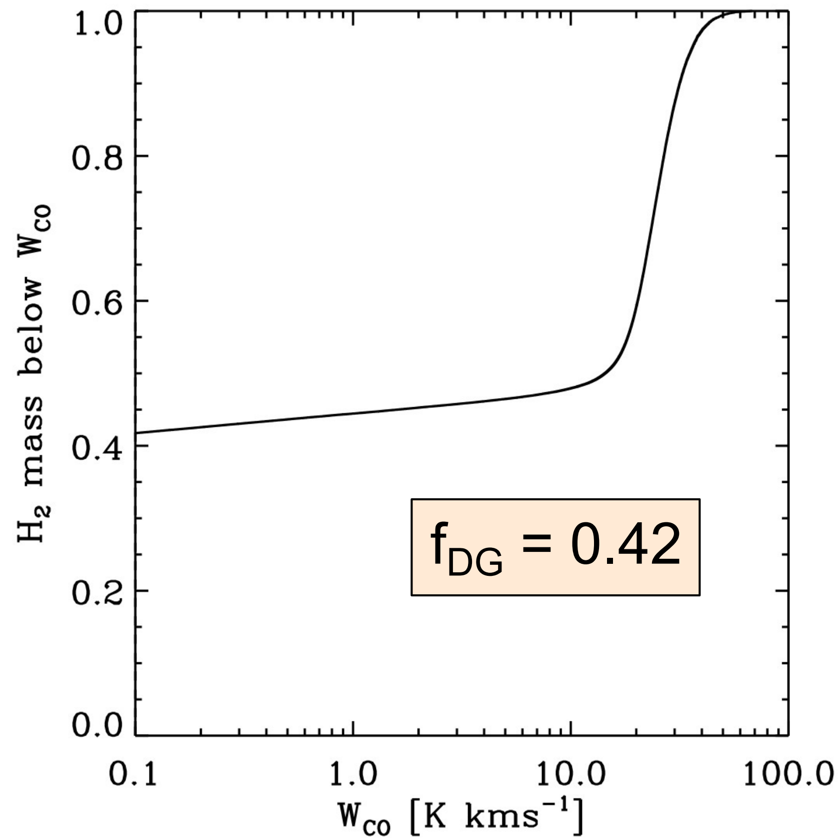

* dust methods have large uncertainties.

(Smith et al., 2014, MNRAS, 441, 1628)

is there CO-dark H_2 gas?

- there is increasing evidence, that a significant fraction of the H_2 gas in galaxies is not traced by CO (e.g. Pringle, Allen, Lubov 2001, Hosokawa & Inutsuka 2007, Clark et al. 2012)

- 3D simulations of colliding HI gas forming molecular clouds at the stagnation region performed by Paul Clark in Heidelberg
  - SPH (also with FLASH)
  - full fledged CO chemistry
  - TREECOL for calculating extinction
  - ‘standard’ dust model
  - sink particles to account for local collapse (star formation)
  - two models: slow and fast flow

further evidence form detailed colliding flow calculations

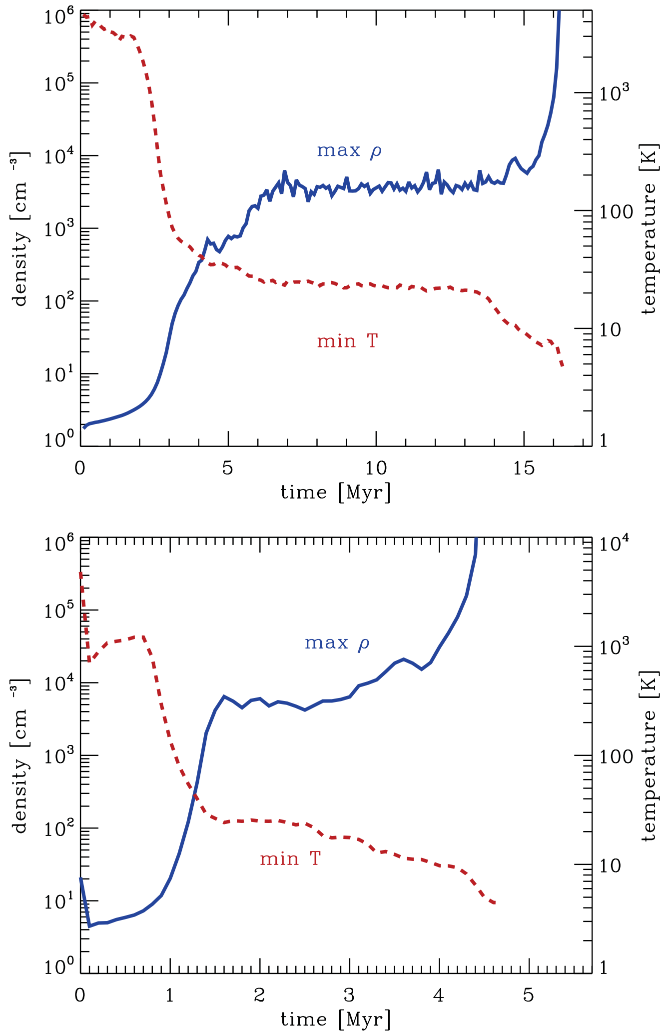

Figure 3. Evolution with time of the maximum density (blue, solid line) and minimum temperature (red, dashed line) in the slow flow (top panel) and the fast flow (bottom panel). Note that at any given instant, the coldest SPH particle is not necessarily the densest, and so the lines plotted are strictly independent of one another.

slow flow

fast flow

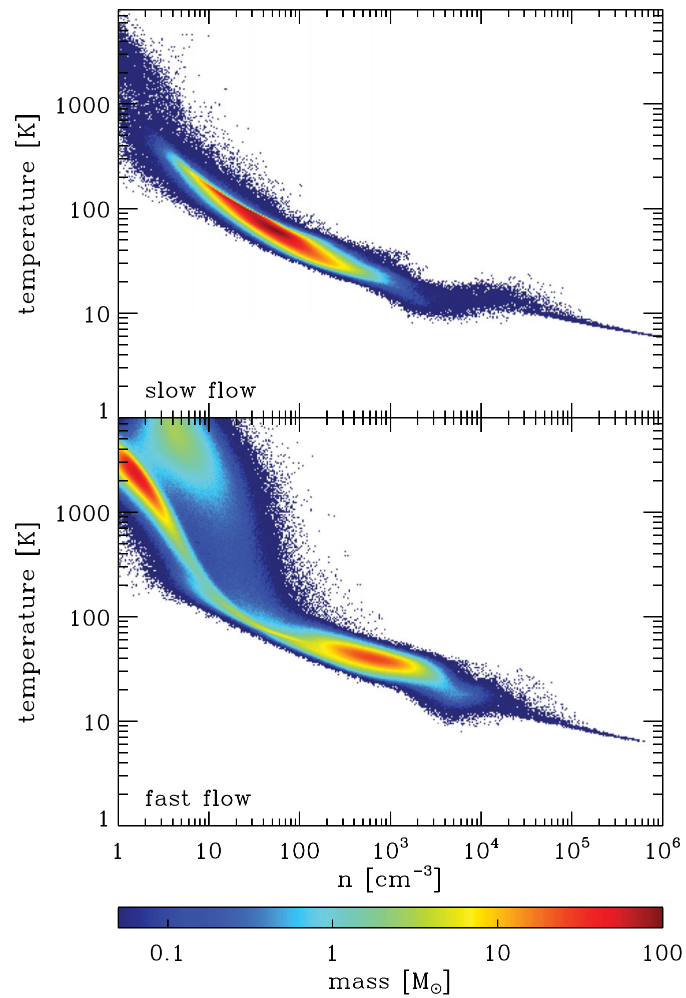

Figure 5. The gas temperature–density distribution in the flows at the onset of star formation.

Clark et al. (2012,MNRAS, 424, 2599)

see also Pringle, Allen, Lubov (2001), Hosokawa & Inutsuka (2007)

further evidence form detailed colliding flow calculations

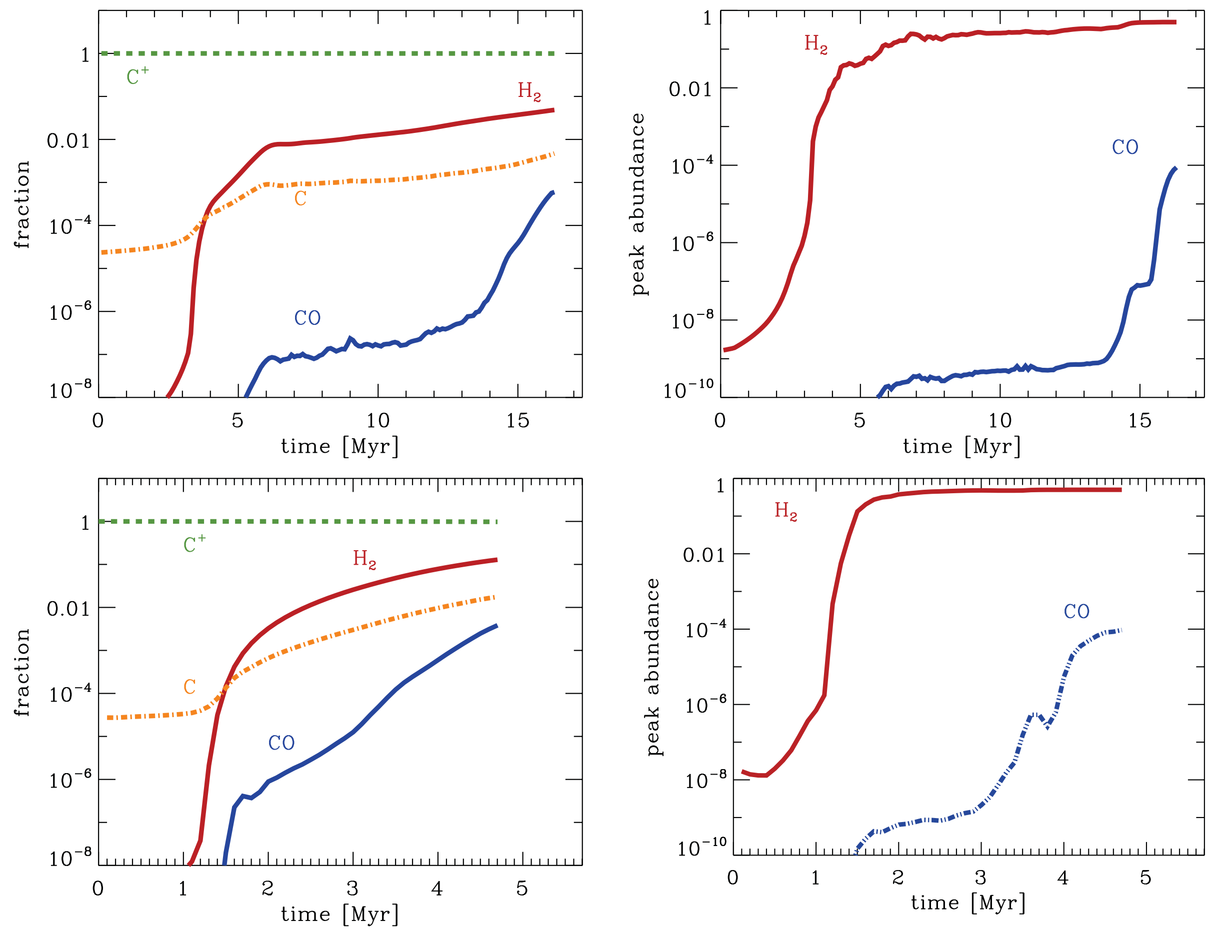

slow flow

fast flow

Figure 6. Chemical evolution of the gas in the flow. In the left-hand column, we show the time evolution of the fraction of the total mass of hydrogen that is in the form of H_2 (red solid line) for the 6.8 km s^{-1} flow (upper panel) and the 13.6 km s^{-1} flow (lower panel). We also show the time evolution of the fraction of the total mass of carbon that is in the form of C^+ (green dashed line), C (orange dot–dashed line) and CO (blue double-dot–dashed line). In the right-hand column, we show the peak values of the fractional abundances of H_2 and CO. These are computed relative to the total number of hydrogen nuclei, and so the maximum fractional abundances of H_2 and CO are 0.5 and 1.4×10^{-4}, respectively. Again, we show results for the 6.8 km s^{-1} flow in the upper panel and the 13.6 km s^{-1} flow in the lower panel. Note that the scale of the horizontal axis differs between the upper and lower panels.

Clark et al. (2012,MNRAS, 424, 2599)

see also Pringle, Allen, Lubov (2001), Hosokawa & Inutsuka (2007)

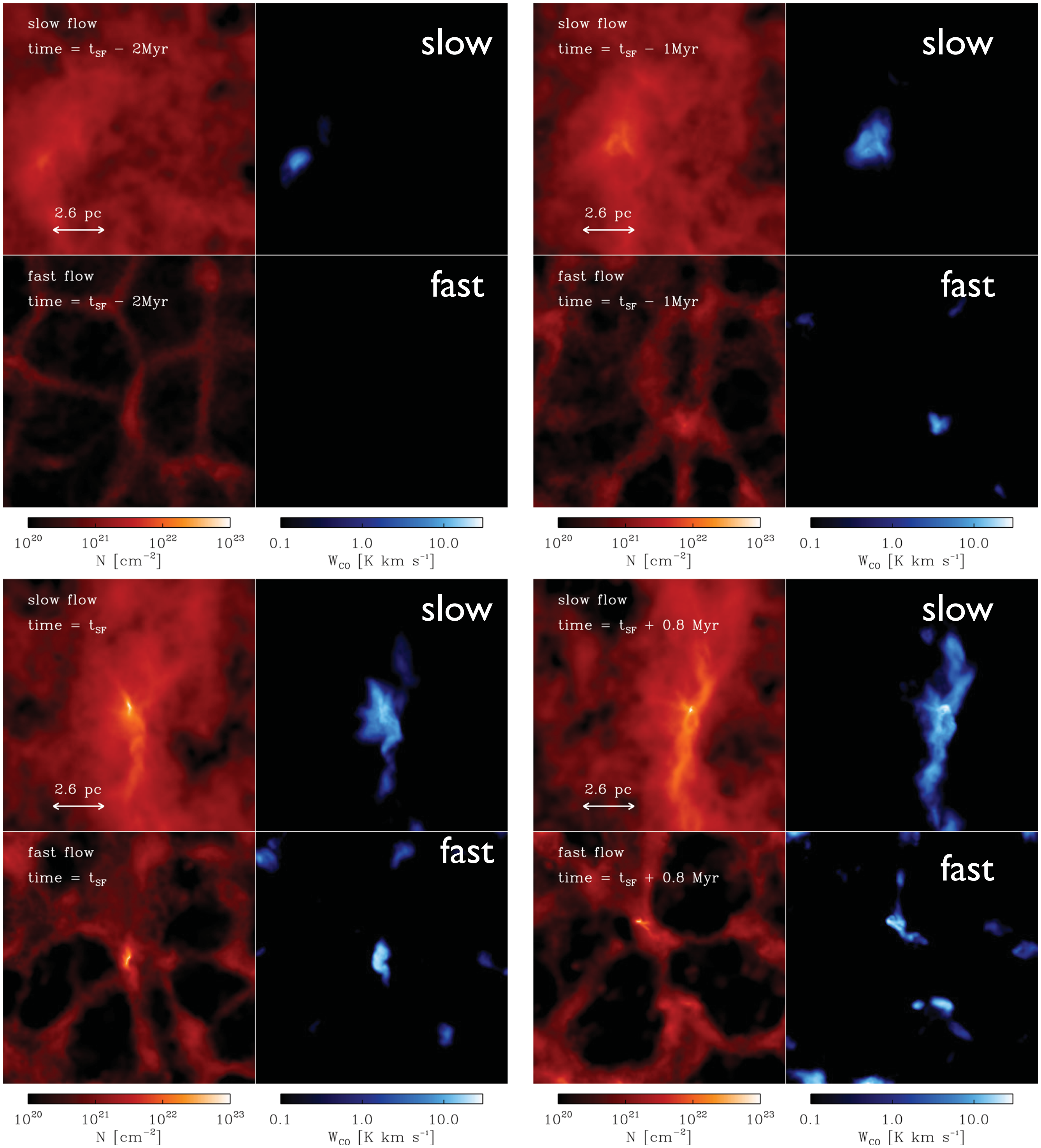

H_2 column

CO emission

fraction of CO dark gas will also change with metallicity and with ambient radiation field

Clark et al. (2012,MNRAS, 424, 2599)

properties of star forming filaments

large-scale filaments

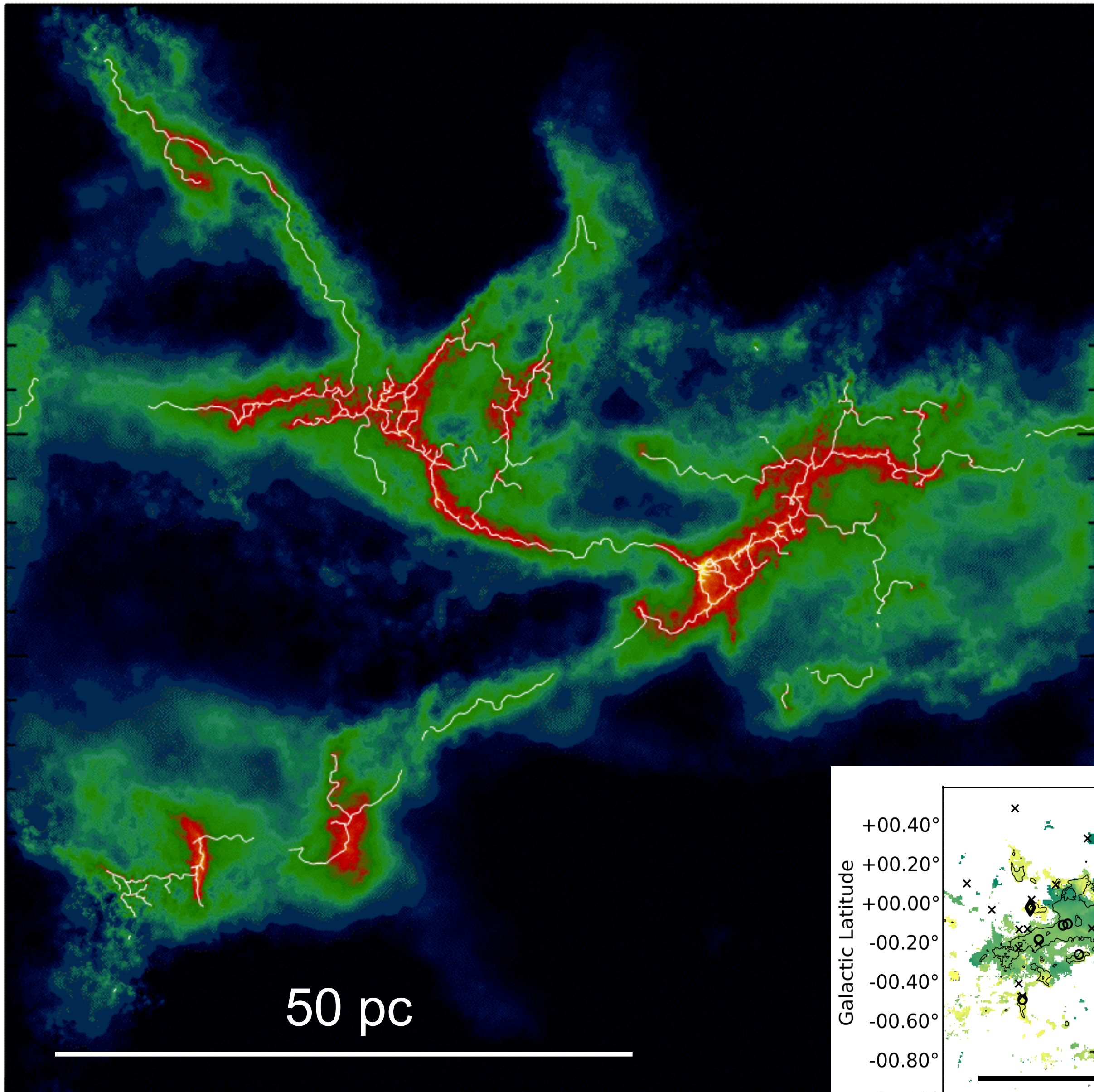

Smith et al. (2014, MNRAS, 445, 2900)

next steps:

studying details of ISM morphology and star formation in dedicated zoom-in simulation

example:

giant molecular cloud complex (~10^6 $M_\odot$) viewed in the plane of the disk.

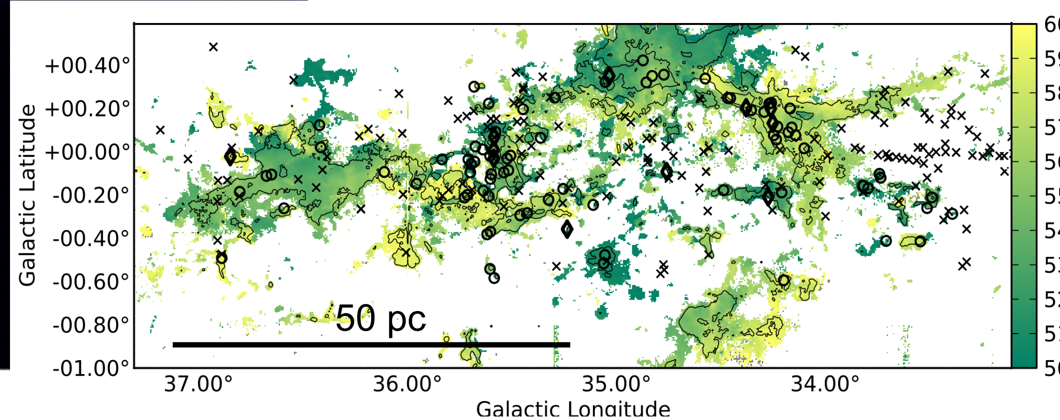

Ragan et al., 2014, A&A submitted, arXiv:1403.1450)

zoom-in on filaments

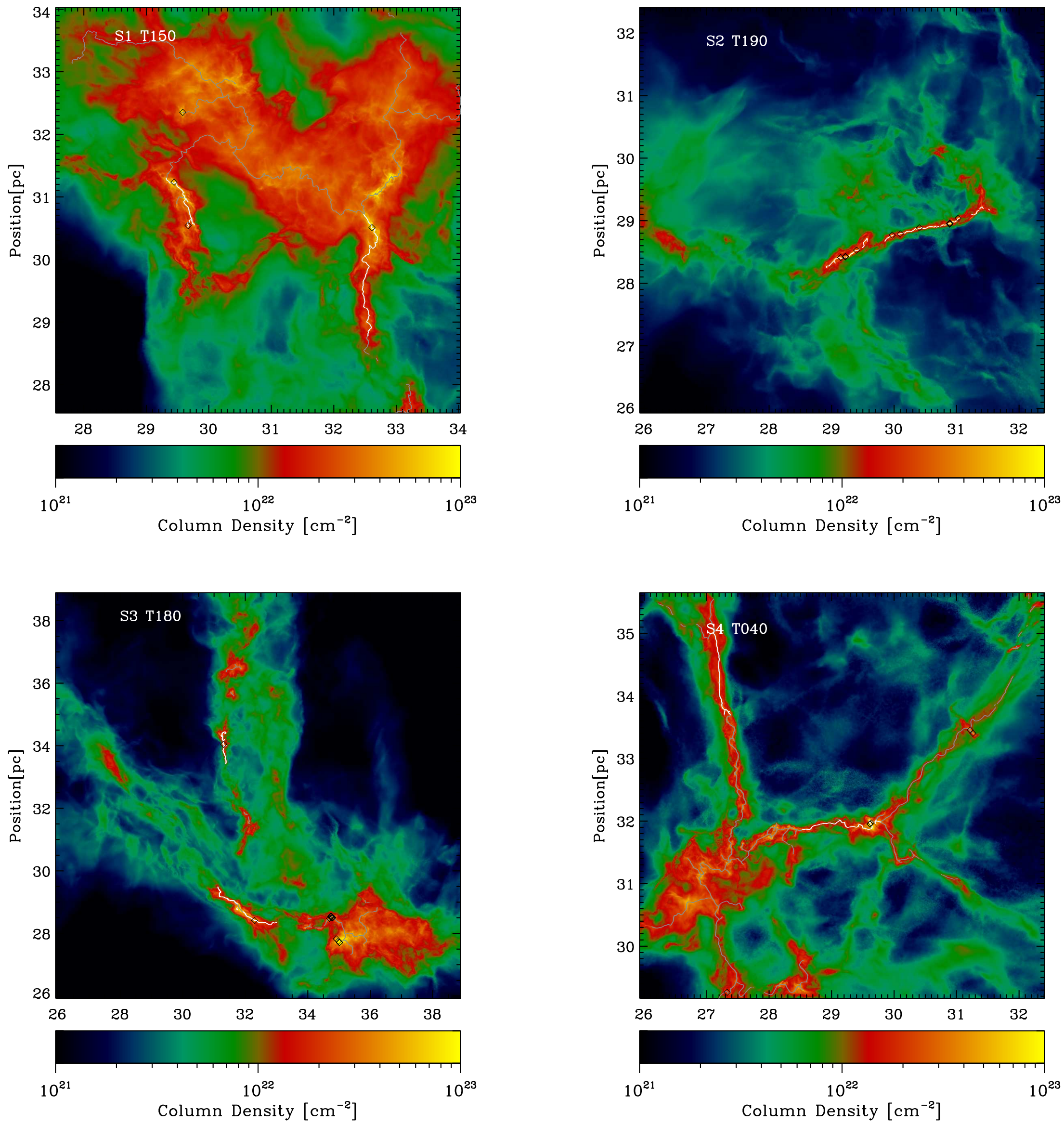

next steps:

studying details of ISM morphology and star formation in dedicated zoom-in simulation *(resolution ≲2000 AU, with full chemistry)*

analysis:

- morphology
- velocity
- chemistry
- observations (dust maps for Herschel, CO, N_2H+, HCN, etc. for line obs.)

Smith et al. (2014, MNRAS, 445, 2900,
also Smith et al. 2012, ApJ, 750, 64, Smith et al. 2013, ApJ, 771, 24, Chira et al., 2014, MNRAS, submitted)

filaments do not have universal width

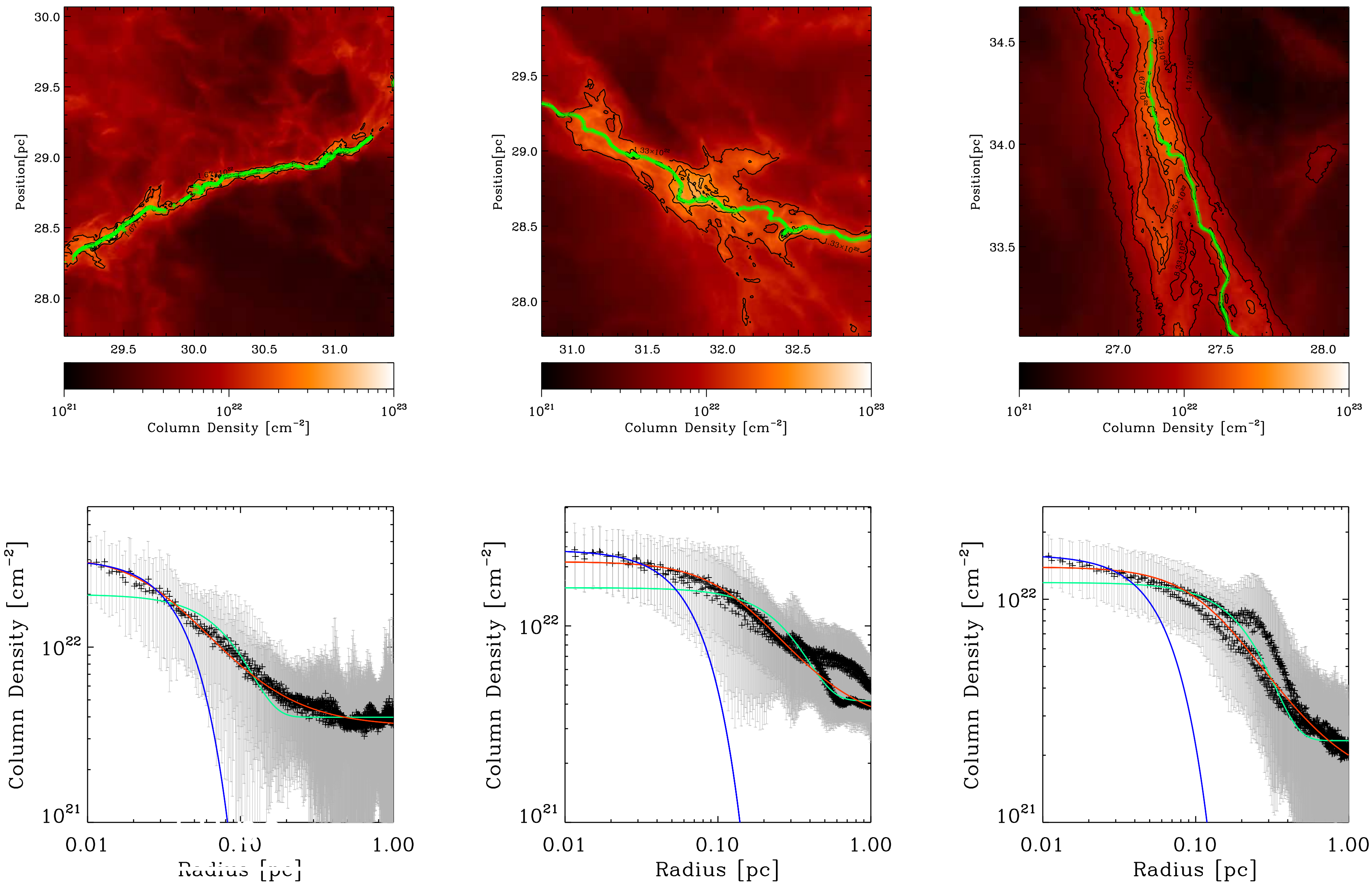

Smith et al. (2014, MNRAS, 445, 2900)

filaments do not have universal width

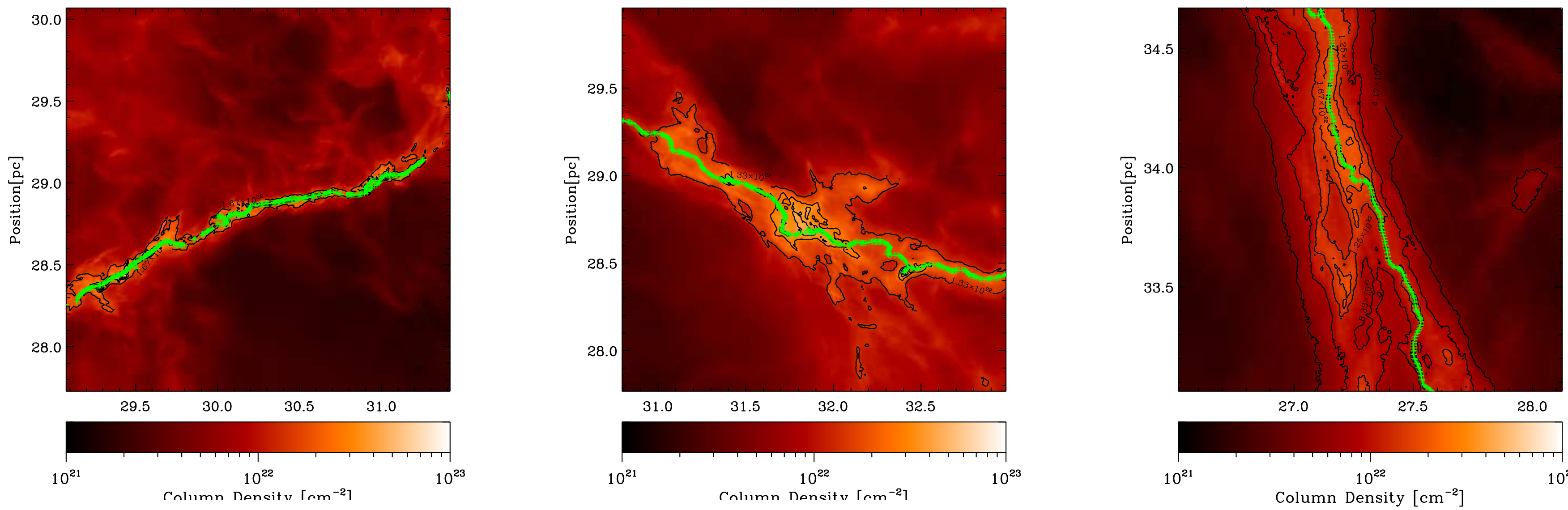

Arzoumanian, et al., 2011, A&A, 529, L6

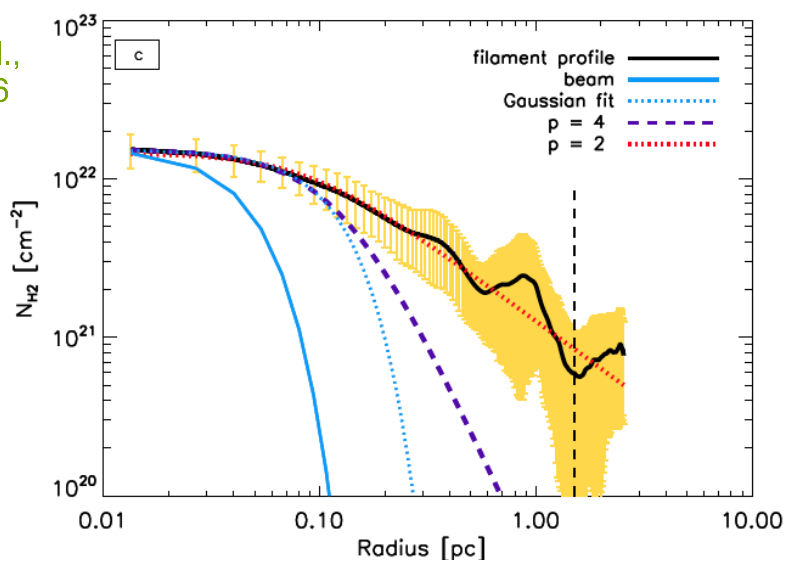

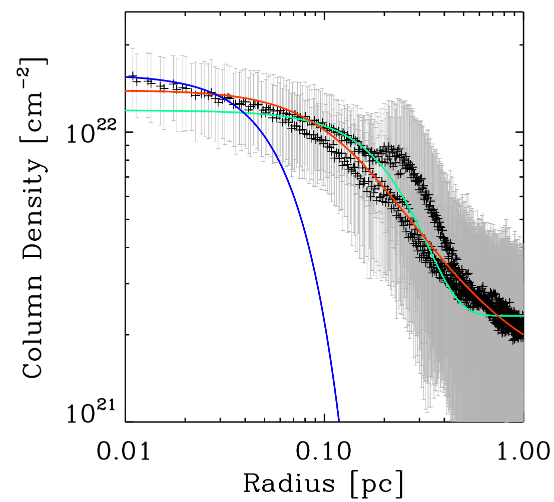

Smith et al. (2014, MNRAS, 445, 2900)

3D filaments have complex structure

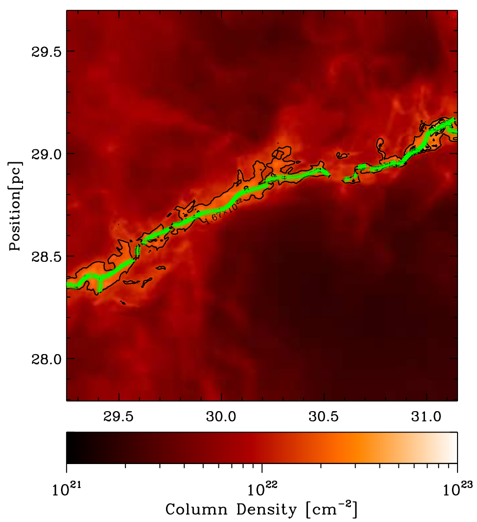

2D filament detection shows nice coherent filament

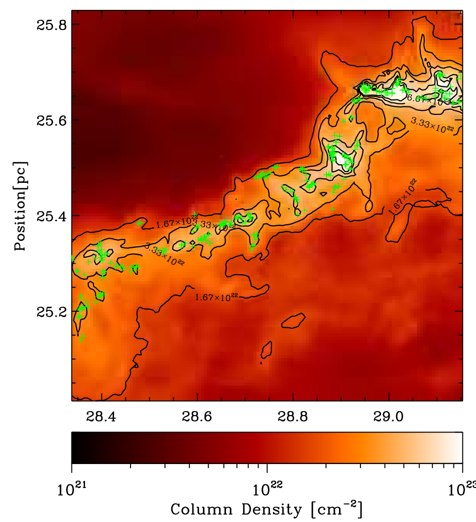

2D + LOS peak detection shows complex structure

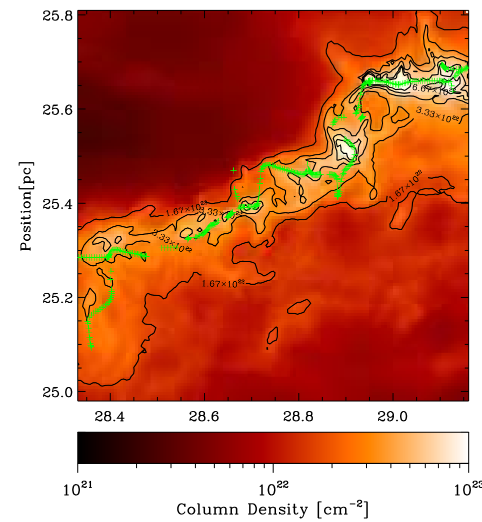

full 3D filament analysis confirms this picture

Smith et al. (2014, MNRAS, 445, 2900)

walk along the filament

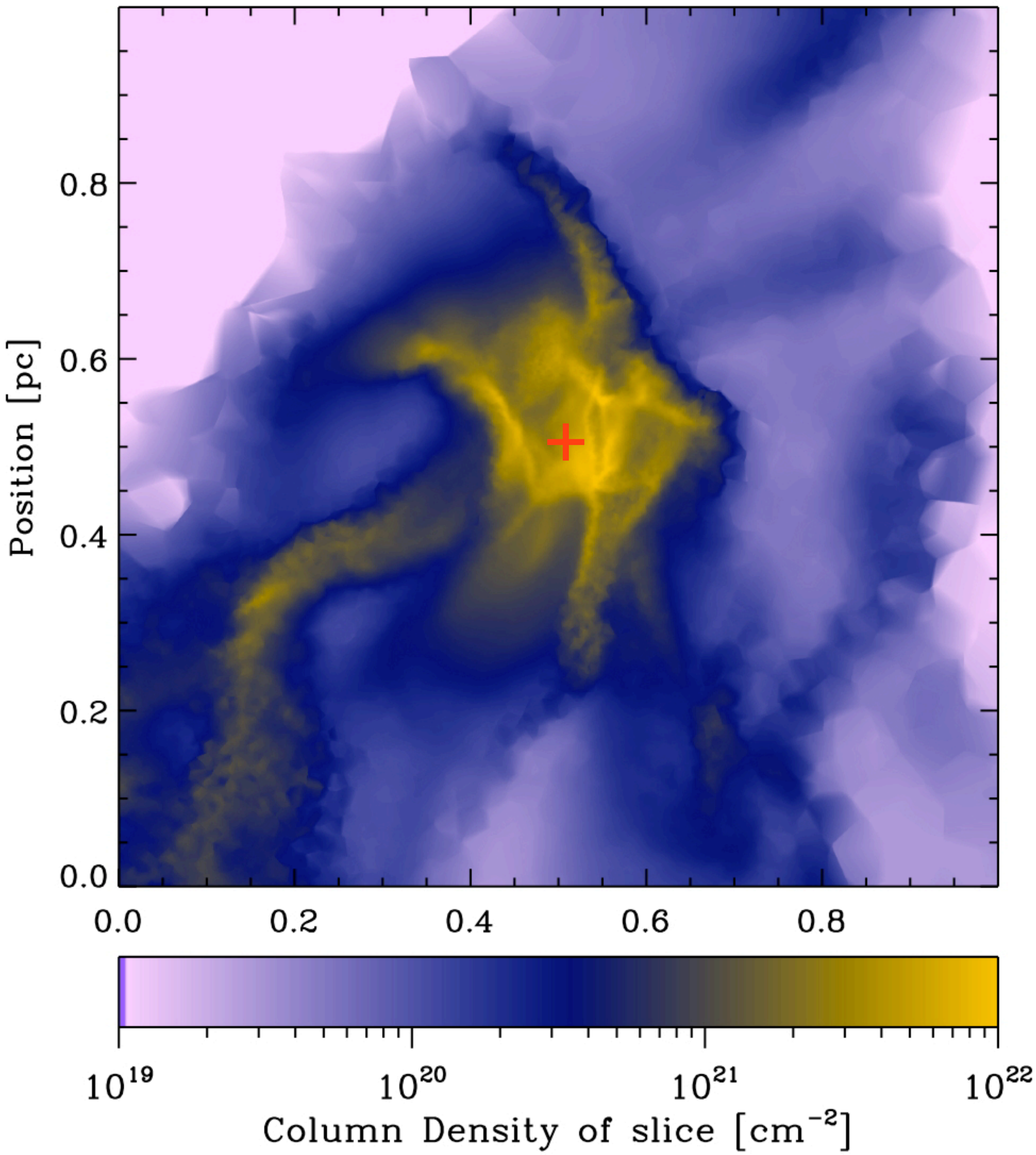

- walking along the filament exhibits complex 3D structure that is now (fully) seen in projected density
- is this similar to the filament fibers proposed by Hacar et al. (2013, A&A, 554, 55)

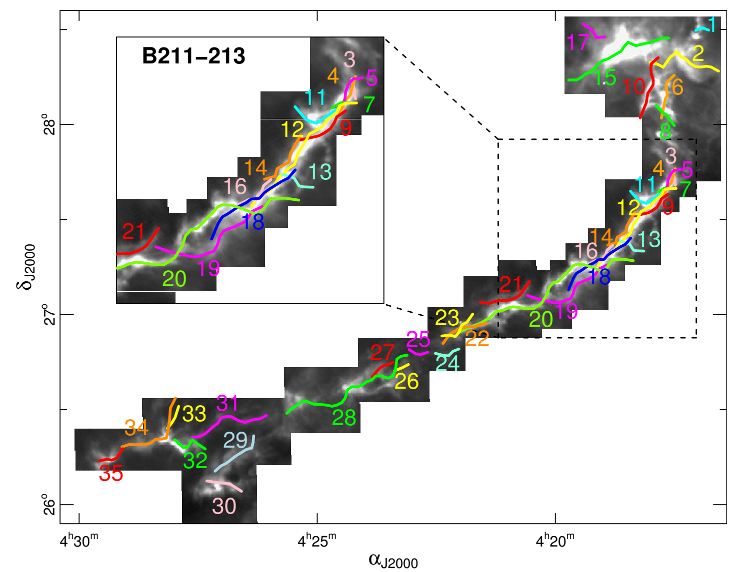

Smith et al. (2014, MNRAS, 445, 2900)

Summary

Star formation is intrinsically a multi-scale and multi-physics problem. Many different processes need to be considered simultaneously.

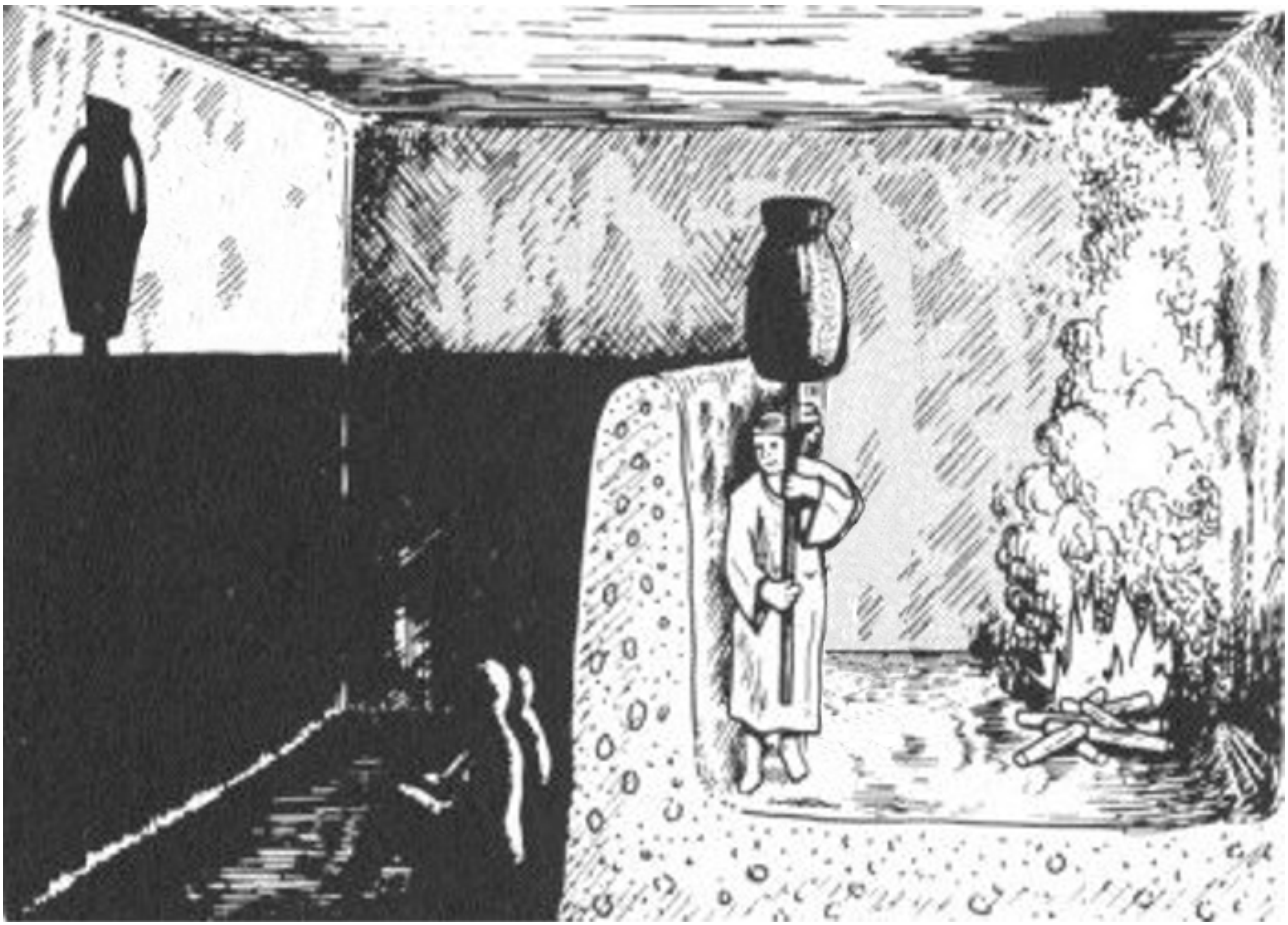

* The Republic (514a-520a)

Laszlo Szücs, image from criticalthinking-mc205.wikispaces.com

Star formation is intrinsically a multi-scale and multi-physics problem. Many different processes need to be considered simultaneously.

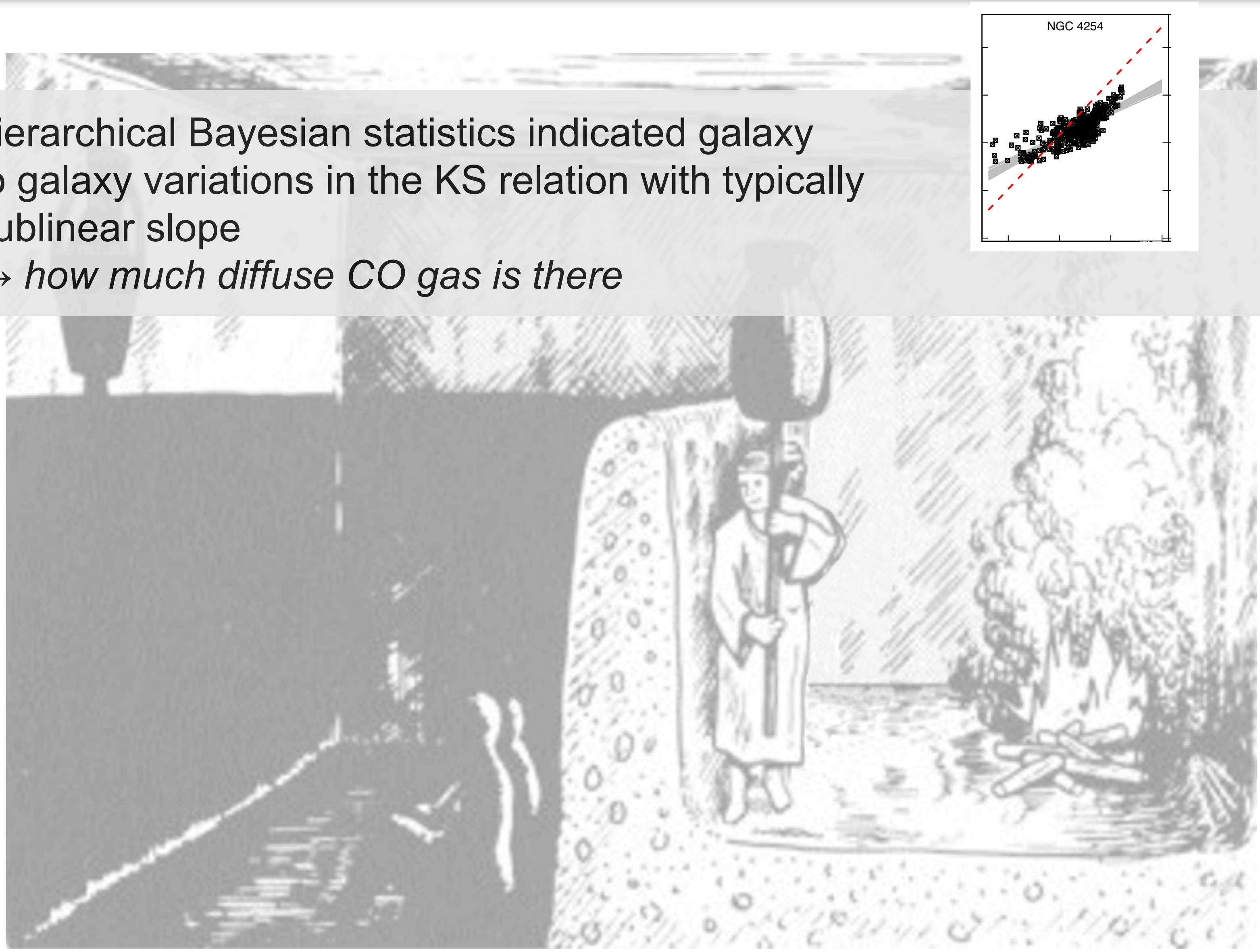

- hierarchical Bayesian statistics indicated galaxy to galaxy variations in the KS relation with typically sublinear slope
  → *how much diffuse CO gas is there*

* The Republic (514a-520a)

Laszlo Szücs, image from criticalthinking-mc205.wikispaces.com

Star formation is intrinsically a multi-scale and multi-physics problem.
Many different processes need to be considered simultaneously.

- hierarchical Bayesian statistics indicated galaxy to galaxy variations in the KS relation with typically sublinear slope
  → *how much diffuse CO gas is there*

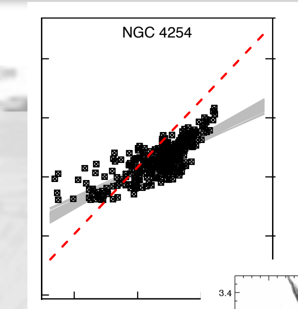

- detailed (M)HD calculations with time-dependent chemistry allow us to study the properties of CO-dark H2 gas
  → *im*

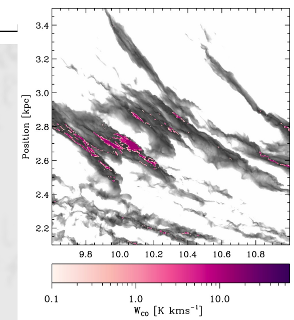

* The Republic
(514a-520a)

Laszlo Szücs, image from criticalthinking-mc205.wikispaces.com

Star formation is intrinsically a multi-scale and multi-physics problem. Many different processes need to be considered simultaneously.

- hierarchical Bayesian statistics indicated galaxy to galaxy variations in the KS relation with typically sublinear slope
  → *how much diffuse CO gas is there*
- detailed (M)HD calculations with time-dependent chemistry allow us to study the properties of CO-dark H2 gas
  → *implications for interpreting observational data?*
- molecular clouds are filamentary, but filament parameters (width, slope, central density) may vary significantly
  → *what does it mean for star cluster formation?*

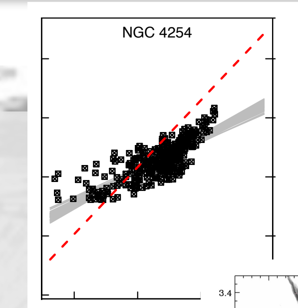

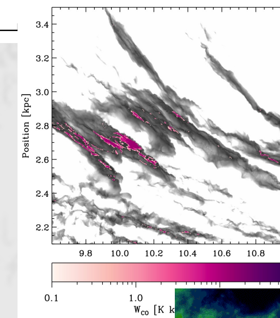

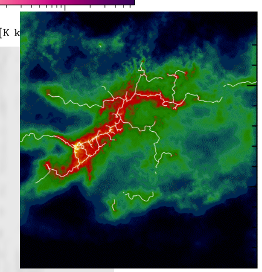

Laszlo Szücs, image from criticalthinking-mc205.wikispaces.com

* The Republic (514a-520a)

Star formation is intrinsically a multi-scale and multi-physics problem. Many different processes need to be considered simultaneously.

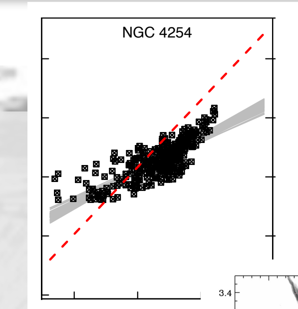

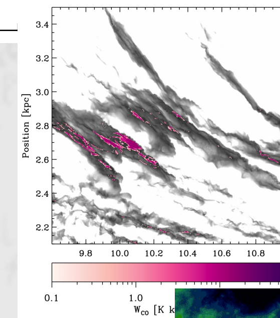

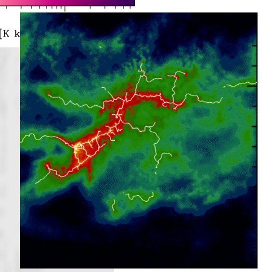

- hierarchical Bayesian statistics indicated galaxy to galaxy variations in the KS relation with typically sublinear slope
  → *how much diffuse CO gas is there*
- detailed (M)HD calculations with time-dependent chemistry allow us to study the properties of CO-dark H2 gas
  → *implications for interpreting observational data?*
- molecular clouds are filamentary, but filament parameters (width, slope, central density) may vary significantly
  → *what does it mean for star cluster formation?*
- next steps:
  multi-physics simulations with Arepo and FLASH for comparison with existing survey data

* The Republic (514a-520a)

Laszlo Szücs, image from criticalthinking-mc205.wikispaces.com

additional slides

large-scale filaments

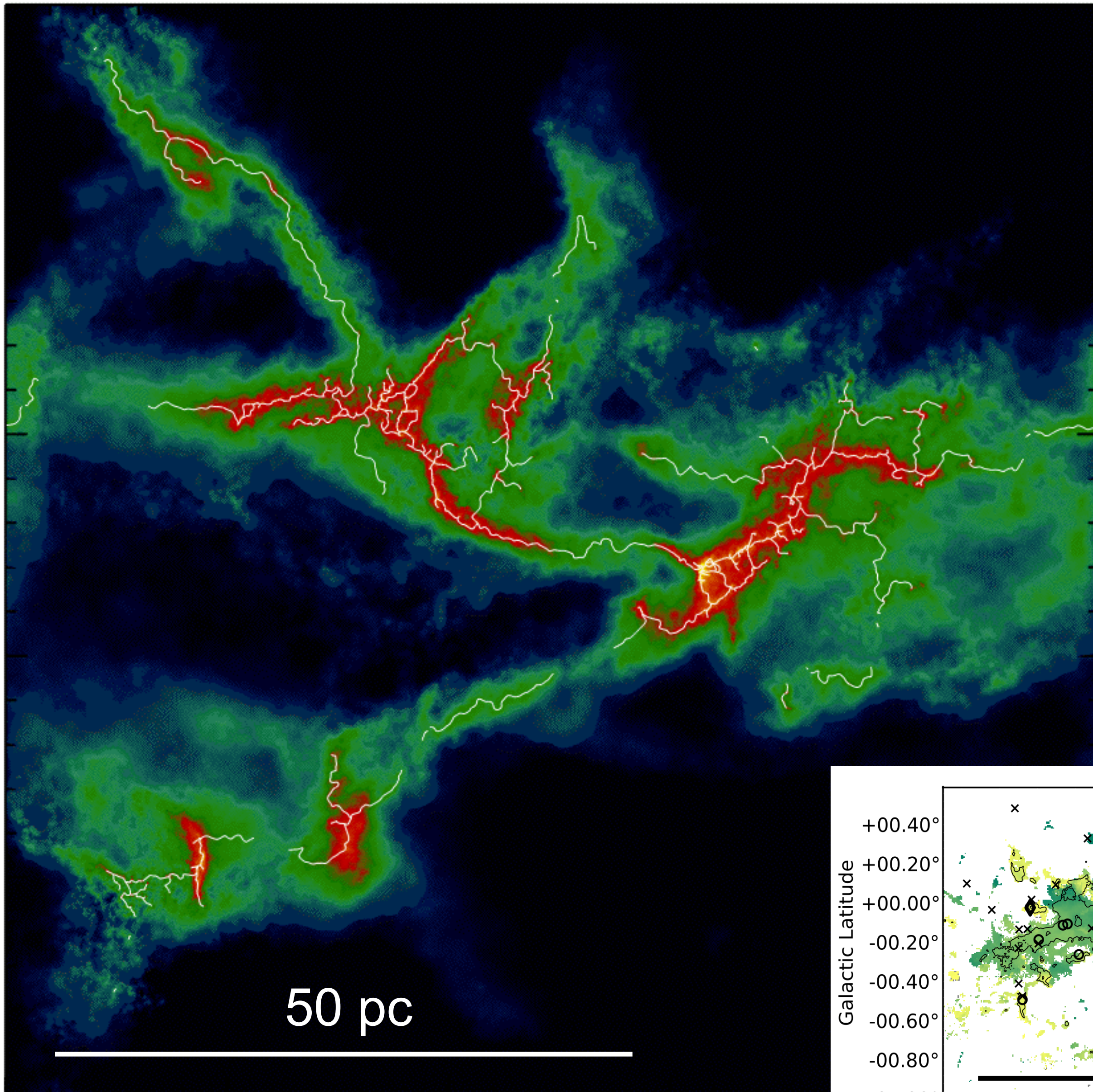

Smith et al. (2014, MNRAS, 445, 2900)

next steps:

studying details of ISM morphology and star formation in dedicated zoom-in simulation

example:
giant molecular cloud complex (~10^6 M$_\odot$) viewed in the plane of the disk.

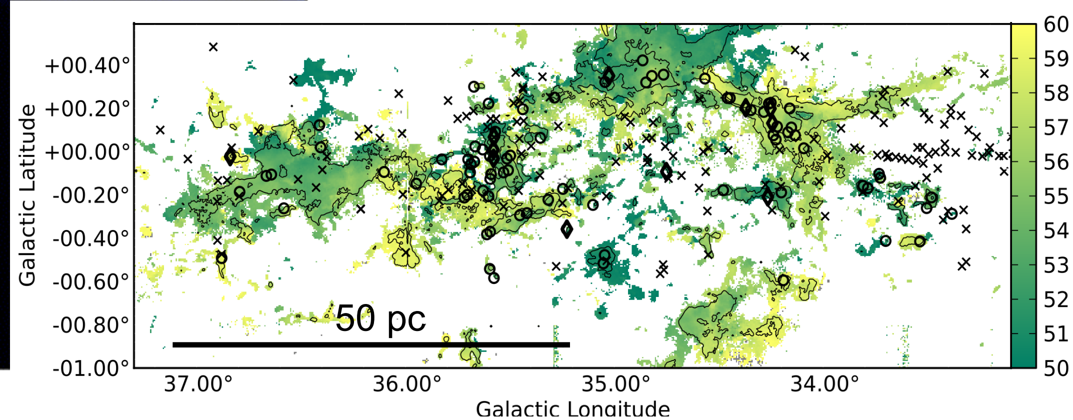

Ragan et al., 2014, A&A submitted, arXiv:1403.1450)

zoom-in on filaments

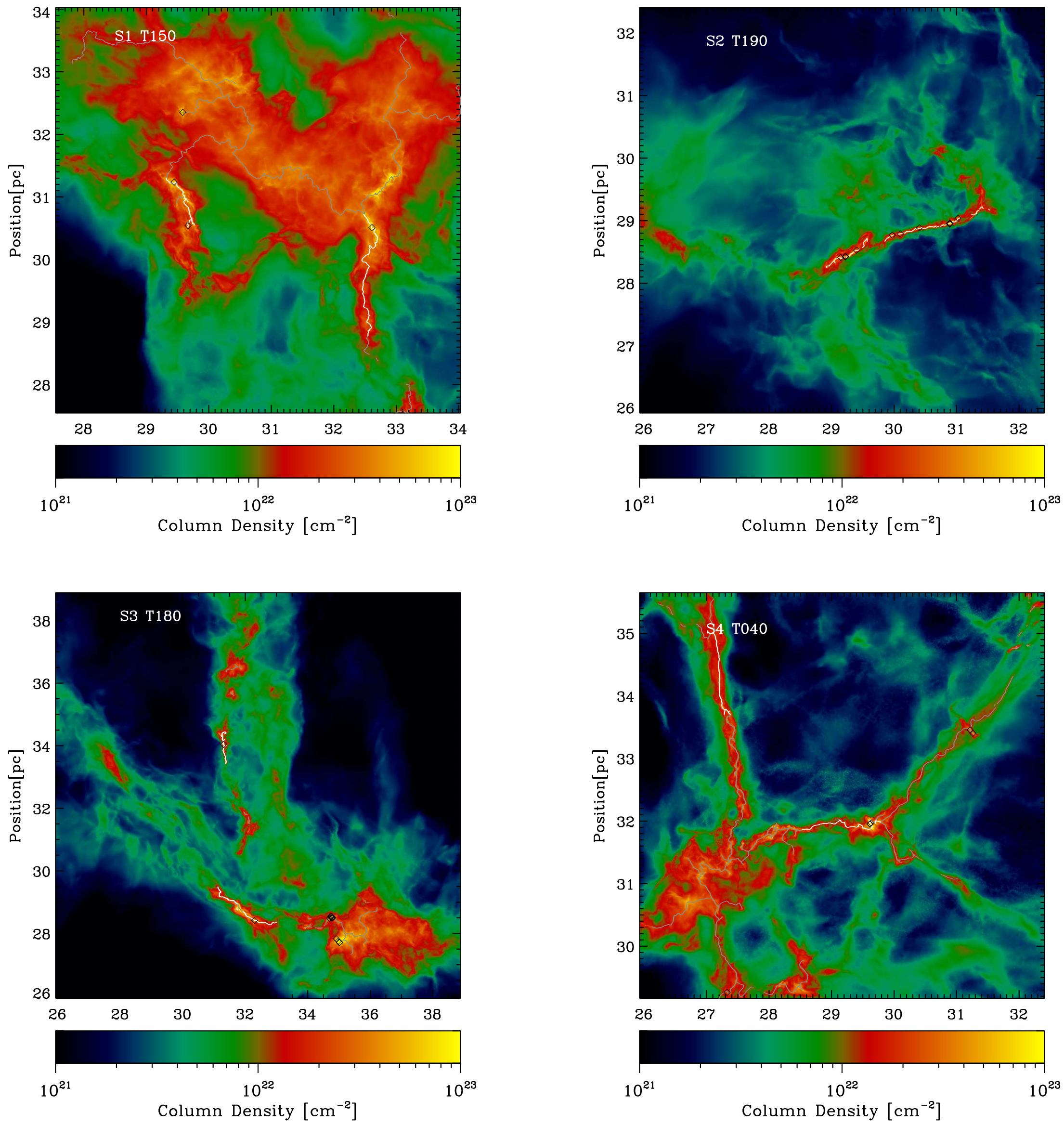

next steps:

studying details of ISM morphology and star formation in dedicated zoom-in simulation *(resolution ≲2000 AU, with full chemistry)*

analysis:

- morphology
- velocity
- chemistry
- observations (dust maps for Herschel, CO, N_2H+, HCN, etc. for line obs.)

Smith et al. (2014, MNRAS, 445, 2900,
also Smith et al. 2012, ApJ, 750, 64, Smith et al. 2013, ApJ, 771, 24, Chira et al., 2014, MNRAS, submitted)

filaments do not have universal width

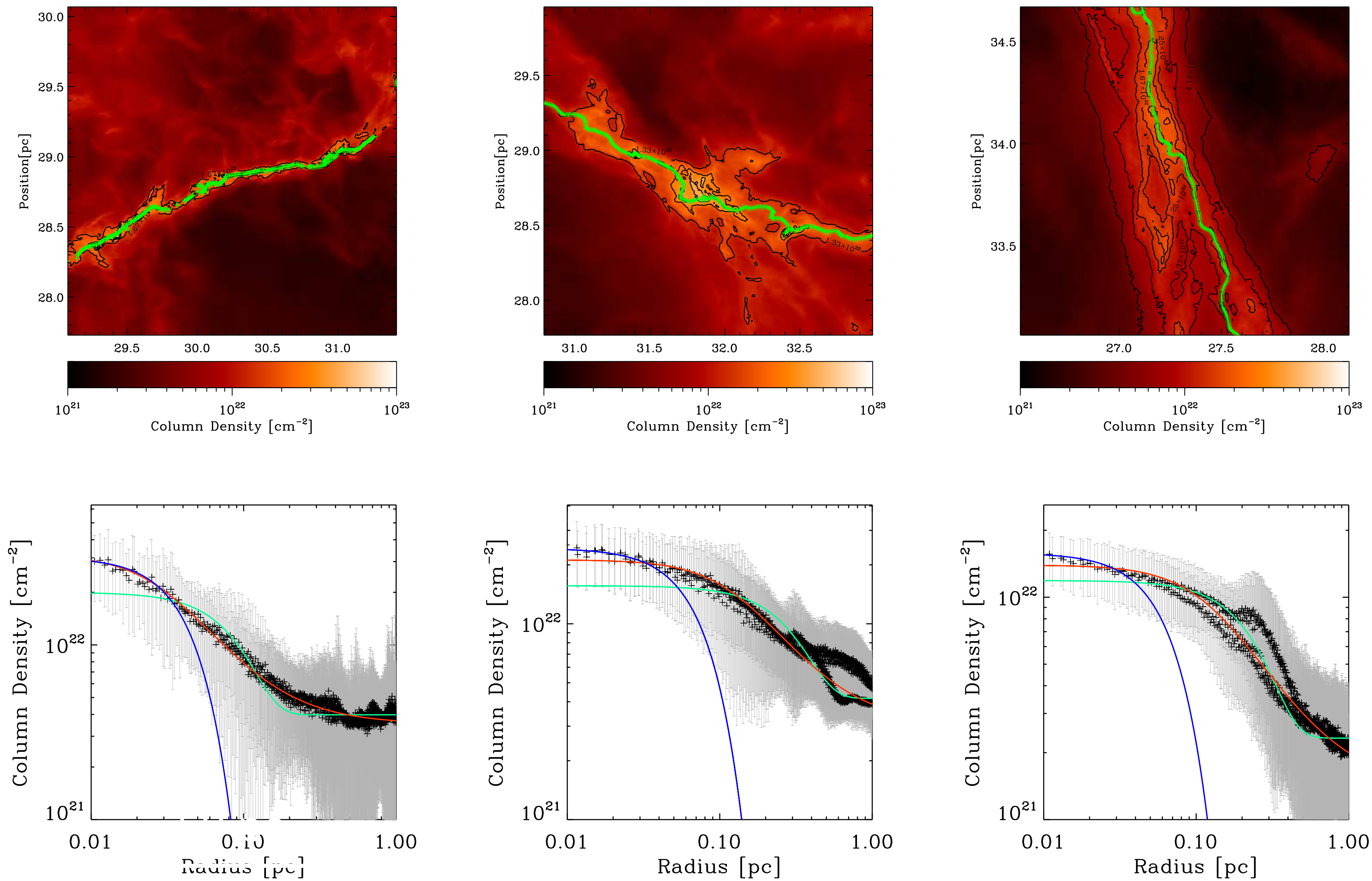

Smith et al. (2014, MNRAS, 445, 2900)

filaments do not have universal width

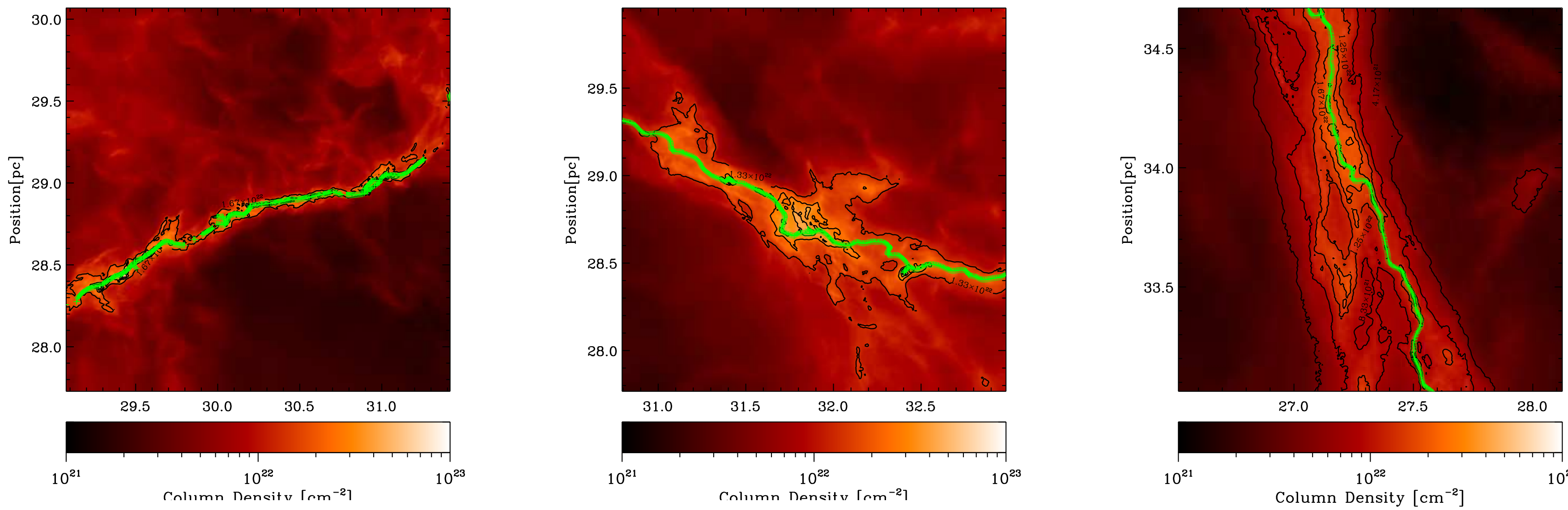

Arzoumanian, et al., 2011, A&A, 529, L6

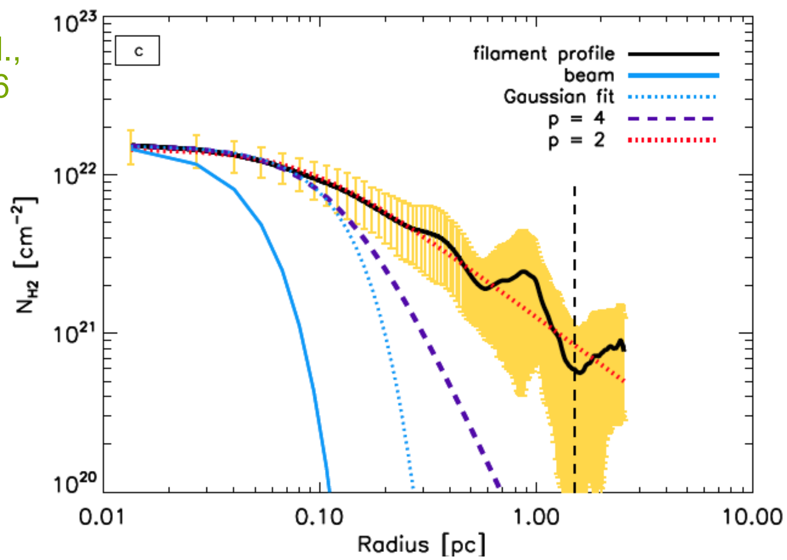

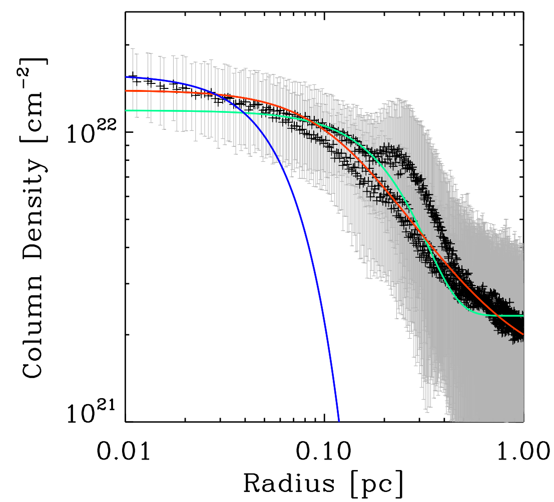

Smith et al. (2014, MNRAS, 445, 2900)

3D filaments have complex structure

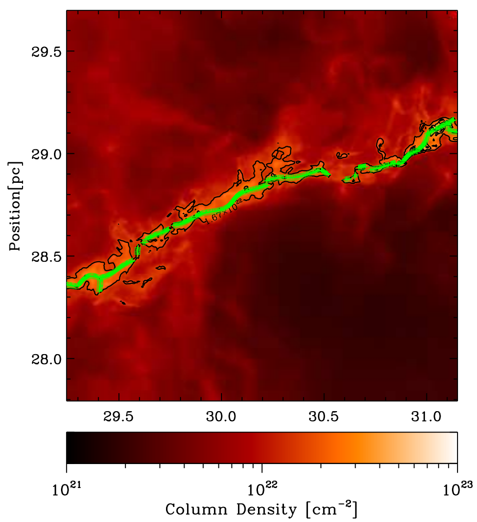

2D filament detection shows nice coherent filament

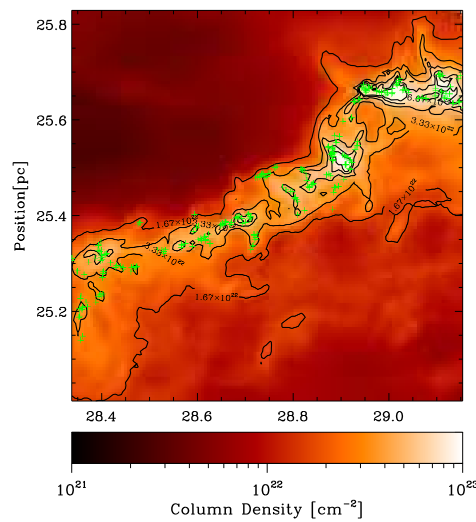

2D + LOS peak detection shows complex structure

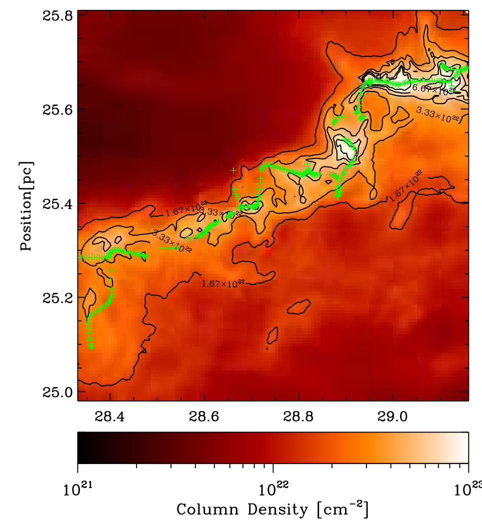

full 3D filament analysis confirms this picture

Smith et al. (2014, MNRAS, 445, 2900)

walk along the filament

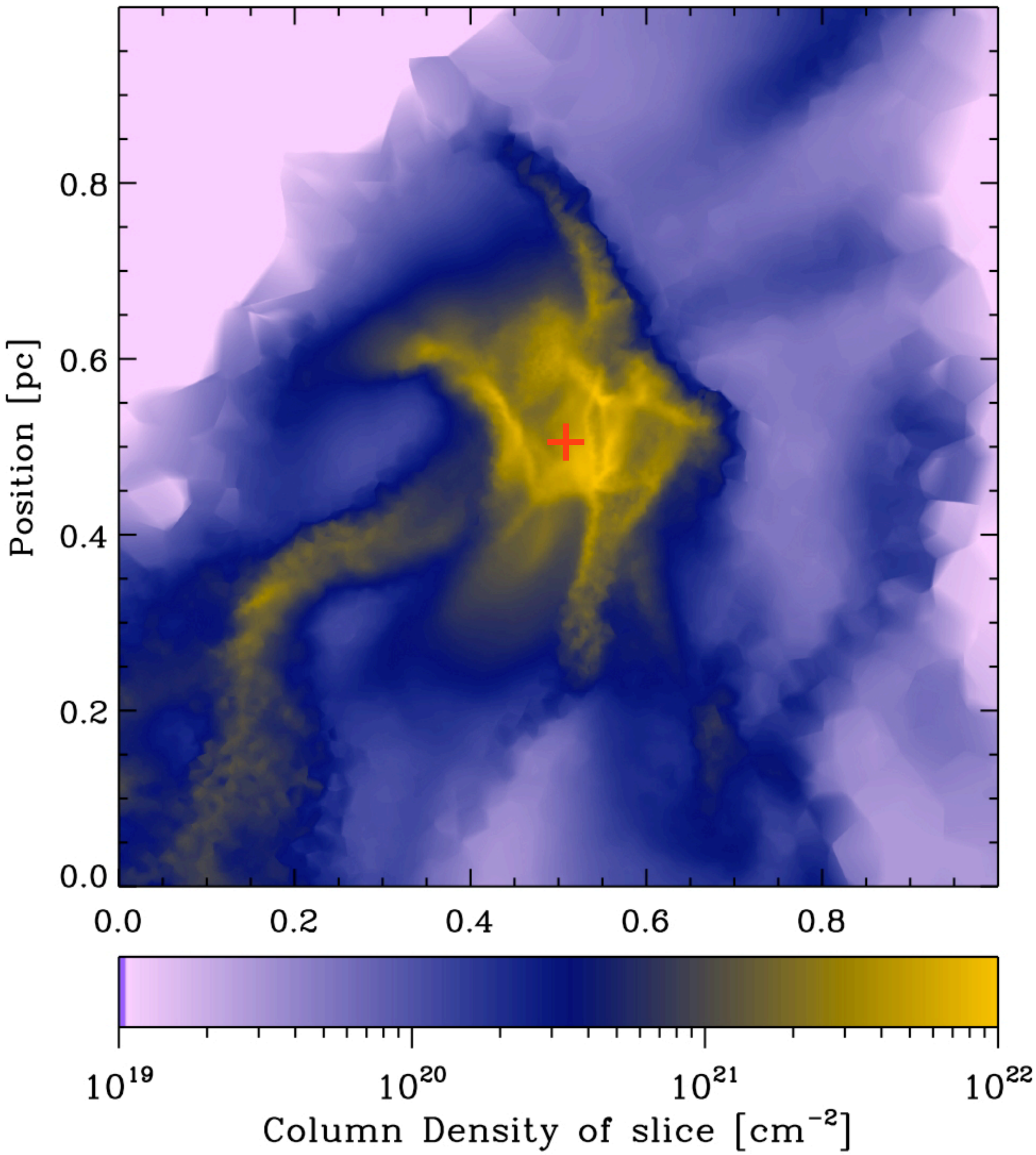

- walking along the filament exhibits complex 3D structure that is now (fully) seen in projected density
- is this similar to the filament fibers proposed by Hacar et al. (2013, A&A, 554, 55)

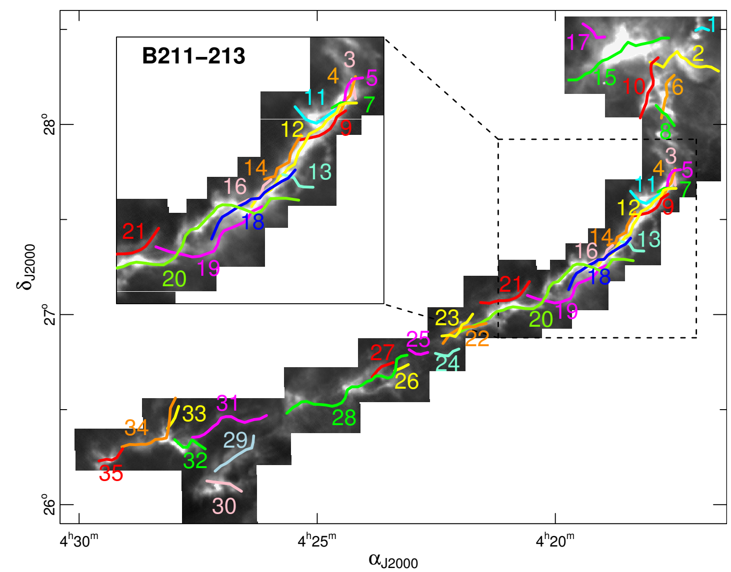

Smith et al. (2014, MNRAS, 445, 2900)

are molecules needed for star formation?

- it has been proposed that molecule formation (H_2, CO, etc.) is a prerequisite for star formation
  (e.g. Schaye 2004; Krumholz & McKee 2005; Elmegreen 2007; Krumholz et al. 2009)
- the idea is that CO is a necessary coolant for collapse
- however, also C+ and C are very efficient coolants
- see what is needed for star formation, by artificially 'switching' of certain chemical pathways
  (Glover & Clark 2011, 2012)

  - no shielding
  - no chemistry, gas remains atomic
  - H2 chemistry, but no CO
  - H2 and CO chemistry, hydrogen initially atomic
  - H2 and CO chemistry, hydrogen initially molecular

  - SPH (and FLASH) simulations of isolated, gravitational bound molecular cloud
  - column densities for H2 self-shielding, dust shielding determined using TreeCol (Clark et al. 2011)

are molecules needed for star formation?

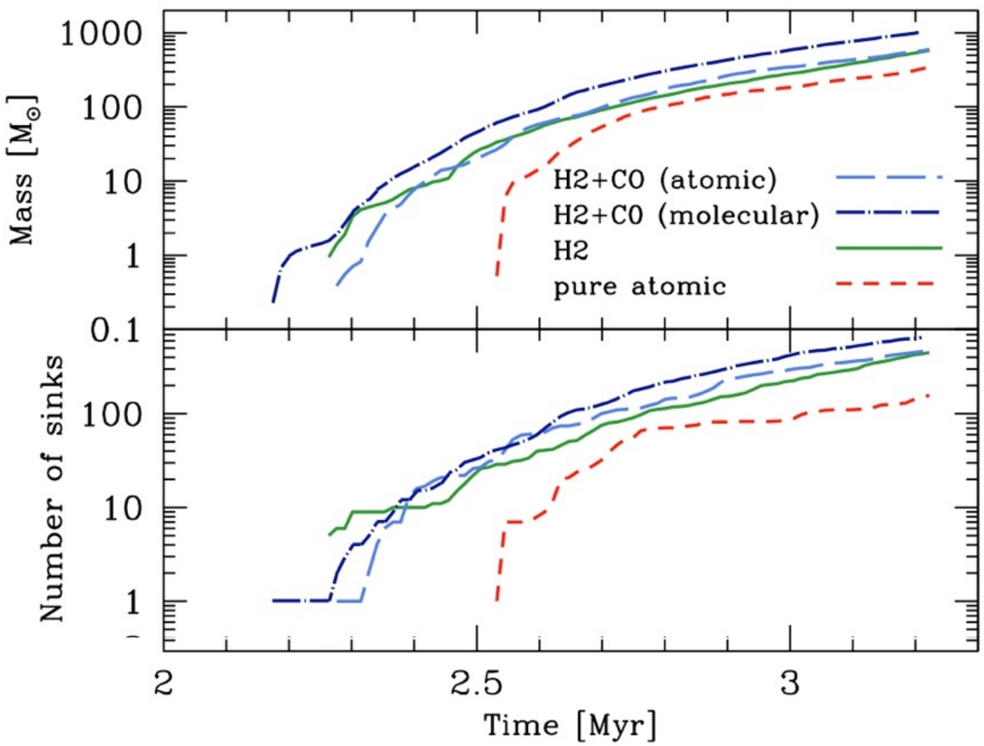

- presence of molecular gas has only very minor influence on ability of cloud to form stars

Glover & Clark (2011)

are molecules needed for star formation?

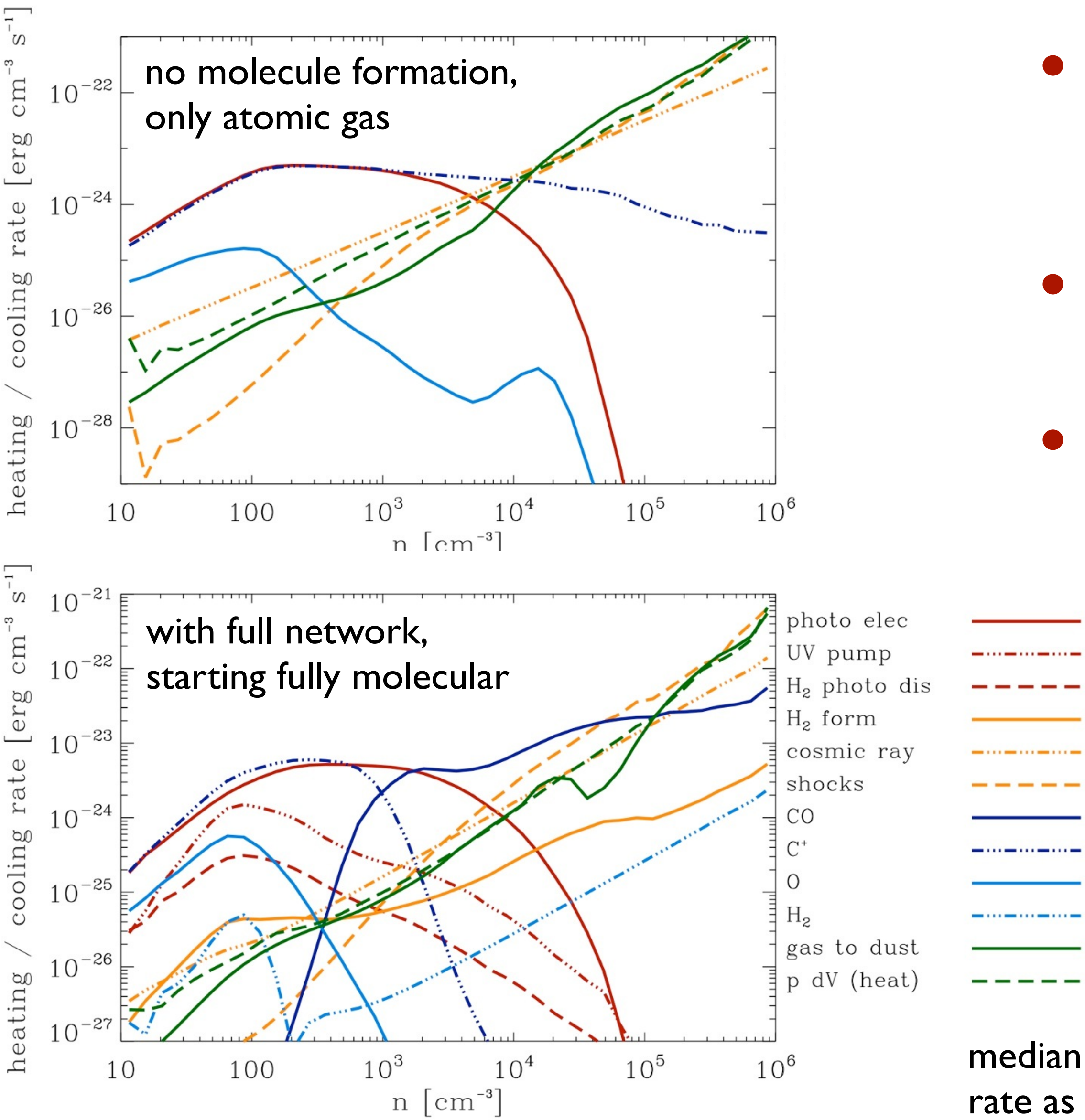

Glover & Clark (2011)

- presence of molecular gas has only very minor influence on ability of cloud to form stars
- C^+ is equally efficient coolant in atomic phase as CO in molecular
- shielding is important at high densities: photoelectric emission from dust grains is not longer dominant heating process

median heating and cooling rate as function of density

are molecules needed for star formation?

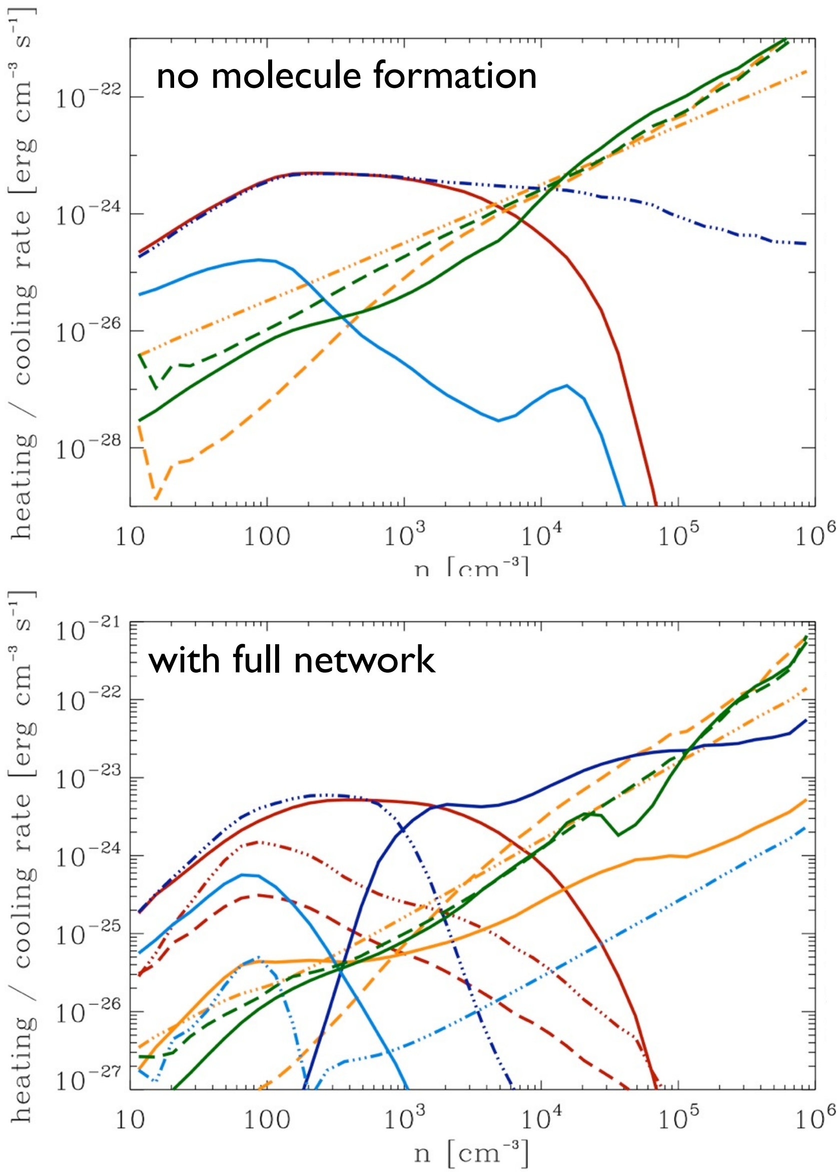

Glover & Clark (2011)

- presence of molecular gas has only very minor influence on ability of cloud to form stars
- C^+ is equally efficient coolant in atomic phase as CO in molecular
- what is crucial is the ability of cloud to shield itself from interstellar radiation field
- but clouds that are big/dense enough to shield themselves will be molecular!

this suggests that the correlation between H_2 and star formation is a coincidence

are molecules needed for star formation?

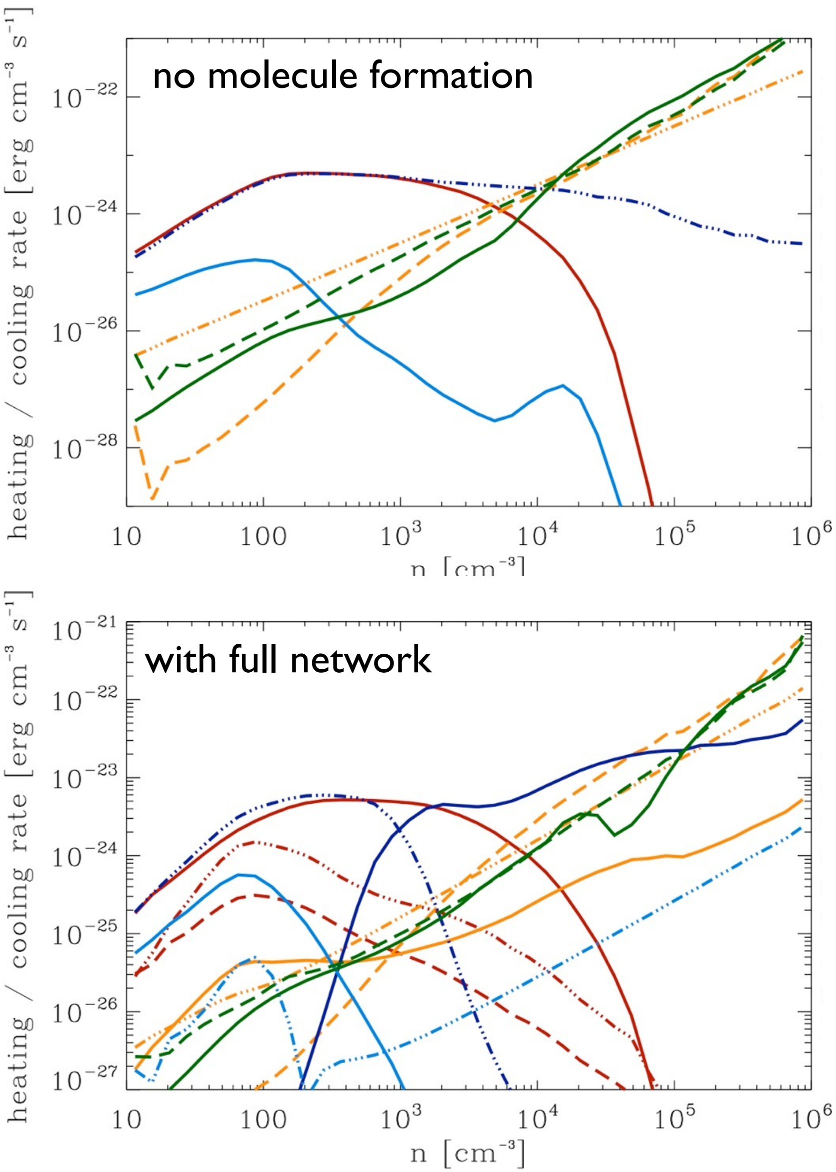

Glover & Clark (2011)

- presence of molecular gas has only very minor influence on ability of cloud to form stars
- C^+ is equally efficient coolant in atomic phase as CO in molecular
- what is crucial is the ability of cloud to shield itself from interstellar radiation field
- but clouds that are big/dense enough to shield themselves will be molecular!

more important is *extinction* (this introduces metallicity dependence)

metallicity dependence

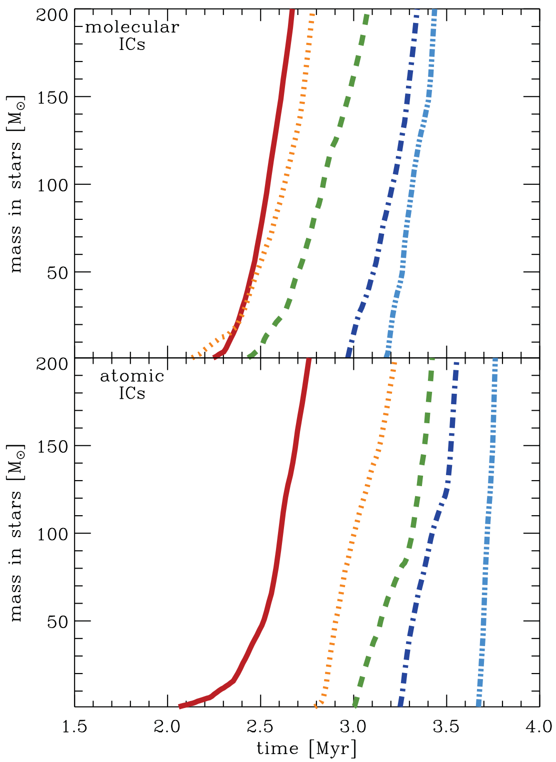

Figure 1. Upper panel: mass in sinks, plotted as a function of time, for runs Z1-M (solid line), Z03-M (dotted line), Z01-M (dashed line), Z003-M (dot–dashed line) and Z001-M (double-dot–dashed line). In these runs, hydrogen was initially in fully molecular form. Lower panel: the same quantity, but for runs Z1-A (solid line), Z03-A (dotted line), Z01-A (dashed line), Z003-A (dot–dashed line) and Z001-A (double-dot–dashed line). In these runs, hydrogen was initially fully atomic.

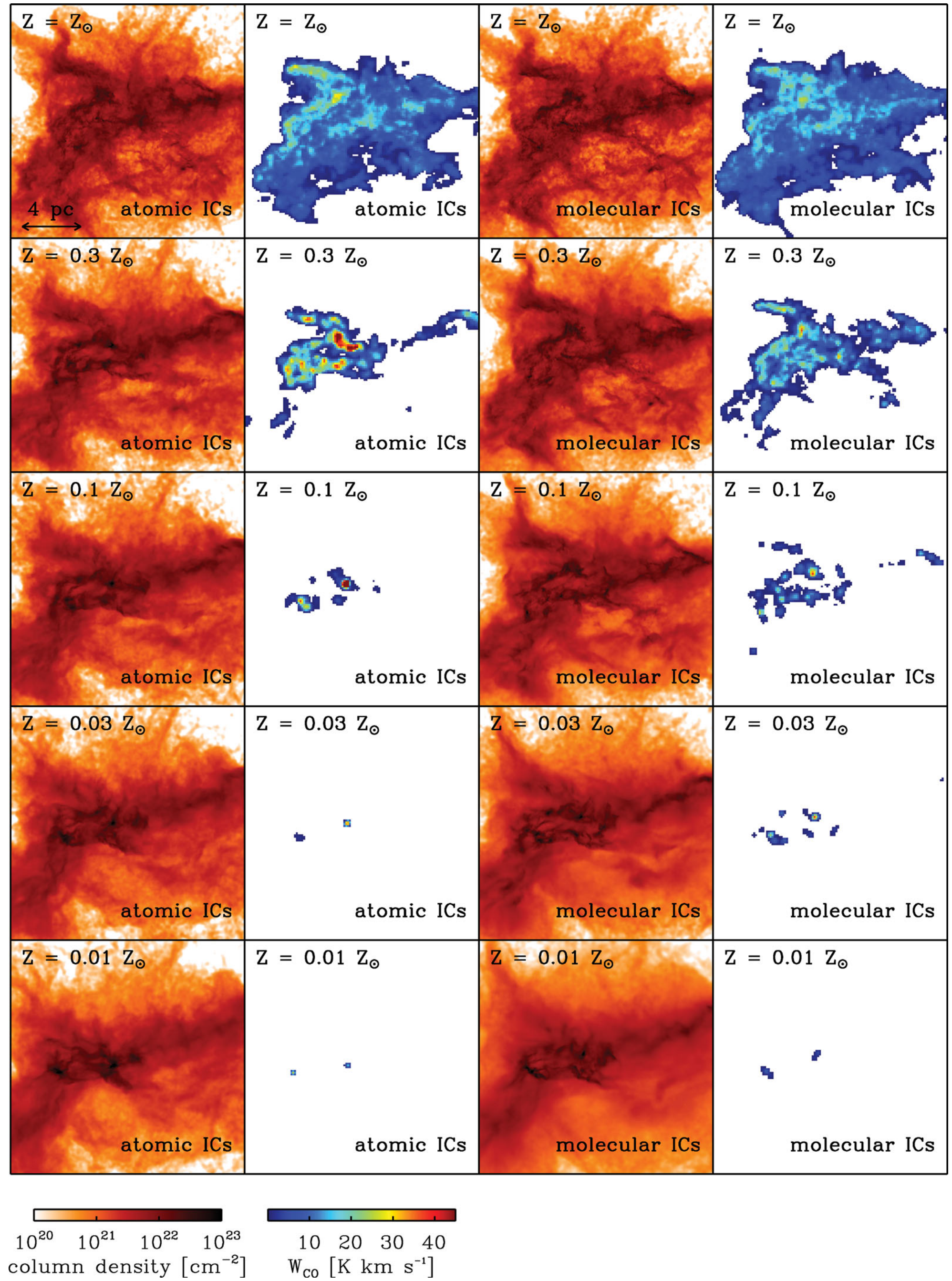

1.0

0.3

0.1

0.03

0.01

Figure 5. Maps of column density (first and third columns) and integrated intensity in the $J = 1$–0 rotational transition of ^{12}CO (second and fourth columns) for each of the simulations. The maps show a region of side length 16.2 pc that includes roughly 80 per cent of the total cloud mass, but almost all of the CO emission. The CO integrated intensity maps were produced using the RADMC-3D radiative transfer code, as described in the text.

Glover & Clark (2012)

BUT: at low metallicities, H2 and HD cooling may indeed matter!

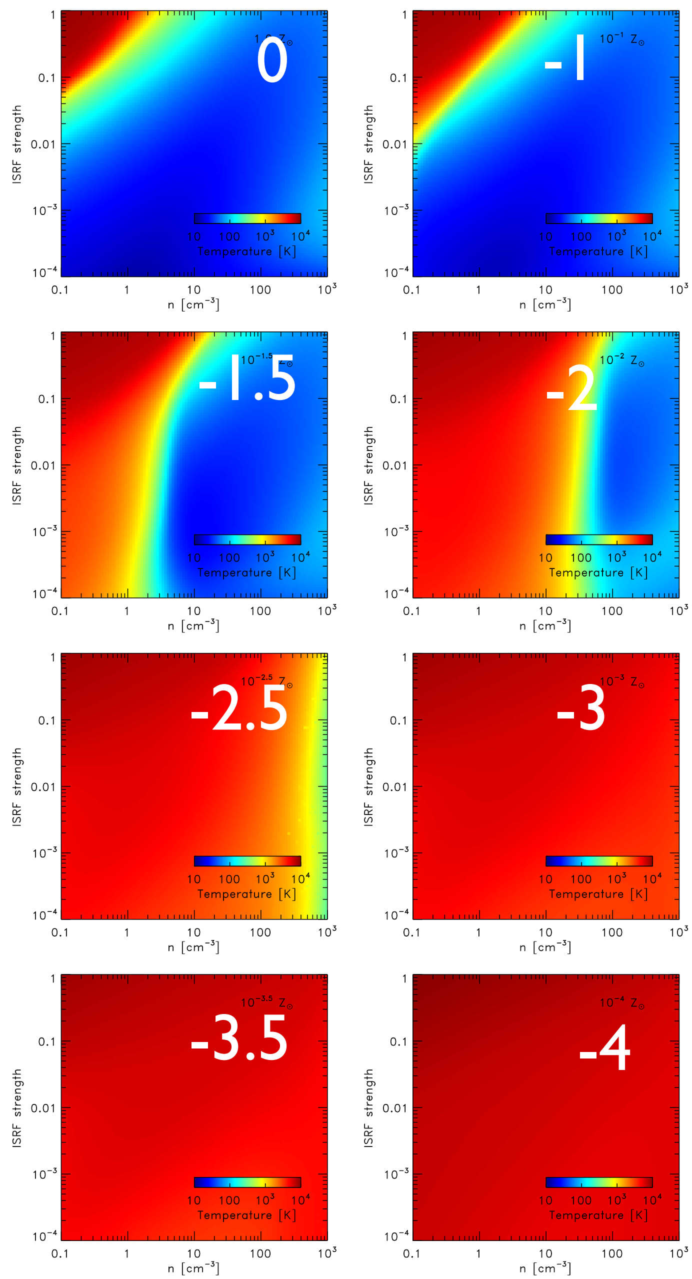

Figure 1. Gas temperature at $t = t_{\rm ff}$, computed as a function of the number density of hydrogen nuclei, n, and the strength of the interstellar radiation field in units of the standard value, G_0, for a set of runs covering a range of metallicities between $Z = Z_{\odot}$ and $Z = 10^{-4}\,{\rm Z}_{\odot}$. In these runs, the effects of H_2 and HD cooling were not included.

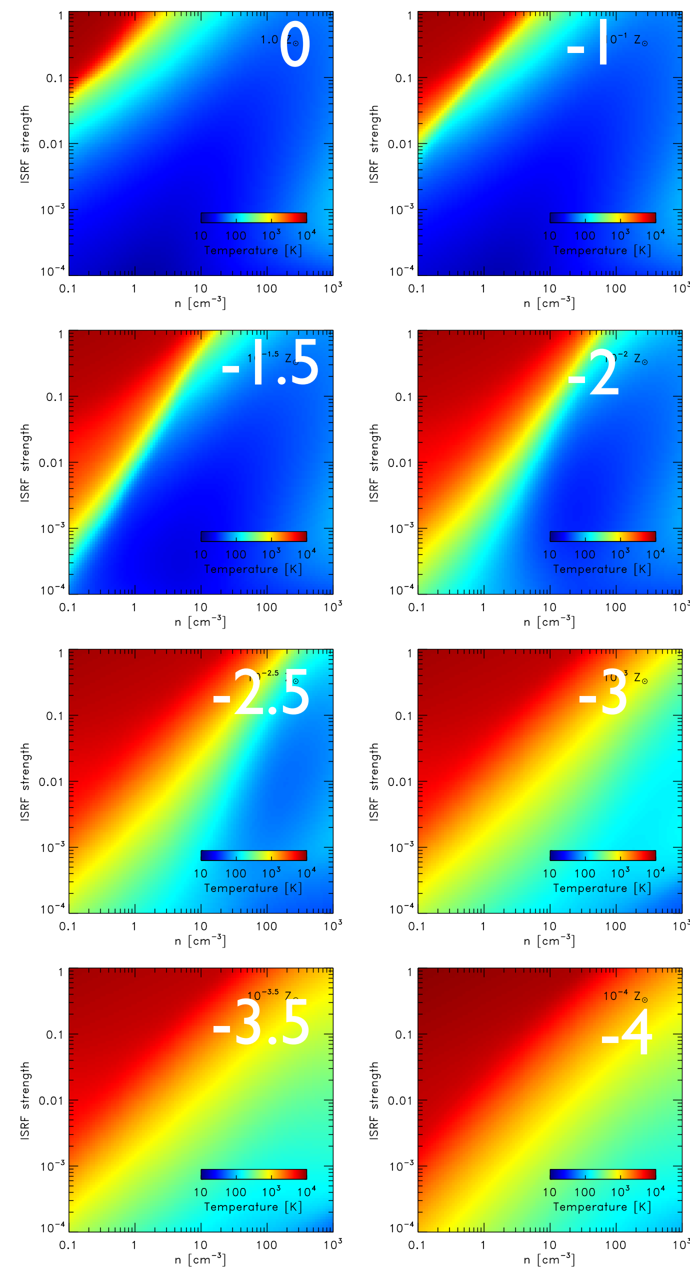

Figure 2. As Figure 1, but for a set of runs that included the effects of H_2 and HD cooling.

Glover & Clark (2013)